Norwegian University
of Life Sciences

Master's Thesis 2023 60 ECTS
Faculty of Chemistry, Biotechnology and Food Sciences

Denitrification and Its Application in High-Cell-Density Cultivation for Single-Cell Protein Production

Marte W. Lindholm-Dahle
MSc in Biotechnology

This page intentionally left blank

DENITRIFICATION AND ITS APPLICATION IN HIGH-CELL-DENSITY CULTIVATION FOR SINGLE-CELL PROTEIN PRODUCTION

Marte W. Lindholm-Dahle

Faculty of Chemistry, Biotechnology and Food Science
Norwegian University of Life Sciences

May 2023

A master's thesis submitted for the degree of
Master of Science in Biotechnology

Master Thesis Supervisors

Linda Liberg Bergaust (Main Supervisor)
Associate Professor
Faculty of Chemistry, Biotechnology and Food Science
Norwegian University of Life Sciences
1432 Ås, Norway
Phone: +47 67 23 24 49
E-mail: linda.bergaust@nmbu.no

Marte Mølsæter Maråk (Co-supervisor)
PhD Candidate
Faculty of Chemistry, Biotechnology and Food Science
Norwegian University of Life Sciences
1432 Ås, Norway
Phone: +47 67 23 29 97
E-mail: marte.molsater.marak@nmbu.no

Acknowledgements

Writing this thesis and performing all the related lab work would not have been possible without the help of a few people I would like to thank. First, I would like to thank my main supervisor, assoc. prof. Linda Liberg Bergaust, for letting me take part in your research. Thank you for designing this thesis's experiments and dedicating your time to give me excellent guidance and feedback during the writing process; I really appreciate it. I am also profoundly inspired by your knowledge and passion for the field.

Secondly, I would like to thank my co-supervisor, Marte Mølsæter Maråk. Thank you for gradually making me work independently at the lab by first giving me top-notch lab protocols and demonstrating different techniques and how to use the machines but then forcing me to try them on my own. Thank you for all the feedback on my work and for always calming me down when I showed up stressed out at your office because of a new experiment or the overwhelming writing process. You said you had never been a supervisor before, but let me say, you could not have done it any better than you did.

I would also like to thank the rest of the Microbial Ecology and Physiology (MEP) group at NMBU for welcoming me and helping me in the lab. Especially Lars M. and Elisabeth for helping me with the robot; Lars B. for giving advice regarding KinCalc and the CO_2 experiment; Martin, Louise and Kristine for help with the molecular work; Else Marie and Rannei for teaching me how to use the haemocytometer and ddPCR respectively; and finally, my lab bench neighbour Gro for help with the flow cytometer, but also spreading joy every day and all the non-lab related conversation about weddings etc.

Finally, I also have to thank all my friends and family for cheering on me through all my years at NMBU and giving me much-needed breaks now and then. I am especially grateful to my fiancé for supporting me through this stressful time and always being there for me emotionally and physically. I also have to mention my dog, Piko, for being an important support for me, offering unlimited cuddles (sometimes against his own will).

Abstract

Denitrification is one of the key processes in the nitrogen cycle, being responsible for the reduction of biologically available nitrate (NO_3^-) and nitrite (NO_2^-) to nitrogen gas (N_2), with nitric oxide (NO) and nitrous oxide (N_2O) as gaseous intermediates. Denitrification is an anaerobic process, and when denitrifying communities are exposed to oxygen, it tends to result in increased emissions of N_2O. It is, therefore, essential to learn more about how oxygen fluctuations affect denitrification to find ways of mitigating the increasing N_2O emissions. Denitrification can also be applied to industrial and biotechnological processes like protein production. With an increased population in the world, sustainable food and feed production is more crucial than ever, and with a shortage of proteins, new methods of producing them are needed. Single-cell protein (SCP) emerges as a tantalising prospect in this context. Existing culturing processes are based on aerobic respiration, however, with the limitations it entails, which denitrification might eliminate.

This thesis focuses on denitrification and its application in high-cell-density cultivation (HCDC) for SCP production through a newly invented process named AnaPro. The fed-batch culturing takes advantage of the alkalising effect of denitrification for the controlled provision of substrates. The process is still under development, and optimisations are needed: 1) As the culturing depends on a "pH-stat", it is essential to consider the acidifying effect of CO_2 produced by respiration. However, accurate measurements of this effect have been lacking. 2) Reactor systems may also be prone to oxygen leakages, and finding an organism which can tolerate potential oxygen fluctuations is required. In line with this, we tested the pH depression by CO_2 at two buffer strengths in the presence and absence of cells. Moreover, we compared the model organism *Paracoccus denitrificans* and the presumably aerobic denitrifier *Paracoccus pantotrophus* in terms of their response to oxygen exposure during denitrification, taking parameters such as cell count, dry weight, gas accumulation, enzyme activity and yield into account.

The results of this work have contributed to optimising the anaerobic HCDC method. The relationship between CO_2 and pH has been established, resulting in improved conditions for cell growth in a pH-stat. The comparative study of *P. denitrificans* and *P. pantotrophus* showed that the two organisms were highly similar, and neither showed signs of aerobic denitrification. However, subtle differences in yield and enzyme activity when exposed to oxygen during denitrification suggest that *P. pantotrophus* is a slightly better candidate for anaerobic HCDC than *P. denitrificans*.

Sammendrag

Denitrifikasjon er en viktig prosess i nitrogensyklusen, og er ansvarlig for reduksjonen av biologisk tilgjengelig nitrat (NO_3^-) og nitritt (NO_2^-) til nitrogengass (N_2), med nitrogenmonoksid (NO) og lystgass (N_2O) som mellomprodukter. Denitrifikasjon er en anaerob prosess, og når aktivt denitrifiserende mikrobielle samfunn eksponeres for oksygen øker ofte emisjonen av N_2O. I prosessen med å finne løsninger for å mitigere økende N_2O emisjoner er det derfor essensielt å lære mer om hvordan oksygenfluktuasjoner påvirker denitrifikasjon. Denitrifikasjon kan også benyttes til industrielle og bioteknologiske prosesser, for eksempel proteinproduksjon. Med en økende befolkning i verden er mat- og fôrproduksjon viktigere enn noen gang, og med en mangel på proteiner kreves nye metoder for å produsere de. Enkeltcelle proteiner (SCP) fremstår som et fristende prospekt i denne sammenhengen. Eksisterende metoder for SCP produksjon er basert på aerob respirasjon, med de begrensningene det medfører, noe denitrifikasjon potensielt kan eliminere.

Denne masteroppgaven fokuserer på denitrifikasjon og utnyttelsen av denne formen for anaerob respirasjon i høydensitetskultivering (HCDC) for SCP produksjon gjennom en nyoppfunnet prosess kalt AnaPro. «Fed-batch»-dyrkingen drar fordel av den alkaliserende effekten av denitrifikasjon for kontrollert tilførsel av substrater. Prosessen er fortsatt under utvikling, og det er behov for optimaliseringer: 1) Siden dyrkingen er avhengig av en "pH-stat", er det viktig å vurdere den forsurende effekten av CO_2 produsert ved respirasjon. Nøyaktige målinger av denne effekten har imidlertid manglet. 2) Reaktorsystemer kan også være utsatt for oksygenlekkasjer, og det er nødvendig å finne en organisme som kan tolerere potensielle oksygenfluktuasjoner. I tråd med dette testet vi pH-depresjonen med CO_2 ved to bufferstyrker i nærvær og fravær av celler. Dessuten sammenlignet vi modellorganismen *Paracoccus denitrificans* og den antatt aerobe denitrifikanten *Paracoccus pantotrophus* med tanke på deres respons på oksygeneksponering under denitrifikasjon, ved å undersøke parametere som celletall, tørrvekt, gassakkumulering, enzymaktivitet og utbytte (biomasse yield).

Funnene i denne oppgaven har bidratt til å optimalisere den anaerobe HCDC metoden. Forholdet mellom CO_2 og pH er etablert, noe som resulterer i forbedrede forhold for cellevekst i pH-stat. Den komparative studien av *P. denitrificans* og *P. pantotrophus* viste at de to organismene var svært like, og ingen av dem viste tegn til aerob denitrifikasjon. Imidlertid antyder subtile forskjeller i utbytte og enzymaktivitet ved eksponering for oksygen under denitrifikasjon at *P. pantotrophus* er en marginalt bedre kandidat for anaerob HCDC enn *P. denitrificans.*

Table of Contents

Abbreviations

cDNA	Complementary DNA (Reverse Transcription of mRNA)
ddPCR	Digital Droplet PCR
Fnr	Fumarate and Nitrate Reduction
gDNA	Genomic DNA
HCDC	High Cell Density Cultivation
HPLC	High-Performance Liquid Chromatography
Nap	Nitrate Reductase (Periplasmic)
Nar	Nitrate Reductase (Cytoplasmic)
Nir	Nitrite Reductase
NOA	Nitric Oxide Analyser
Nor	Nitric Oxide Reductase
Nos	Nitrous Oxide Reductase
N-oxides	Collective Term for NO_3^-, NO_2^-, NO and N_2O
PBS	Phosphate Buffered Saline
PCR	Polymerase Chain Reaction
qPCR	Quantitative PCR
SCP	Single-Cell Proteins
w/v	Weight per Volume

List of Tables and Figures

List of Appendix Tables and Figures

1 Introduction

1.1 The Nitrogen Cycle

Nitrogen is essential for all life on earth as it is a crucial element in proteins, nucleic acids, vitamins and hormones, making up about 6.25% of the dry weight of living organisms (Bothe et al., 2007). Vast nitrogen reservoirs are found in the atmosphere as nitrogen gas (N_2) and in the crust of Earth as ammonium (NH_4^+), but both forms are biologically unavailable for most organisms. Organisms depend on access to reactive nitrogen for assimilatory and dissimilatory processes. Microorganisms are central in making nitrogen biologically available through nitrogen fixation and in the circulation of reactive nitrogen in the biosphere, a process called the nitrogen cycle (Pepper et al., 2015b).

The nitrogen cycle (Fig. 1.1) consists of many key processes like nitrification, ammonification, nitrogen fixation, denitrification, anaerobic ammonium oxidation (anammox), complete ammonia oxidation to nitrate (comammox) and dissimilatory nitrate reduction to ammonium (DNRA) (Burns et al., 1996; Russow et al., 2009). This thesis focuses on denitrification as an environmentally relevant process, and as a biotechnological prospect, but before diving into the topic, a short description of the other microbial processes which are a part of the nitrogen cycle is included below.

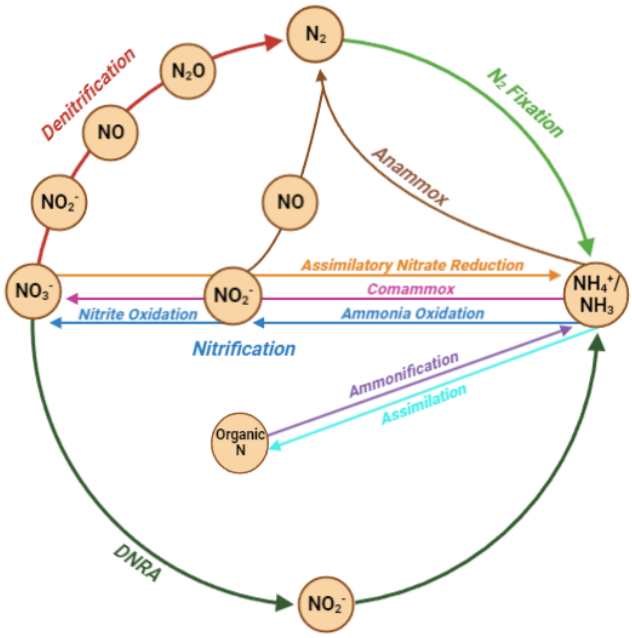

Figure 1.1 The Nitrogen Cycle. *Schematic overview of key processes of the nitrogen cycle.*

Nitrification

Nitrification is the oxidation of either ammonia (NH_3) or NH_4^+ to nitrite (NO_2^-) and, finally nitrate (NO_3^-). The process can be divided into two parts: first the NH_3/NH_4^+ oxidation to hydroxylamine (NH_2OH) and further to NO_2^-, catalysed by the enzymes ammonia monooxygenase (Amo) and hydroxylamine dehydrogenase (Hao) respectively, and second the nitrite oxidation to NO_3^- catalysed by nitrite oxidoreductase (Nxr). NH_4^+ and NO_2^- are used as electron donors, while O_2 works as the electron acceptor when generating energy for CO_2 fixation.

$$1)\ NH_4^+ \leftrightarrow NH_3 + O_2 + 2\,e^- \xrightarrow{\text{Amo}} NH_2OH + H_2O \xrightarrow{\text{Hao}} NO_2^- + 5\,H^+ + 4\,e^-$$

$$2)\ NO_2^- + \frac{1}{2}O_2 \xrightarrow{\text{Nxr}} NO_3^-$$

Nitrification is performed by ammonia-oxidizing bacteria (AOB), ammonia-oxidizing archaea (AOA) and nitrite-oxidizing bacteria (NOB), and they are all autotrophic aerobes (Ward, 2008). Recent discoveries also involve a fourth group of bacteria within the *Nitrospira* genus called comammox bacteria, which completely oxidises NH_3 to NO_3^- (Hu & He, 2017).

Ammonification

Ammonification is the process of converting organic nitrogen to inorganic nitrogen compounds. The organic nitrogen, like NH_2 from amino groups, can originate from animal excrements or the animal's tissue when it dies. Decomposers like fungi and prokaryotes will break it down and convert it to inorganic nitrogen compounds which plants and bacteria can use, like NH_3 and NH_4^+. Without ammonification, the organic nitrogen compounds would accumulate in large amounts as bacteria, plants and biofilms prefer inorganic compounds as their substrate (Strock, 2008).

Nitrogen Fixation

Nitrogen fixation is the process of fixing the N_2 gas in the atmosphere as NH_3 by an enzyme called nitrogenase, which makes the nitrogen accessible to plants and other bacteria.

$$N_2 + 8H^+ + 8\,e^- \xrightarrow{Nitrogenase} 2\,NH_3 + H_2$$

Nitrogen fixation is an energy-costly process which requires hydrolysis of 16 ATP molecules per N_2 molecule (Barney et al., 2006; Seefeldt et al., 2009). The process is carried out by nitrogen-fixing bacteria, which utilize the nitrogenase enzyme. Nitrogen-fixing bacteria live in

aquatic environments (cyanobacteria) and soil as free-living bacteria (e.g., *Azotobacter*) or in symbiosis with legumes (e.g., *Rhizobium* and *Bradyrhizobium*) (Postgate, 1982).

Anaerobic Ammonium Oxidation (Anammox)

Anammox is the process of anaerobic oxidation of NH_4^+ to N_2, also involving the reduction of NO_2^- to nitric oxide (NO), where the latter is combined with NH_4^+ to form hydrazine (N_2H_4) which finally is oxidized to N_2 (Hayatsu et al., 2008). The process is commercially used in the treatment of wastewater to remove NH_4^+. The anammox bacteria belong to the Planctomycetota phylum and possess a lipid bilayer membrane-bound compartment called an anammoxosome inside the cytoplasm. The process is divided into three steps:

1) $NO_2^- + 2\,H^+ + e^- \xrightarrow{\text{Nir}} NO + H_2O$

2) $NO + NH_4^+ + 2\,H^+ + 3\,e^- \xrightarrow{\text{HH}} N_2H_4 + H_2O$

3) $N_2H_4 \xrightarrow{\text{Hzo}} N_2 + 4\,H^+ + 4\,e^-$

First, NO_2^- is reduced to NO by using nitrite reductase (Nir) enzymes. Further, hydrazine hydrolase (HH) catalyses the production of N_2H_4. The final reaction where N_2 is formed is catalysed by hydrazine oxidoreductase (Hzo) (Jetten et al., 2001; Kraft et al., 2011; Kuenen, 2008).

Dissimilatory Nitrate Reduction to Ammonium (DNRA)

Dissimilatory nitrate reduction to ammonium (DNRA) is an anaerobic process favoured under high C:N ratios. NO_3^- is reduced to NO_2^-, mainly by periplasmatic nitrate reductase (NapAB). Next, NO_2^- is reduced to NH_4^+ by a pentaheme cytochrome *c* nitrite reductase (NrfA).

1) $NO_3^- + 2\,e^- + 2\,H^+ \xrightarrow{\text{NapAB}} NO_2^- + H_2O$

2) $NO_2^- + 8\,H^+ \xrightarrow{\text{NrfA}} NH_4^+ + 2\,H_2O$

When the C:N ratio is low, the other main anaerobic process of the nitrogen cycle, denitrification, is favoured (Kraft et al., 2011; Liu et al., 2021).

1.2 Denitrification

Denitrification is a form of anaerobic respiration where the different nitrogen compounds serve as the electron acceptor. This results in a stepwise reduction of NO_3^- to N_2 via the intermediates NO_2^-, NO and nitrous oxide (N_2O).

$$NO_3^- \xrightarrow{Nitrate\ reductase} NO_2^- \xrightarrow{Nitrite\ reductase} NO \xrightarrow{Nitric\ oxide\ reductase} N_2O \xrightarrow{Nitrous\ oxide\ reductase} N_2$$

It is a widely studied process as it is widespread and the most significant biological source of N_2O, the third most important greenhouse gas after CO_2 and methane (Tian et al., 2016). Additionally, denitrification is the most critical reason for stratospheric ozone depletion (Thompson et al., 2019). The following subsections describe denitrifying organisms in general, the denitrification apparatus, thermodynamics, regulation, physiology and the environmental perspective of denitrification.

1.2.1 Organisms

Denitrification is found in all domains (Bacteria, Archaea and Eukarya), but so far, no reduction of N_2O from the eukaryotes has been reported. Among the prokaryotes, the most studied microorganism is bacteria, which is also this thesis's focus. Denitrifying bacteria are found in water, sediments and soil, making up about 10 - 15% of the bacterial population in these areas. They can use both inorganic and organic compounds as their carbon source (Ambus & Zechmeister-Boltenstern, 2007). Many denitrifying bacteria are found in the *Paracoccus*, *Bacillus* and *Pseudomonas* genera, but they have been identified in over 50 genera, mainly belonging to the α-, β-, and γ-classes of the Proteobacteria phylum (Eldor, 2015; Ji et al., 2015). Denitrifying bacteria generate ATP through denitrification when oxygen is absent but generally switch to aerobic respiration when oxygen is present, making most denitrifying bacteria facultative aerobic heterotrophs (Bothe et al., 2007; Zumft, 1997).

1.2.2 Denitrification Apparatus

Denitrification is modular, and denitrifying bacteria can have either one, some or all of the enzymes nitrate reductase (Nar/Nap), nitrite reductase (Nir), nitric oxide reductase (Nor) and nitrous oxide reductase (Nos). Bacteria possessing only the former are not regarded as denitrifiers, as denitrification *sensu stricto* requires at least a reduction of NO_2^- to NO (Lycus et al., 2017).

All the steps of denitrification require the transfer of electrons (Fig. 1.2). The N-oxides (NO_3^-, NO_2^-, NO and N_2O) serve as electron acceptors, and the electron donor is the reduced form of nicotinamide adenine dinucleotide (NADH), which releases two electrons and a proton when oxidated to NAD^+ (Shi et al., 2020). The electrons from the oxidation of NADH are transferred to a quinone pool in the membrane by NADH dehydrogenase (complex I) (Sazanov & Hinchliffe, 2006). The *bc*$_1$ complex (complex III) will transfer the electrons from the quinone pool to cytochrome *c* in the periplasm (Berry et al., 2000). Cytochrome *c* is a small protein with covalently bound heme and cysteine and is an important electron carrier in cellular respiration. Under aerobic respiration, the electrons would be transferred to complex IV, which is a terminal oxidase, but under denitrification, the electrons are transferred to Nir, Nor and Nos instead (Chen & Strous, 2013).

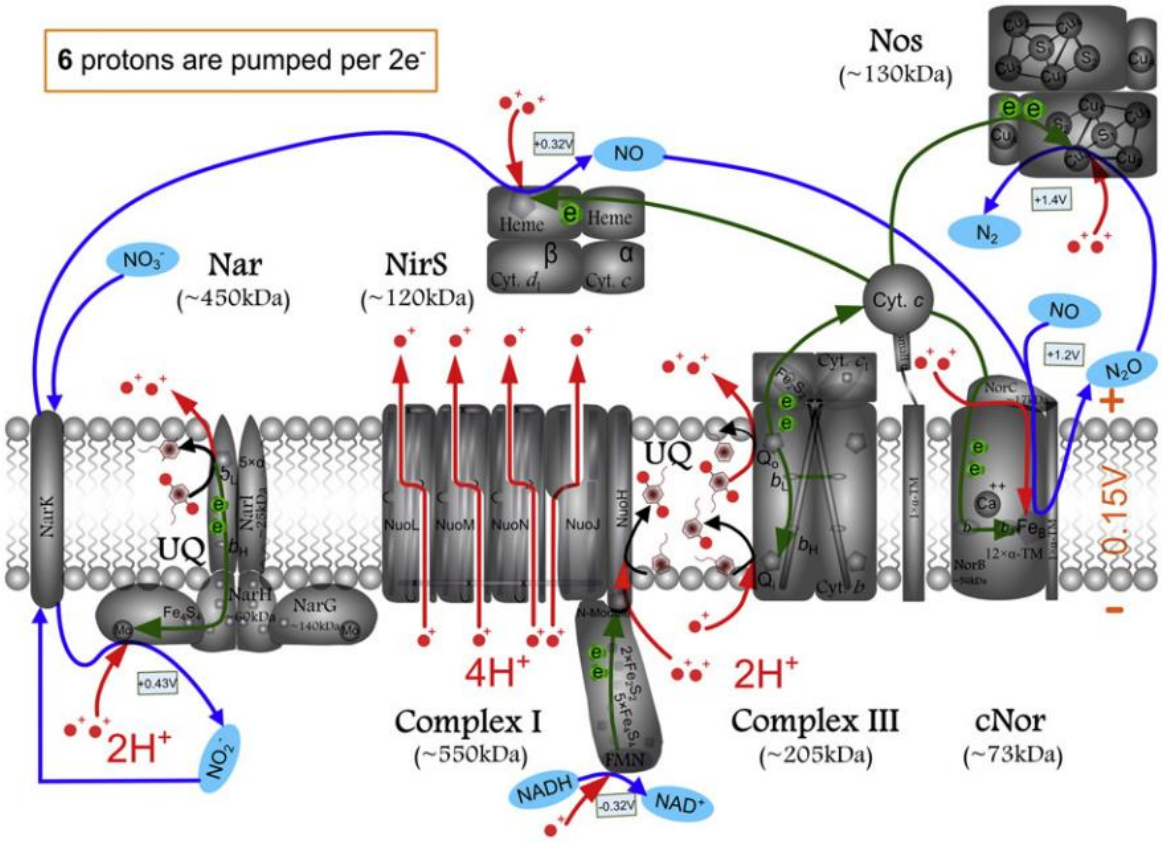

Figure 1.2 Schematic Diagram of Canonical Denitrification Electron Respiratory Chain. *Electrons are transferred from the electron donor NADH to the N-oxide reductases (which serve as the electron acceptors) via complex I, ubiquinone/ubiquinol, complex III, and cytochrome c. Complex I and III and cytoplasmic reductase also remove protons from the cytoplasm, which results in an overall contribution of 6 protons per electron pair to the proton motive force (PMF). Figure from Chen and Strous (2013).*

Nitrate Reductase (Nar/Nap)

The first denitrification step is catalysed by the dissimilatory nitrate reductases Nar or Nap. These enzymes are members of the vast family of molybdopterin oxidoreductases and can be found in the cytoplasm (NarGH) or the periplasm (NapAB). Some organisms have both, while others have only one (Richardson et al., 2001).

$$NO_3^- + 2\,H^+ + 2\,e^- \rightarrow NO_2^- + H_2O$$

NarGH conserves more energy than NapAB due to the extra consumption of protons from the cytoplasm (Bertero et al., 2003). For NapAB, the energy is only conserved through complex I (Richardson, 2000; Simon et al., 2008). In some versions of the complex, NarGH is located in the periplasm but coupled with a complex III-like cytochrome *b* subunit which allows the conservation of energy (Martinez-Espinosa et al., 2007).

Nitrite Reductase (Nir)

The reduction of NO_2^- to NO can be catalysed by two structurally different enzymes: cd_1 nitrite reductase and cobber-type nitrite reductase, encoded by *nirS* and *nirK*, respectively, and both are located in the periplasm (Godden et al., 1991; Shapleigh, 2006).

$$NO_2^- + 2\,H^+ + e^- \rightarrow NO + H_2O$$

As electron donors, both cytochrome *c* and small copper proteins can be used (Koutný et al., 1999; Moir et al., 1993; Shapleigh, 2006). Neither of the enzymes can contribute to proton motive force (PMF) directly due to their periplasmic localization (Chen & Strous, 2013).

Nitric Oxide Reductase (Nor)

The next step of the denitrification is reduction of NO to N_2O, which is performed by the nitric oxide reductases (Nor).

$$2\,NO + 2\,H^+ + 2\,e^- \rightarrow N_2O + H_2O$$

There are three different types of Nor, distinguished by their electron donor: qNor, which is encoded by *norZ* and accepts electrons from quinols, cNor, which is encoded by *norBC* and accepts electrons from cytochrome *c*, and the less common qCu_ANor, which can accept electrons from both menaquinol and cytochrome *c* (Hino et al., 2012; Matsumoto et al., 2012; Suharti et al., 2004). The Nor enzymes are capable of oxygen reduction as well as nitric oxide reduction, the only difference is the affinity. For each N_2O molecule made, two molecules of NO and two electrons are required (Chen & Strous, 2013).

Nitrous Oxide Reductase (Nos)

The final step of denitrification is the reduction of N_2O to N_2 gas, which is only possible with the enzyme nitrous oxide reductase (Nos). Nos is a periplasmic homodimer encoded by *nosZ* and is the only enzyme which reduces N_2O under physiological conditions (Berks et al., 1995).

$$N_2O + 2\,H^+ + 2\,e^- \rightarrow N_2 + H_2O$$

Two different clades of NosZ are found, called clade I and clade II (Sanford et al., 2012). There are genomic differences between the two clades (Hallin et al., 2018), and physiological differences regarding affinity to N_2O and reduction rates are also reported (Yoon et al., 2016).

NosZ consists of two copper centres, Cu_A and Cu_Z, where the latter is unique for NosZ. Cu_A is a common copper centre situated at the N-terminal. Its responsibility is the electron transfer from cytochrome *c* to Cu_Z, which is a copper centre situated at the C-terminal and is the catalytic site. Within the same monomer, the distance between Cu_A and Cu_Z is 40 Å, which is too far for electron transfers. Therefore, the homodimers are arranged head-to-tail, where one of the monomers' N-terminal domain will interact with the other monomer's C-terminal domain and vice versa, reducing the distance between Cu_A and Cu_Z to 10 Å, resulting in efficient electron transfers. The reaction occurs in the periplasm, resulting in no contribution to the formation of a PMF and no conservation of energy (Schneider et al., 2014).

1.2.3 Thermodynamics of Denitrification

From a theoretical thermodynamic point of view, NO_3^- and oxygen are nearly equally good electron acceptors, and the redox potential is quite similar. However, regarding bioenergetics and kinetics, oxygen is a better electron acceptor than NO_3^- due to the much higher amount of energy conserved through aerobic respiration compared to denitrification. During aerobic respiration, up to ten protons are translocated as opposed to a maximum of six protons during denitrification, a difference caused by the fact that no denitrification modules translocate protons (Flock et al., 2009), except from Nar (Chen & Strous, 2013).

The other disadvantage of denitrification is in regard to kinetics, as it requires several different enzyme complexes, as well as the space in the membrane and periplasm is restricted. This restricted space leads to a smaller amount of each complex per cell and, thus, a lower maximum substrate conversion rate and increased distances between electron donors and acceptors (Chen & Strous, 2013). Due to the difference in energy yield, it makes sense for denitrifying bacteria to suppress denitrification in the presence of oxygen, which is what is generally observed.

1.2.4 Regulation of Denitrification

As established above, aerobic respiration yields more energy than denitrification. Therefore, strict regulation of denitrification in facultative anaerobes is likely a fitness trait. In line with this, all of the reductases described in section 1.2.2 are regulated on a transcriptional level responding to intra- and extracellular signals such as oxygen and N-oxide concentrations (Strohm et al., 2007). Moreover, coordination of the N-oxide reductases is essential to prevent the accumulation of toxic intermediates like NO (Baumann et al., 1997).

Regulatory Proteins and Oxygen Signalling

The expression of denitrification genes is regulated by O_2 and the presence of N-oxides via two-component systems or factors belonging to the cyclic-AMP receptor protein/fumarate and nitrate reductase (Crp/Fnr) family of transcriptional regulators. The details of how the regulation is organised vary in different organisms. In the regulation of denitrification genes of the model organism *Paracoccus denitrificans* (Fig. 1.3), there are three Fnr-type regulators: FnrP, NarR, and NNR (Van Spanning et al., 1997). The former controls the oxygen-dependent transcription activation, the second controls nitrate reduction and the latter control the expression of genes encoding the reductases Nir and Nor. FnrP is sensitive to oxygen, while NarR is sensitive to NO_3^- and NO_2^-, and NNR is sensitive to both oxygen and NO (Wood et al., 2001)

The cells will start building their denitrification proteome when the O_2 concentration falls below a set threshold. However, if the O_2 is suddenly removed, the cells cannot synthesise the denitrification enzymes as energy from O_2 is needed, resulting in the cells being entrapped in anoxia. Rapid sensing of decreasing O_2 levels is therefore crucial for survival (Højberg et al., 1997). When the cells sense the low O_2 concentration, activation of FnrP is induced. The activation of FnrP, along with the presence of NO_3^- or NO_2^-, or both, will, in turn, activate NarR. Further, NarR induces transcription of the *nar* gene, encoding Nar. NNR is activated by rising NO concentrations and will induce the transcription of *nirS*, encoding Nir. The transcription of *nor*, encoding Nor, is induced by NO via NNR. Transcription of *nosZ*, encoding Nos, on the other hand, is induced by NNR and FnrP, and not the N_2O concentration directly (Bergaust et al., 2012). The transcription of *nar* and *nirS* become autocatalytic as their activity produces the intermediate, which also induces their transcription (Hassan et al., 2014).

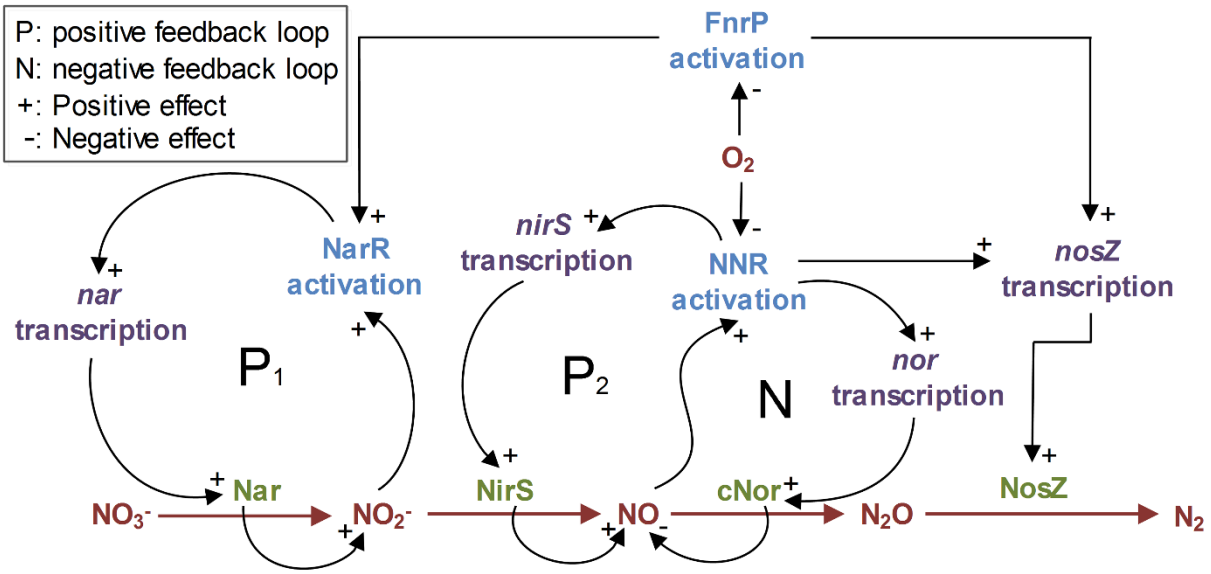

Figure 1.3 Schematic Diagram of Regulatory Network in P. denitrificans. *Figure from Hassan et al. (2014).*

It becomes evident that O_2 is a crucial regulator of denitrification, as high O_2 concentrations generally inactivate the entire denitrification pathway and make the bacteria switch to aerobic respiration (van Spanning et al., 2007). Over time, a population grown in oxic environments will result in a destroyed denitrification proteome as the enzymes will be diluted for each generation. If the environment turns anoxic, the cells must start the energy-costly rebuilding of their denitrification apparatus. In other words, having an intact denitrification proteome is only rewarding if the anoxic conditions remain over time, which the organisms have no way of predicting, resulting in a bet-hedging strategy to increase the overall fitness of the species across generations at the expense of the fitness of the current generation (Lycus et al., 2018; Veening et al., 2008).

1.2.5 Physiology of Denitrifiers in Natural Environments

From an environmental perspective, it is interesting to understand what makes denitrification go all the way to N_2 and what is causing the accumulation of intermediates, especially the greenhouse gas N_2O, as it contributes to global warming and the destruction of the ozone layer (Ravishankara et al., 2009). Much of the atmospheric N_2O originates from anthropogenic activity, and about half of the anthropogenic N_2O emission comes from cultivated soil (Stehfest & Bouwman, 2006). Agriculture affects N_2O emissions through drainage, liming, tillage, fertilization, and cropping, but other factors like climate and soil type also play a role (Bakken et al., 2012).

It is not the agriculture itself which leads to emissions of N_2O, but rather the microbial processes involved in the transformation of the nitrogen from fertilizers, such as nitrification and denitrification. Nitrification has a low N_2O/NO_3^- product stoichiometry, suggesting denitrification is a more potent N_2O source (Mørkved et al., 2007). An important factor when investigating the emissions is the N_2O / (N_2 + N_2O) product ratio of denitrification, as it is an indication of how much N_2O is emitted compared to N_2, which is the final product of complete denitrification. Establishing the N_2O/N_2 ratio can be challenging *in situ* compared to simple systems like pure cultures. Especially measuring N_2 production is challenging, but understanding it is crucial when developing ways to mitigate N_2O emissions (Bakken et al., 2012).

The emission of N_2O due to denitrification is also affected by factors in the natural environment, such as oxygen and pH (Liu et al., 2014; Liu et al., 2010). In the model organism *P. denitrificans*, all cells can express the *nosZ* gene, which encodes Nos. However, in slightly acidic soil (pH 6), the last step of denitrification does not take place. The lack of reduction to N_2 leads to N_2O emission, even though both the *nirS* and *nosZ* genes are expressed at the same rate as during pH 7. Bergaust et al. (2010) showed that even a slight decrease in pH from 7 (the optimal pH of denitrification) to 6 was enough to inhibit the protein synthesis and assembly of N_2O reductase, thus leading to a high N_2O/N_2 product ratio. As the relevant genes were expressed, this suggests the affected part of Nos is the post-translational regulation rather than the expression itself (Bergaust et al., 2011; Bergaust et al., 2010).

As well as being affected by pH, the Cu_Z copper-centre of Nos is oxygen sensitive, which previously was said to lead to incomplete denitrification as the final step of denitrification cannot happen in the presence of oxygen. The result is the emission of N_2O during so-called aerobic denitrification. However, a recent study by Wang et al. (2023) shows that the denitrifiers can develop a defence mechanism, which will theoretically lead to continuous reduction of N_2O to N_2 in the presence of oxygen. Natural environments where denitrifying bacteria exist are rarely anoxic permanently, which would result in low concentrations of NO_3^- and NO_2^- over time. Oxygen fluctuates, and it is therefore essential for denitrifiers to be able to keep their respiratory metabolism. If not, they might find themselves trapped in anoxia with little to no available electron acceptors, resulting in insufficient energy for protein synthesis. Another outcome is the accumulation of NO to a toxic level, which will lead to the death of the bacteria (Bergaust et al., 2010; Højberg et al., 1997; Richardson, 2000).

1.3 Applications of Denitrification

Denitrification can be utilized in a broad range of biotechnological processes. The most common application of denitrification is in the process of wastewater treatment. A novel invention explores the possibility of using denitrifying bacteria to produce single-cell proteins by anaerobic high-cell-density cultivation.

1.3.1 Wastewater Treatment

Denitrification plays an important role in returning reactive nitrogen species to the atmosphere, removing biological nutrients, and improving water quality (Grady Jr et al., 2011). By combining nitrification and denitrification, nitrogen can be removed from wastewater using the activated sludge process. Generally, the activated sludge process can be divided into two systems, either a single sludge system where the sludge is sent through a series of aerobic and anaerobic tanks, where nitrification and denitrification take place respectively, or a multi-sludge system where carbonaceous oxidation, nitrification, and denitrification are carried out in separate tanks. A third, modified process is the Bardenpho process which consists of five stages: fermentation, anoxic denitrification, oxic nitrification, anoxic denitrification, and finally, re-aeration (Pepper et al., 2015a).

More recently, anammox and comammox have been discovered, and their potential in wastewater treatment, as well as the phenomenon known as aerobic denitrification, assuming complete reduction to N_2, or else there would be a considerable risk of N_2O emissions. Aerobic denitrification is particularly interesting, as the nitrogen removal will be achieved in one step in contrast to the previously described methods of nitrification and denitrification in designated tanks. With bacteria performing aerobic denitrification, the nitrogen can be removed in an oxic tank with supplied organic carbon (Xi et al., 2022).

1.3.2 Production of SCP by Anaerobic HCDC

The population in the world is constantly increasing, leading to an increased demand for food and feed. As a supplement to conventional protein sources, single-cell protein production by high-cell-density cultivation is an alternative, which has recently been shown to be possible using denitrifying bacteria (Bergaust et al., 2022).

Single-Cell Proteins (SCP)

Single-cell proteins (SCP) originate from dried cells from microorganisms (fungi, algae, and bacteria). The exploitation of such microorganisms is relatively inexpensive as the microorganisms utilize waste products as their source of energy and carbon. SCP has a high content of vitamins, essential amino acids, proteins, and lipids, making them suitable for food and feed, especially the latter (Huang & Kinsella, 1986; Nasseri et al., 2011).

High-Cell-Density Cultivation (HCDC)

High-cell-density cultivation (HCDC) is the cultivation of microorganisms (bacteria, archaea, and yeast) in high densities. The exact density needed to classify as high density varies as the lower limit ranges from 20-50 g dw L^{-1} to 100 g dw L^{-1}, and in extreme cases, as high as 200 - 300 g dw L^{-1} (Riesenberg & Guthke, 1999; Subramaniam et al., 2018). HCDC was primarily established to produce SCP, ethanol, and biomass using yeast but was later applied for other microorganisms and productions, such as antibiotic production using dense bacterial cultures of streptomycetes (Suzuki et al., 1987). HCDC has also been used for the production of high concentrations of biomass, using fermentation technology and *Escherichia coli* (Kleman & Strohl, 1994; Lee, 1996; Riesenberg, 1991). There is an increasing industrial demand for food, feed, and medicine. Thus, more research is needed regarding HCDC's biotechnological potential (Riesenberg & Guthke, 1999).

AnaPro – SCP Production by Anaerobic Respiration

Under conventional, aerobic HCDC, oxygen becomes rate-limiting as oxygen has very low solubility in liquid (Garcia-Ochoa & Gomez, 2009). Further, this can result in anaerobic conditions and fermentation. An alternative to the conventional, aerobic HCDC is anaerobic HCDC using denitrifying bacteria (Bergaust et al., 2022).

By doing so, the rate-limiting step of oxygen transfer is removed as the electron acceptor is provided as NO_3^- dissolved in liquid rather than O_2 gas. A potential problem of doing so occurs if NO_3^- is provided as a salt, resulting in alkalization of the medium and salt accumulation. To avoid this, NO_3^- is provided as HNO_3, avoiding the accumulation of salt and maintaining the pH and NO_3^- concentration within an acceptable range.

The principle of the anaerobic HCDC is to supply the stirred culture with HNO_3 and minerals through an acid pump and glucose as a carbon source through a glucose pump to balance the growth of the cells (Fig. 1.4). The pumps are programmed by a given setpoint which triggers the supply when reached. In that way, the cells will always have access to both electron acceptors (NO_3^-) and carbon (glucose), resulting in the following loop:

$$Denitrification \rightarrow Reduction\ of\ NO_3^- \rightarrow Increase\ in\ pH$$
$$\rightarrow Triggering\ the\ Acid\ Pump\ and\ Glucose\ Pump$$
$$\rightarrow Addition\ of\ HNO_3\ and\ Glucose \rightarrow Denitrification$$

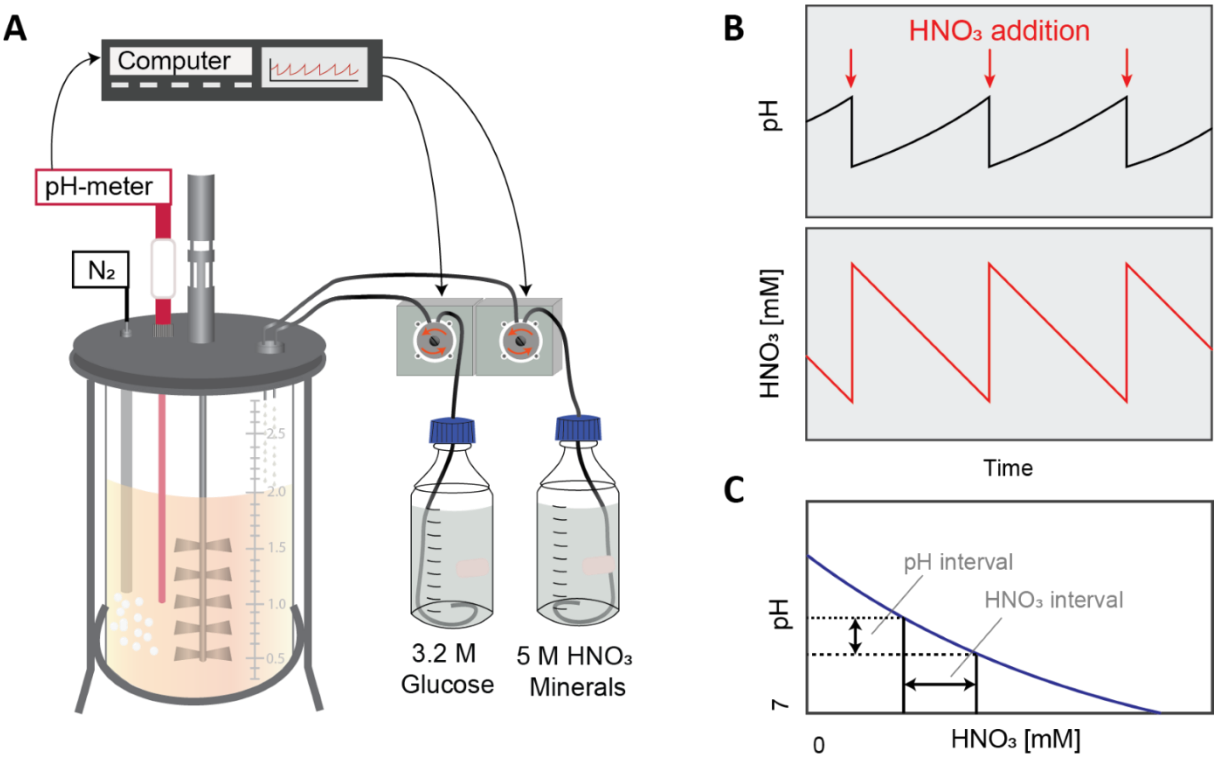

Figure 1.4 Principle of Anaerobic HCDC. *A) Experimental Setup B) Supply of HNO_3 based on pH C) pH and HNO_3 concentration interval based on a titration curve. Figure adapted by Marte M. Maråk, based on figure by Linda Bergaust.*

1.4 Optimization of Industrial Processes

The anaerobic HCDC process described under AnaPro is still under development, and optimization is still needed. Two main challenges are 1) the so-called "CO_2 problem" of how CO_2 affects the pH and 2) how oxygen leakage affects the denitrifying bacteria.

1.4.1 Carbonate Chemistry in a pH-stat for HCDC

During anaerobic HCDC, the pH increases when the cells are denitrifying, and CO_2 is produced. However, when CO_2 is dissolved in water, the pH is lowered due to carbonic acid formation (Appelo & Postma, 2004).

$$CO_2(aq) + H_2O \leftrightarrow H_2CO_3$$

$$H_2CO_3 \leftrightarrow H^+ + HCO_3^-$$

$$HCO_3^- \leftrightarrow H^+ + CO_3^{2-}$$

Changes in pH trigger the acid pump of the pH-stat. The challenge is that the net pH increase is too small as denitrification increases the pH, but dissolved CO_2 lowers it, resulting in a minimal change in pH. Without the supply of HNO_3, the cells will stop growing when NO_3^- is depleted. Eventually, the CO_2 will be "blown out", and the pH will further increase and trigger the acid pump, resulting in the addition of HNO_3, and denitrification will resume.

However, this pause in cell growth and denitrification makes the process less efficient than it theoretically could be. The actual loop observed is:

$$Denitrification \rightarrow Reduction\ of\ NO_3^- + Production\ of\ CO_2 \rightarrow Minimal\ Change\ in\ pH$$
$$\rightarrow Depletion\ of\ NO_3^- \rightarrow Cell\ Growth\ Stops$$
$$\rightarrow Eventually\ CO_2 is\ \text{blown out} \rightarrow Increase\ in\ pH$$
$$\rightarrow Acid\ Pump\ is\ Triggered \rightarrow Addition\ of\ HNO_3 \rightarrow Denitrification$$

1.4.2 Sensitivity to Oxygen in HCDC

One of many factors to consider when choosing an organism for HCDC is its sensitivity to potential oxygen leakages. There are presumably differences in both the threshold for when denitrification ceases and the amount of N_2O emitted. Aerobic denitrifiers have the potential and could eliminate this problem, as oxygen fluctuations would be tolerated.

Multiple studies by Robertson & Kuenen (1983; 1984; 1985) claim that *Paracoccus pantotrophus* can perform aerobic denitrification, suggesting that the generally oxygen-sensitive Nos enzyme may exist in different forms, where some of them are not sensitive to oxygen. This conclusion is based on the observation of N_2 as one of the end products after denitrification in an environment with >80% O_2 saturation. On the other hand, Chen and Strous (2013) explain this with the fact that actively respiring bacteria can effectively consume oxygen and keep the oxygen concentration low, or this could be due to flaws in the experiments, such as insufficient stirring or aggregation of the bacteria. They further conclude that aerobic denitrification does not make sense bioenergetically as the most considerable electron flow is to complex IV rather than N-oxide reductases, and aerobic respiration is preferred over denitrification regarding growth.

1.5 Aim and Outline of Thesis

This thesis had two main aims: The first was to find a way to solve the so-called "CO_2 problem" of how CO_2 affects the pH during anaerobic HCDC. The second aim was multi-pronged: to investigate whether a so-called aerobic denitrifier continues complete denitrification if exposed to hypoxic and oxic conditions and compare it to an organism known not to perform aerobic denitrification. This has implications for our understanding of the effect of oxygen fluctuations in complex systems vis a vis N_2O emissions and for the choice of an organism for HCDC regarding tolerance for oxygen leakages. In an attempt to do so, the two closely related species of denitrifying bacteria were investigated and compared: The model organism *P. denitrificans* (strain Pd1222) and the believed aerobic denitrifier *P. pantotrophus* (type strain GB17; DSM 2944).

P. denitrificans was first isolated in 1910 by Beijerinck and Minkman (1910), who gave the bacterium the name *Micrococcus denitrificans*. In 1969 it was renamed *P. denitrificans* by Davis et al. (1969). Pd1222 is a genetic modification of the *P. denitrificans* type strain DSM413^T with enhanced conjugation frequencies (De Vries et al., 1989). *P. pantotrophus* was formerly known as *Thiosphaera pantotropha* (Robertson & Kuenen, 1984) but was reassigned to the new species *P. pantotrophus* in 1999 (Rainey et al.). Both organisms are gram-negative bacteria said to be facultatively chemolithoautotrophic, nonmotile and able to use reduced sulphur compounds and organic compounds under aerobic and anaerobic conditions (Ludwig et al., 1993).

Prior to the main experiments, preliminary experiments were done to establish factors like cell count, optical density and dry weight. Further, the first main experiment with CO_2 was conducted to establish the influence CO_2 has on the pH. Finally, the second main experiment was done by monitoring the chosen bacterial strain under denitrification and how oxygen fluctuations affect the accumulation of NO, N_2O and N_2, as well as monitoring the activity of the N-oxide reductases.

2 Materials and Methods

2.1 Bacterial Strains

The bacteria used in the experiments were *P. denitrificans* (strain Pd1222) and *P. pantotrophus* (type strain GB17). Glycerol stocks of both strains were made by mixing 700 µL of a dense, late-exponential culture with 300 µL of 50% glycerol in cryotubes. The glycerol stocks were kept at -80°C for long-term storage and at -20°C for short-term storage. After thawing, an entire glycerol stock was added directly to the desired growth medium for each new experiment.

2.2 Medium and Cultivation Conditions

2.2.1 Sistrom's Medium and Preparation of Aerobic Vials

In all experiments, unless otherwise stated, a modified version of Sistrom's medium A (Sistrom, 1960) was used as a growth medium. The original version (Appendix A1) includes carbon sources such as succinate, L-glutamic acid and L-aspartic acid. However, the carbon source was excluded from the basal stock (10x concentrated) in the version used in these experiments (Appendix A2). The medium was prepared in 10x stocks and kept at -20°C. Due to precipitation, drops of 5 M HCl were added until the solution cleared. The finished medium was prepared by diluting the 10x solution in distilled MQ water and adjusting the pH to 7.0 by stepwise addition of 10 M KOH. The medium was distributed into 120 mL serum vials (50 mL each). One PFTE triangular stirring bar (35 X 9 mm, VWR 442-0388) was added to each vial before autoclaving. Glucose syrup (sterile filtered, 3.125 M stock) was added to a final glucose concentration of 20 mM before inoculation.

2.2.2 Preparation of Anaerobic Vials

The vials were sealed for the anaerobic parts of the experiments, and the atmosphere was replaced with He-gas. This process is called He-washing and is accomplished by replacing the protective aluminium foil on the autoclaved vials with sterile butyl-rubber septa and sealing them with aluminium crimp caps. With a system consisting of an Edwards vacuum pump, valves connected to a He-line and a vacuum line, cycles of evacuation and He-filling were performed. The vials were placed on a magnetic stirrer to ensure optimal gas exchange between liquid and headspace, and needles were used to pierce the septa.

The vials were repeatedly evacuated and then filled with helium in seven cycles of 180 s evacuation and 30 s He-filling. The He-washing resulted in three orders of magnitude lowering of N_2 and O_2 concentrations. The final He-filling resulted in an overpressure, which was removed by piercing the septa with a needle attached to a syringe filled with ethanol after the vials had been equilibrated to the desired temperature (Molstad et al., 2007).

2.2.3 Cultivation Conditions

P. denitrificans has an optimum growth temperature of approximately 37°C (Hahnke et al., 2014; Nokhal & Schlegel, 1983). *P. pantotrophus* share the same optimum growth temperature (Vikromvarasiri et al., 2015). All cultivations were done in temperature-controlled water baths. The temperature was set lower than the optimum growth temperature, ranging from 17 - 30°C, to make the cells grow slower. The decreased growth rate allowed harvesting of the cells in the exponential growth phase and at specific optical densities and resulted in a higher resolution data set when monitoring the gas kinetics in the robot incubation system described in section 2.3.1.

In order to adapt cultures to anoxic conditions and denitrification, transition cultures were made. These were made by inoculating the desired strain to an oxic vial and incubating until a late-exponential culture was reached. Then 1 mL of the culture was transferred to a capped vial with hypoxic conditions (1% O_2 in headspace) and 4 - 5 mM of either NO_3^- or NO_2^-. The addition of NO_3^- or NO_2^- ensured that the cells had enough energy from O_2 to be used to synthesise the denitrification enzymes, thus resulting in a culture where most of the population carried a full-fledged denitrification proteome (Lycus et al., 2017).

2.2.4 Fixation of Cells

Formalin preserves the proteins of the cell, and the cell will be preserved in the same condition as it was at the time of sampling. In some experiments, the cells were fixated with formalin (37% w/v formaldehyde). When fixating cells, 1 800 µL of the culture was mixed with 200 µL formalin to a final concentration of ~ 4% w/v formaldehyde. The fixated cells were stored at 4°C until further research, in general, within five days.

2.3 Analytical Methods

2.3.1 Robot Incubation System

A robotized incubation system designed and built in-house was used to monitor the concentration of gases during the experiments (Fig. 2.1). This incubation system allows studies of the gas kinetics in multiple vials simultaneously in a thermostatic water bath. Magnetic stirring was used in all liquid cultures to ensure full gas exchange between the headspace and liquid phase. The stirring speed was set to 600 rpm unless otherwise stated. In addition to stirred cultures, calibration standards called "Low" (ambient air: 21% O_2, 78% N_2), "NO" (25 ppm NO in N_2) and "High" (1% CO_2 and 151 ppm N_2O in Helium) were used in the robot incubation system.

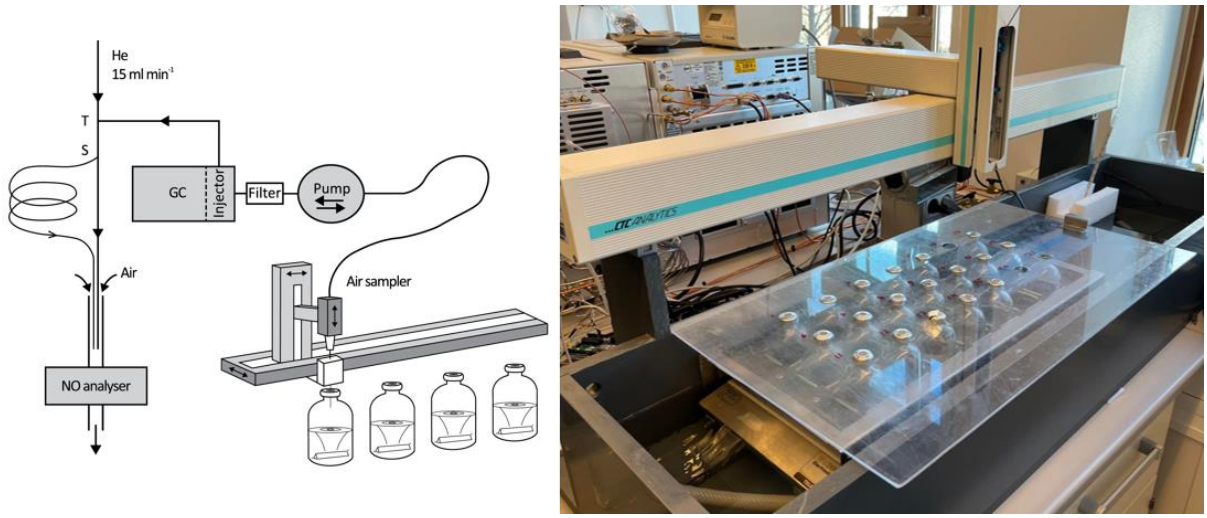

Figure 2.1. Robot Incubation System. *Left: Schematic diagram of the robot incubation system, showing the gas flow to the gas chromatograph and NO-analyser. Figure from Molstad et al. (2007). Right: The newest robot at the lab of a total of three robots. This specific robot incubation system can take 21 vials simultaneously in a temperature-regulated water bath, where 15 vials are placed at a magnetic stirrer plate, and six vials are placed without stirring.*

Samples from the headspace of the vials are taken by a CTC GC-PAL autosampler, replacing the volume sampled with helium gas and ensuring constant pressure. The autosampler is connected to an Agilent 7890A gas chromatograph equipped with three detectors (TCD, FID and ECD) and two PLOT columns, one for separation of N_2 and O_2 and one for separation of CH_4, N_2O and CO_2. The gas chromatograph determines the concentration of O_2, CO_2, N_2 and N_2O, and the sample flows through a chemiluminescence NO analyser to determine NO concentration (Molstad et al., 2007).

The principle of the NO analyser is described further in section 2.3.3. The data (peak areas) were sorted by gas, vial and time stamps using a Python script and exported to .xlsx format for further analysis in Excel using a KinCalc spreadsheet as described in the following section.

2.3.2 KinCalc

KinCalc[1] is an Excel spreadsheet for analysing gas data sets made by Professor Lars Bakken (NMBU). In all robot experiments done as a part of this master's thesis, the September 2022 version of KinCalc was used to analyse the gas data. In a master sheet, the user fills the pH and temperature, and NO_2^- and NO_3^- values can be filled in by interpolation. Additional information and experimental set-up are written in a dedicated sheet, making KinCalc suitable for integrating offline experimental data.

The data sorted by time, gas and vial for each incubation experiment were imported into an empty KinCalc file. The three gas standards used in the robot incubation system were used to calibrate the KinCalc spreadsheet by converting the peak areas to ppm and to determine the leakage factor, sampling volume and dilutions due to replacing the sampled volume with He-gas during the experiment. The temperature-dependent solubility of gases was used to calculate liquid concentrations of gases at each timepoint, assuming 1 atm pressure (Wilhelm et al., 1977) and taking the transport rate between the gas and liquid phase into account. For CO_2, the solubility is also a function of pH (Appelo & Postma, 1993). After calibration, the KinCalc spreadsheet facilitates detailed gas kinetics analyses, such as aerobic/anaerobic respiration, growth rates, and stoichiometry of substrates vs intermediates and products.

2.3.3 Nitrite Measurements and the Nitric Oxide Analyzer (NOA)

NO_2^- was analysed with a Sievers Nitric Oxide Analyzer (NOA) 280i. The NOA enables the quantification of NO_2^- in the low µM to mM scale after reduction to NO. 10 µL of the sample was injected through the rubber septa that seals a purging vessel containing reducing agent, sodium iodide (NaI) in 50% acetic acid, with a constant flow of N_2 (Fig. 2.2). NO_2^- will then be reduced to NO. With the inert N_2 bubbles in the reducing agent, the NO gets carried through the system and into the NOA. By chemiluminescence, NO reacts with ozone to produce O_2 and NO_2* in an excited state.

[1] Available for all at https://www.nmbu.no/en/research/groups/nitrogen/spreadsheets-

When the excited NO_2* returns to its ground form, it emits light which is converted from photons to electrical signals by a photomultiplier and then the electrical signals are detected by the computer (Rümer et al., 2016). As the outcome of the NOA is peak areas, a standard curve was needed to convert the peak areas to NO_2^- concentrations in mM. A dilution series of KNO_2 with known concentrations were made and injected into the NOA three times for each dilution to create a standard curve (Appendix B1). The dilution series consisted of KNO_2 in the following concentrations: 0 mM, 0.1 mM, 0.5 mM, 1.0 mM, 5.0 mM, 10 mM and 50 mM in MQ H_2O.

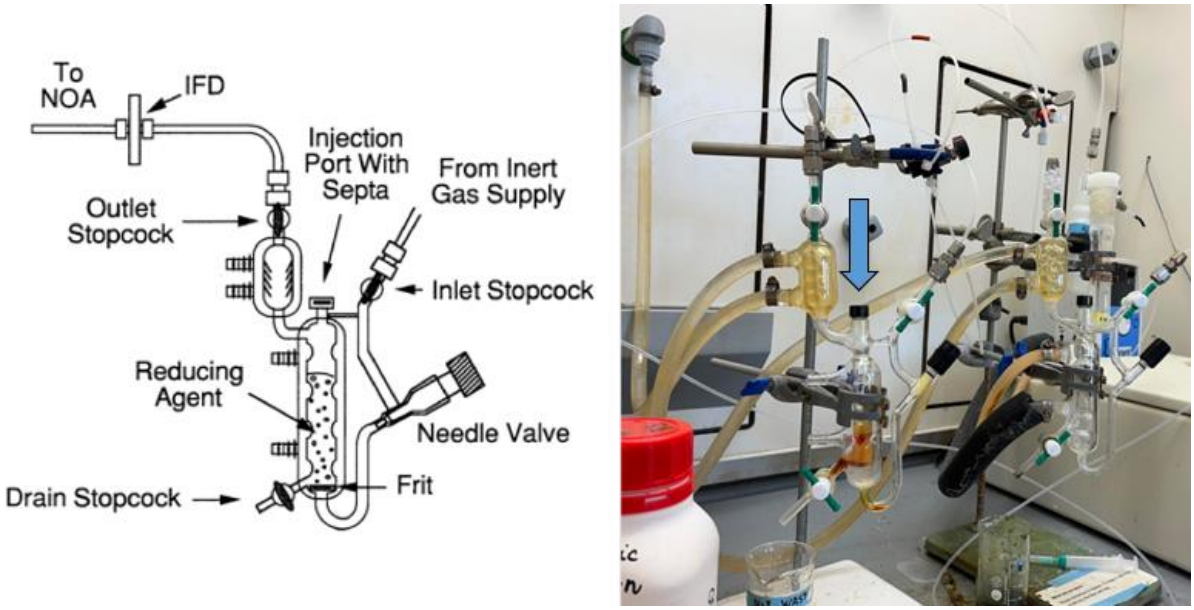

Figure 2.2. Nitric Oxide Analyzer (NOA) System. *Left: Schematic diagram of purge vessel for nitrite reduction. The sample is injected through the injection port with septa. Figure from Sievers Nitric Oxide Analyzer NOA 280i Operation and Maintenance Manual. Right: The complete setup of the NOA apparatus. The injection port with septa is marked with a blue arrow.*

2.3.4 Optical Density Measurements (Spectrophotometry)

The cultures' optical density (OD) was measured to evaluate the cell density in growing cultures. When measuring the OD of the samples, 1 mL of the culture was transferred to a cuvette and placed in a spectrophotometer to measure the cell density based on light scatter. The wavelength was set to λ = 660 nm unless otherwise stated. For samples with an OD_{660} above 1.00, a 10x dilution was made and measured as the sample will be too concentrated for the spectrophotometer to give an accurate measurement as the upper limit for the linear range is reached.

2.3.5 Bürker Counting Chamber (Haemocytometry)

A Bürker counting chamber (haemocytometer) was used to count cells manually under a microscope. 10 µL of the sample was applied into a Bürker counting chamber under a microscope with a 40x objective and PH2. Depending on which square was used for counting, the number of cells counted in the square was multiplied by the respective factor listed in Table 2.1 to give the estimated number of cells mL^{-1} to the corresponding OD_{660} value. For all samples, ten squares were counted, and the mean was calculated.

Table 2.1 Calculation of Cells mL^{-1} by Haemocytometry. *Based on the square type used for counting the cells, different equations to calculate the cells mL^{-1} were used. Table retrieved from lab protocol by Skaar and Aasen (2021).*

Square	Volume (mm^3)	Calculation of Cells mL^{-1}
A	1/10	(#cells in square A · 10) · 10^3
B	1/160	(#cells in square B · 160) · 10^3
C	1/1000	(#cells in square C · 1000) · 10^3
D	1/4000	(#cells in square D · 4000) · 10^3
E	1/250	(#cells in square E · 250) · 10^3

2.3.6 Flow Cytometry

Flow cytometry is a method to analyse single cells in solution. This rapid method produces scattered fluorescent light signals with lasers as light sources. It has detectors to read the light signals and convert them to electronic signals analysed by a computer (McKinnon, 2018). The flow cytometer used was the CellStream™ Flow Cytometer by Sigma-Aldrich. The software used for analysis was the associated CellStream™ Analysis Software. The channels used were:

Forward scatter: FSC – 456/51 – D2

Side scatter: SSC – 773/56 – A1

SYBR®Green positives: 488 – 528/46 – C3

Figure 2.3 below illustrates an example of the gating used for all flow cytometry experiments.

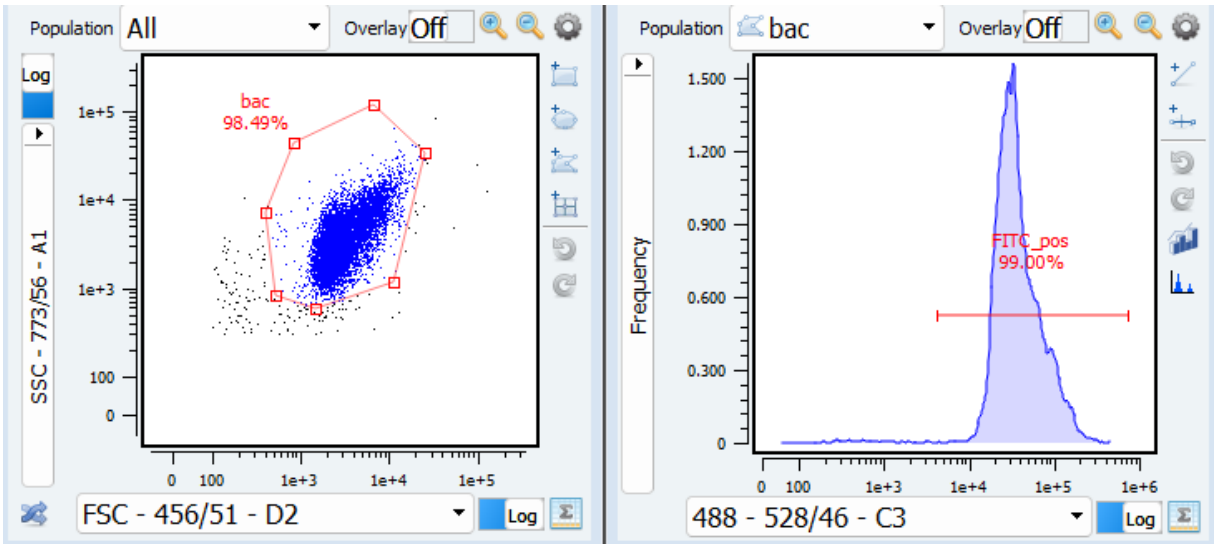

Figure 2.3 Channels and Gating for Flow Cytometry. *A typical result regarding the gating of bacteria out of all particles (left) and* SYBR®Green *positive (FITC_pos) cells out of the defined bacteria (right).*

The flow cytometry experiments used both aerobically and anaerobically raised cells of Pd1222 and GB17. Prior to running the samples through the flow cytometer, OD_{660} was measured, 10x dilutions were made, and the cells were fixated with formalin. Some were left unstained, while most were stained using SYBR®Green by Molecular Probes™ and incubated in the dark for 20 min before flow cytometry. As the optimal concentration of both cells and SYBR®Green was unknown, different combinations of dilutions were made and tested. SYBR®Green was originally in the concentration 10 000x in DMSO (dimethyl sulfoxide). For further use, new Eppendorf tubes were prepared with diluted SYBR®Green to the concentration of 100x. Then SYBR®Green was tested in 0.5x, 1x and 5x final concentrations combined with undiluted and 10x diluted cells, as shown in Table 2.2.

Table 2.2 Ratio of SYBR®Green and Cells. *The table shows how much SYBR®Green was used in different concentrations for undiluted and diluted cells.*

	SYBR®Green Concentration		
	0.5x	1x	5x
Undiluted cells	2.5 µL SYBR®Green 497.5 µL cells	5 µL SYBR®Green 495 µL cells	25 µL SYBR®Green 475 µL cells
10x diluted cells	2.5 µL SYBR®Green 497.5 µL cells	5 µL SYBR®Green 495 µL cells	25 µL SYBR®Green 475 µL cells

The samples were then inserted into the flow cytometer, and the events s^{-1} was monitored. The desired events s^{-1} was around 300 - 400. When the events s^{-1} were higher, the sample needed to be diluted either 10x or 100x.

2.3.7 Dry Weight Determination

For dry weight determination, cells were harvested by centrifugation at 10 000 rcf in 10 min and 10°C. Pellets were washed twice in filtered Milli-RO water before they were resuspended in 1 mL of filtered Milli-RO water in Eppendorf tubes and placed in a heating cabinet at 100°C until the water was evaporated to constant weight. Clean Eppendorf tubes were also placed in the heating cabinet to follow the natural weight loss of the tubes due to the heat. All of the tubes were weighed before adding the cells and after the incubation in the heating cabinet to calculate the actual dry weight of the cells (g L^{-1} OD_{660}^{-1}).

2.3.8 Glucose Measurements

The glucose measurements were performed using an ab65333 Glucose Assay Kit from abcam. This kit contains a Glucose Assay Buffer, Glucose Probe, Glucose Enzyme mix and Glucose Standard (100 nmol μL^{-1}). Prior to the assay, the Glucose Assay Buffer was equilibrated to room temperature. The Glucose Probe was placed on a 37°C heat block for 1 - 5 min. The Glucose Enzyme Mix was reconstituted in 220 µL Glucose Assay Buffer and kept on ice during the assay. The Glucose Standard was diluted to 1 nmol μL^{-1} and used to make six standards ranging from 0 nM to 10 nM with 2 nM intervals. These standards were used to make a standard curve (Appendix B2).

A reaction mix was made by mixing 46 µL Glucose Assay Buffer, 2 µL Glucose Probe and 2 µL Glucose Enzyme Mix per sample. On a 96 Well Titer plate, 50 µL reaction mix and 50 µL sample or standard were added to each well. For each sample and standard, duplicates were made. The 96 Well Titer plate was then placed in a Varioskan LUX Multimode Microplate Reader by ThermoFisher, and the wavelength was set to λ = 570 nm. The average of the duplicate readings was calculated to find the glucose concentration in the samples. The mean absorbance value of the blank was then subtracted from all other samples. Based on the trendline from the standard curve (Appendix B2), the values from the corrected absorbance were multiplied by this factor along with the dilution factor.

2.4 Molecular Methods

2.4.1 Purification of DNA

The QIAmp DNA Mini Kit from Qiagen was used for cell lysis and DNA purification. Cell pellets (approximately $3.09 \cdot 10^8$ - $1.33 \cdot 10^9$ cells) were thawed at room temperature and resuspended in 100 µL of tissue lysis buffer (Buffer ATL). Then 20 µL of proteinase K (20 mg mL^{-1}) was added to the sample and mixed by vortexing prior to incubation at 56°C for 1 hour. The sample was then centrifuged to collect the drops. 4 µL of RNase A (100 mg mL^{-1}) was added to the sample and mixed by vortexing in pulses for 15 s. Following was a 2 min incubation at room temperature. Another centrifugation was performed, and then 200 µL of lysis buffer (Buffer AL) was added to the sample. A similar pulse-vortexing was done, and the sample was incubated at 70°C for 10 min. 200 µL of absolute ethanol was added to the sample and mixed. The mixture was then applied to the QIAmp Mini spin column and centrifuged at 6 000 rcf for 1 min.

The column was then transferred to a clean collection tube, and the old one was discarded. 500 µL wash buffer 1 (Buffer AW1) was applied to the column and then centrifuged at 6 000 rcf for 1 min before transferring the column to a clean collection tube. 500 µL wash buffer 2 (Buffer AW2) was applied to the column, centrifuged at 14 100 rcf for 3 min, and then another minute after changing the collection tube. The column was then transferred to a clean Eppendorf tube, and 200 µL elution buffer (Buffer AE) was applied. After 1 min of incubation at room temperature, the column was centrifuged at 6 000 rcf for 1 min. The elution was repeated once to increase the yield.

2.4.2 Polymerase Chain Reaction (PCR)

A polymerase chain reaction (PCR) was performed to amplify target genes. Preparation for PCR was done by preparing PCR reaction mix (20 µL total volume) in 8-strip PCR tubes, each containing the template (gDNA 1 – 10 ng μL^{-1}), DreamTaq Green PCR master mix (1x) by ThermoFisher, forward/reverse primer (1 mM) and nuclease-free water. The strip was then placed in the PCR machine with the program described in Table 2.3 below. The annealing temperature was adjusted to the primers' melting temperature (Tm) in Appendix C.

Table 2.3 PCR Program for the PCR Machine.

Temperature	Time	Cycles	Step
95°C	3 min	1x	Initial Denaturation
95°C	30 s		Denaturation
Tm - 5°C	30 s	30x	Annealing
72°C	1 min per kb		Extension
72°C	7 min	1x	Final Extension

2.4.3 Gel Electrophoresis

Gel electrophoresis was performed to verify the amplification of target genes from PCR and the absence of other DNA fragments. This method separates the different DNA fragments based on molecular weight, and by taking a picture of the gel, bands representing the different molecules are visible. To make the agarose gel, 2 g of ultrapure agarose was dissolved in 100 mL 1x TAE buffer solution, a buffer solution containing 40 mM Tris base, 20 mM acetic acid and 1 mM EDTA.

4 µL of peqGREEN was added to the gel solution prior to casting as an alternative to ethidium bromide to stain the DNA. After the gel had hardened, it was put in a gel tank and covered with 1x TAE buffer. 5 µL of the respective samples and ladder (Appendix D) were applied to the wells. The gel was run at 80V for 45 min. A picture of the gel was taken using Gel Doc™ XP Molecular Imager® and the Quanta One 4.6.7 Software to verify that the PCR had been successful and that the products had the expected size.

2.4.4 Purification of PCR Product

The E.Z.N.A.® Cycle Pure Kit from Omega Bio-tek was used to purify the PCR products. The kit removes DNA fragments smaller than 200 bp, such as primers, nucleotides, enzymes and salts. 5x volume of CP Buffer (Citrate-Phosphate) was added to the PCR product and mixed thoroughly by vortexing and centrifuging. The sample was then applied to a HiBind® DNA Mini Column with a collection tube and centrifuged at 14 100 rcf for 1 min. The flowthrough was discarded, and 700 µL DNA Wash Buffer was applied to the column before centrifuging again at the same speed and time. The wash steps were repeated once before centrifuging the

column while being empty to dry it thoroughly. The column was then transferred to an Eppendorf Tube, and 50 µL of Elution Buffer was applied to the column. After 2 min of incubation at room temperature, the column was centrifuged at 14 100 rcf for 1 min. The column was removed, and the eluate was stored at -20°C.

2.4.5 Purification of RNA

The Monarch Total RNA Miniprep Kit from New England BioLabs was used for RNA purification. Cell pellets (approximately $3.09 \cdot 10^8$ - $1.33 \cdot 10^9$ cells) were thawed at room temperature and resuspended in 800µL of 1x DNA/RNA Protection Reagent and transferred to a lysis tube with beads for mechanical lysis. The tube was placed in a FastPrep-24™ Classic Bead Beating Grinder and Lysis System at 4.5 m/s for 40 s · 2. The tube was centrifuged at 14 100 rcf for 2 min, and 400 µL of the sample volume was transferred to an Eppendorf tube along with an equal volume of RNA Lysis Buffer. The sample was loaded on a gDNA removal column with a collection tube and centrifuged for 30 s at 14 100 rcf. The flowthrough was mixed with an equal volume of absolute ethanol before transferring it to an RNA purification column with a collection tube. The column was centrifuged at 14 100 rcf for 20 s, and the flowthrough was discarded.

A wash step with 500 µL RNA Wash Buffer was performed by adding the buffer to the column and spinning for 30 s, and the flowthrough was discarded. 5 µL of DNase I (2 000 units mL^{-1}) and 75 µL of DNase I Reaction Buffer was then mixed and applied to the column. After 15 min of incubation at room temperature, 500 µL of RNA Priming Buffer was applied to the column and spun for 30 s, and the flowthrough was discarded. Two additional wash step was performed before the column was transferred to an Eppendorf tube. Finally, 50 µL of Nuclease-free water was added to the column and spun for 30 s. The eluate was kept on ice for further treatment and testing for residual gDNA by real-time PCR as described below (section 2.4.7) using primers targeting the *norB* gene, as that primer was confirmed to work for both organisms.

After on-column DNase treatment, an additional DNase treatment was performed for samples containing residual gDNA. The kit used for this was the TURBO DNA-free™ Kit from ThermoFisher. 0.1 volume of 10x TURBO DNase™ Buffer was added to the RNA and mixed gently. 0.5 µL of TURBO DNase™ Enzyme was added, and the sample was incubated at 37°C for 30 min. Another 0.5 µL of TURBO DNase™ Enzyme was added before incubating for an

additional 30 min. After the incubation, a 0.2x volume of DNase Inactivation Reagent was added, and the sample was incubated at room temperature for 5 min. The sample was centrifuged at 10 000 rcf for 1.5 min, and 50 µL of the sample volume was transferred to a new Eppendorf tube.

2.4.6 Reverse Transcription

the Maxima First-Strand cDNA Synthesis Kit from ThermoFisher was used to transform RNA to cDNA. Template RNA (1 pg – 5 µg) was mixed with 4 µL 5x Reaction Mix (containing reaction buffer, dNTPs, oligo$(dT)_{18}$ and random hexamers), 2 µL Maxima Enzyme Mix and nuclease-free water to a total volume of 20 µL. The samples were mixed gently and centrifuged to collect the droplets before being placed in a PCR machine. The program used is described in Table 2.4 below.

Table 2.4 PCR program for Reverse Transcription.

Temperature	Time	Cycles	Step
25°C	10 min	1x	Annealing
50°C	30 min	1x	Reverse Transcription
85°C	5 min		Inactivation
4°C	∞	Hold	

2.4.7 Quantitative PCR (qPCR)

Two different qPCR techniques were used to quantify transcripts: real-time PCR and droplet digital PCR (ddPCR). Real-time PCR was also used to establish the number of gDNA residues after RNA extraction.

Real-Time PCR

Real-time PCR is based on detecting fluorescence signal (e.g., SYBR®Green) that increases proportionally with the sample's target DNA amount. Ideally, the amount of target DNA doubles for each cycle. The cycle threshold (Ct-value) indicates which cycle the fluorescence signals increase above the background, a threshold set automatically or manually (Gibson et

al., 1996). A so-called absolute quantification is acquired by comparing the Ct-value of a sample with a relevant standard curve.

The samples were prepared by mixing the template (1 – 10 ng) with Power SYBR Green PCR Master mix (1x), forward/reverse primer (0.4 µM) and nuclease-free water. The real-time PCR was performed using a StepOnePlus™ Real Time System by ThermoFisher, and the program used is described in Table 2.5 below. The annealing temperature was adjusted to the Tm of the primers (Appendix C). The samples were held at 95°C for 15 s for the melt curve stage before dropping the temperature to 60°C. The temperature increased stepwise back to 95°C with an increment of +0.3°C for each fluorescence measurement.

Table 2.5 PCR Program for real-time PCR.

Temperature	Time	Cycles	Step
95°C	10 min	1x	Incubation
95°C	15 s		Denaturation
Tm -5°C	60 s	40x	Annealing
72°C	1 min per kb		Extension

Droplet Digital PCR (ddPCR)

ddPCR is based on water-in-oil emulsions and segments samples by creating droplets using a droplet generator (Mathekga et al., 2022). The target is dyed, which allows the detection of the target by measuring the fluorescence. The target molecule gets amplified inside each droplet it is present in by PCR. With a droplet reader, the droplets are streamed in a single file, and by detecting the fluorescence of the target, positive and negative droplets are counted to calculate the copy number of the target sequence in the sample. The estimation is based on Poisson distribution which gives the probability that a droplet will contain a given number of copies of the target. The target molecules are assumed to be distributed randomly into droplets, meaning a given target molecule is equally likely to end up in any droplets and move independently of other target molecules without interaction (Lin, 2016).

For ddPCR, the QX200™ Droplet Digital PCR System from Bio-Rad was used. The samples were prepared using the QX200™ ddPCR™ EvaGreen® SuperMix (1x) to allow the detection of the target DNA. Samples were diluted to be within the upper limit of ddPCR, which is 10^6 copies (Mathekga et al., 2022). If the copy number exceeds the limit, the sample gets saturated, and only positive droplets are generated.

Prior to running ddPCR, droplets were generated by adding 20 µL of the sample and 70 µL of QX200™ Droplet Generation Oil to dedicated wells in a DG8™ Cartridge, covering the cartridge with DG8™ Gaskets. The cartridge was then placed in a QX200™ Droplet Generator, and after a short period, 20 000 nanoliter-sized droplets were made in each sample, which was transferred to a 96-well plate. The plate was sealed using a PX1 PCR Plate Sealer and placed in a PCR machine with a program designed for ddPCR (Table 2.6). The annealing temperature was adjusted to the Tm of the primers (Appendix C). After running the PCR program, the samples were kept at 12°C for at least 2 hours to stabilize the droplets. Finally, the plate with the samples was put in the QX200™ Droplet Reader.

Table 2.6 PCR program for ddPCR.

Temperature	Time	Cycles	Step
95°C	5 min	1x	Initial Denaturation
95°C	30 s	40x	Denaturation
Tm - 5°C	30 s		Annealing
72°C	1 min per kb		Extension
4°C	5 min	1x	Final Extension
90°C	5 min		
12°C	2 hours		

2.4.8 Primer Design

To amplify the denitrification genes, *narG, nirS, norB* and *nosZ*, primer pairs for each gene were made, specifically for both Pd1222 and GB17, as the gene sequences differ slightly. The gene sequences were found in KEGG's database, where Pd1222 has the accession number T00440 and GB17/DSM2944 has the accession number T06495. The primers were designed using the Primer3 software and verified by checking the Tm and potential primer dimers in Sigma-Aldrich's DNA Oligo in Tubes tool.

The requirements set for the primers were to be specific to the gene and organism they were designed for and to give a product between 600 and 650 bp, and the primers' lengths were 20 bp. Regarding the Tm of the primer, Primer3 and Sigma-Aldrich gave two different estimates (Appendix C). The first one estimated the primers to have a Tm between 58 and 60, whereas the latter generally estimated them to be between 65 and 68. The denitrification gene primers are listed in Table 2.7 below.

Table 2.7 Primers for Amplification of Denitrification Genes. *Primer pairs designed to amplify the denitrification genes narG, nirS, norB and nosZ.*

Organism	Gene	Primer (5'→ 3')
Pd1222	*narG*	Forward: GAAGTTCGGCGACATCTGG Reverse: CCCGGTCCAGGCTGTAATTG
	nirS	Forward: GACGCCCAATACAACGAAGC Reverse: TGGCGTATTTGTCCTCCCAG
	norB	Forward: CCTTGCCTTCCTGATGCTCA Reverse: GTCCTGCACGTCCATGAAGA
	nosZ	Forward: TGGAGGACGTGGCGAATTAC Reverse: CAGCTTGTCCTTGATCGGGT
GB17	*narG*	Forward: GAACACCTCGGACATGCATC Reverse: TGGGCGAGGAGATGATCTTC
	nirS	Forward: GATCAAGATCGGCTCGGAGG Reverse: TTCGGGTGCGTCTTGATGAA
	norB	Forward: TCGCCTTCCTGATGCTCAAG Reverse: GTCCTGCACGTCCATGAAGA
	nosZ	Forward: TCTCGACCTCCTACAACTCG Reverse: CCTTCGAGAACTTGCACAGC

New primers were made for the same genes to make a standard curve for the qPCR reaction, but this time with a slightly bigger product size of 750 - 800 bp and with the requirement of covering the original primers. These primers were designed using the same procedure and programs. The standard curve primers are listed in Table 2.8 below.

Table 2.8 Standard Primers for Standard Curve. *The primer pairs were designed to amplify the denitrification genes narG, nirS, norB and nosZ and cover the previous primers.*

Organism	Gene	Primer (5'→ 3')
Pd1222	*narG*	Forward: CGCGCATTTCTATACCGAGG Reverse: CTGGATGATCTTGTCGCGAC
	nirS	Forward: AGGATCACAAGACCAAGACG Reverse: TCTCGCCGTCCATGATGAC
	norB	Forward: ATACTGGTGGTGGGTCATCC Reverse: CACGGCATAGATGAACAGCA
	nosZ	Forward: GTCAACGACGGCACCAAC Reverse: CGGTCCTTCGAGAACTTGGA
GB17	*narG*	Forward: TGCTGGTGACGATCGACTT Reverse: CTCATGCACGTTGGTCCAG
	nirS	Forward: CTGTGGATGAAGGAGCCCA Reverse: GGTCTTGAACTCGGGGTCC
	norB	Forward: ATACTGGTGGTGGGTCATCC Reverse: CACCGCATAGATGAACAGCA
	nosZ	Forward: GAACGTCTTCACCGCTGTC Reverse: CATCTGGTCGCCCGAAATG

The last set of primers, 27F and 1492R (Lane, 1991), was for the 16S rRNA gene, and this primer pair was universal for both Pd1222 and GB17. The primers were tested in Benchling to check if they would bind to both organisms and that the product would be slightly different from each other to make it possible to differentiate them later. The 16S primers are listed in Table 2.9 below.

Table 2.9 Primers for 16S. *Primer pairs to amplify the 16S gene in both Pd1222 and GB17. The products have slightly different lengths and are confirmed to have mismatches for easy distinguishing of products after sequencing. Primers from Lane (1991).*

Organism	Gene	Primer (5'→ 3')
Pd1222 and GB17	*16S*	27F: AGAGTTTGATCCTGGCTCAG 1492R: GGTTACCTTGTTACGACTT

2.5 Experiments

Three series of experiments were conducted. 1) Linking OD_{660} to cell density and dry weight; 2) Investigating the correlation between CO_2 and pH, improving the estimation of CO_2, thus biomass yield, in KinCalc, and facilitating optimization of the AnaPro process; 3) Aerobic denitrification: effect of oxic spells on actively denitrifying cultures, with implications for the AnaPro process.

2.5.1 Linking Cell Density to Dry Weight and Cell Numbers

These experiments aimed to establish the most reliable method to estimate the cell count during the main experiments. One of the methods used was counting cells by flow cytometry (section 2.3.6) and linking this number to optical density. The other method was counting the cells manually with a Bürker counting chamber under the microscope, linking this to optical density and dry weight. As the latter seemed the most reliable, the estimates made by microscopy were used to determine the cell numbers.

To estimate the cell number per OD_{660} and dry weight, cultures of Pd1222 and GB17 were raised and counted under the microscope using a Bürker counting chamber. As aerobic and anaerobic cells may differ in size, the experiment was done in two parts; one with aerobically raised cells and one with anaerobically raised cells. Twelve cultures (six aerobic and six anaerobic) were made of each strain, which allowed double triplicates of each strain and growth condition. One triplicate was used for optical density measurements. The other triplicate was untouched (except for additions of KNO_3) until the OD_{660} had reached 1.00 when the entire cultures were harvested and used for dry weight measurements (Fig. 2.4).

During the experiment, the vials were incubated in a robot incubation system with a water bath holding 30°C. The robot monitored the transition culture and the anaerobic vials to know when to supply the cultures with KNO_3 when N_2 production decreased. The optical density was measured by spectrophotometry. Three of the vials for each strain were sampled and fixated when the OD_{660} was ~ 0.05, 0.10, 0.25, 0.50, 0.75 and 1.00, and stored in the refrigerator (4°C) until microscopy. The remaining three untouched vials of cells from each strain were used for dry weight determination (section 2.3.7).

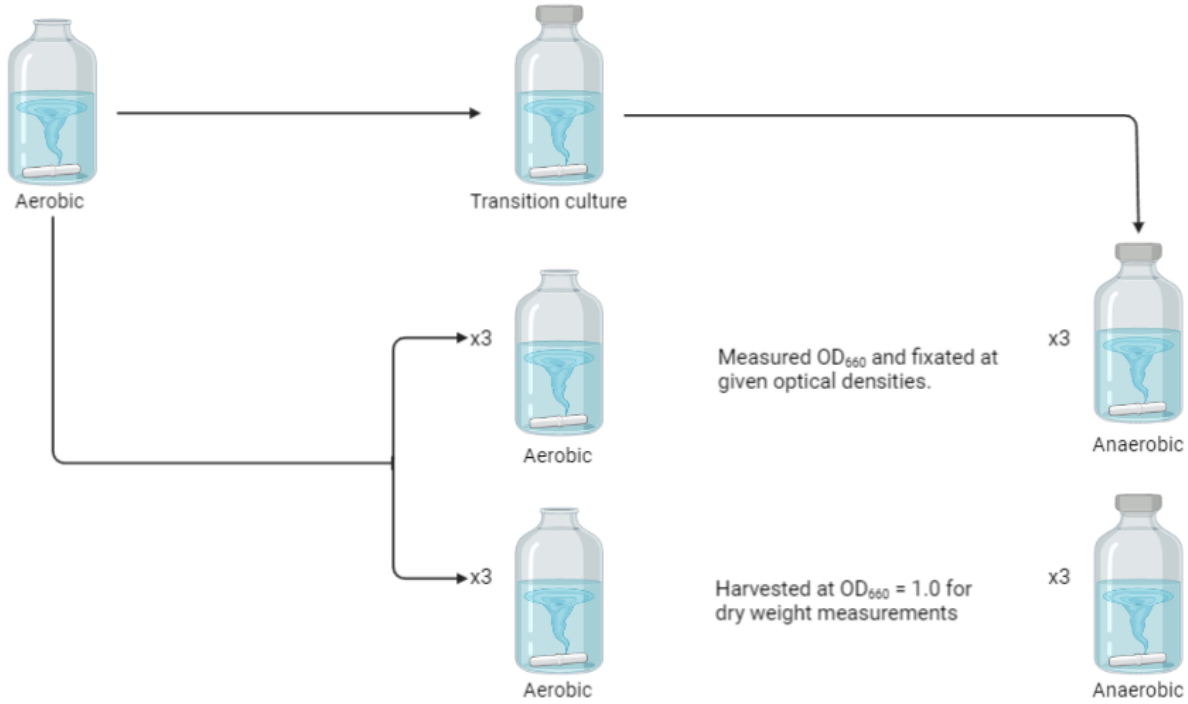

Figure 2.4 Schematic Overview of Experimental Setup for Dry Weight and Microscopy. *Aerobically raised cells were used to inoculate 2 · 3 aerobic vials for each strain, along with one transition culture. 2 · 3 anaerobic vials were inoculated by cells from the transition culture after two days of incubation.*

The fixated samples from each OD_{660} were analysed by microscopy and a Bürker counting chamber as described (section 2.3.5). All three replicates were counted for the samples with an OD_{660} of 0.05, 0.50 and 1.00, while only the first replicate was counted for 0.10, 0.25 and 0.75.

2.5.2 The Solubility of Carbon Species in PBS Under Different Partial Pressures

This experiment aimed to investigate how dissolved CO_2 affects the pH of the growth medium and vice versa. For this experiment, the concentration of the different carbon species was calculated based on pH and pressure measurements along with gas data from the robot incubation system. While placed in the robot incubation system, different volumes of pure CO_2 were injected into the vials. The medium used was PBS (Appendix A5) with different phosphate concentrations: a 20 mM concentration which represents the conditions found in the buffer for the Sistroms medium, and a 100 mM concentration, which represents the medium used in HCDC, to investigate if a stronger buffer was required to counteract the acidifying effect of CO_2. The starting point for both media was a pH of 7.00.

After equilibrium was reached, the fraction of CO_2 found in the headspace, pH and pressure were measured. The pH was measured using the Thermo Scientific™ Orion™ Versa Star Pro™ Benchtop Meter with a Thermo Scientific™ Orion™ Micro pH Electrode, allowing pH measurements without breaking the anoxic conditions by piercing through the septum of the vials. The pressure in the vials was measured using a manometer with a needle to pierce the septum. This experiment was done twice; abiotic with only medium and biotic with aerobically raised Pd1222 cells (approximately $1.07 \cdot 10^9$ cells mL^{-1}). The cells were washed twice in PBS before inoculation to ensure no metabolic activity would affect the results. What was desired to investigate was whether the cells themselves would influence the carbonate chemistry.

Preliminary Experiments

Prior to the main experiment, the amount of time needed to reach equilibrium between CO_2 in the headspace (g) and dissolved in water (aq) was tested. 2 mL of pure CO_2 was injected into vials with 20 mM PBS and a vial with 100 mM PBS while monitoring them in the robot incubation system to investigate how long it would take for the CO_2 concentration in the headspace to stabilise. An additional 2 mL of pure CO_2 was injected stepwise until the total injected volume of CO_2 reached 8 mL. After reaching the last equilibrium, the amount of H_2SO_4 needed to force all CO_2 into headspace (g) (pH ~ 5.00) was also tested. Both tests were done to avoid constant monitoring of the vials in the robot incubation system during the main experiment and to know approximately how much H_2SO_4 was needed to avoid adding too much and risking destroying the samples.

Abiotic Experiment

Triplicates of each PBS molarity and CO_2 concentration were made. As mentioned, the PBS medium was prepared with either 20 mM or 100 mM phosphate, and the CO_2 injection was either 0, 2, 4, 6 or 8 mL, which is equivalent to 0 ppm, 28 571 ppm, 57 143 ppm, 85 714 ppm and 114 286 ppm, respectively. After equilibrium was reached, pH and gas measurements were done. Further on, H_2SO_4 was added until the pH dropped to approximately 5.00. Finally, another pressure measurement was done, and the vials were returned to the robot incubation system to get final gas data readings.

Biotic Experiment

The experiment previously described was repeated, this time with aerobically raised cells of Pd1222. Prior to inoculation, the cells were washed twice in PBS of the same molarity as they were to be inoculated. Between each wash, the cells were placed in a centrifuge at 10 000 rpm and 20°C for 15 min. The supernatant was discarded, and the pellet was resuspended in 1 mL buffer. After reaching equilibrium, the same measurements were done before and after adding H_2SO_4.

2.5.3 Aerobic Denitrification

One of the main experiments was to determine if Pd1222 and GB17 can complete the denitrification process in the presence of oxygen and whether the intermittent presence of oxygen affected apparent yield per mol electron to terminal electron acceptors in cultures adapted to anoxia.

Part 1 – Gas Accumulation and Electron Flow Analysis

Ten vials of anaerobically raised cells of both strains were inoculated and incubated in the water bath until the OD_{660} had reached approximately 0.1. At this point, the OD_{660}, glucose and NO_2^- concentration was measured prior to oxygen injection. For each strain, this resulted in triplicates of each of the test volumes of O_2, set to 0%, 7% and 21%, and one vial was left untouched as a control (Fig. 2.5). An Eppendorf tube was filled with 1 mL of sample and then spun down in a centrifuge at 10 000 rpm for 5 min to get a supernatant and pellet. The supernatant was transferred to a clean Eppendorf tube and used for the NO_2^- and glucose concentration measurements. After these measurements, the original vials were injected with 0%, 7% and 21% O_2, respectively, and the vials were left in the robot incubation system and monitored until

the O_2 concentration was back to 0%. Then new OD_{660}, glucose and NO_2^- concentration measurements were taken, along with pH measurements.

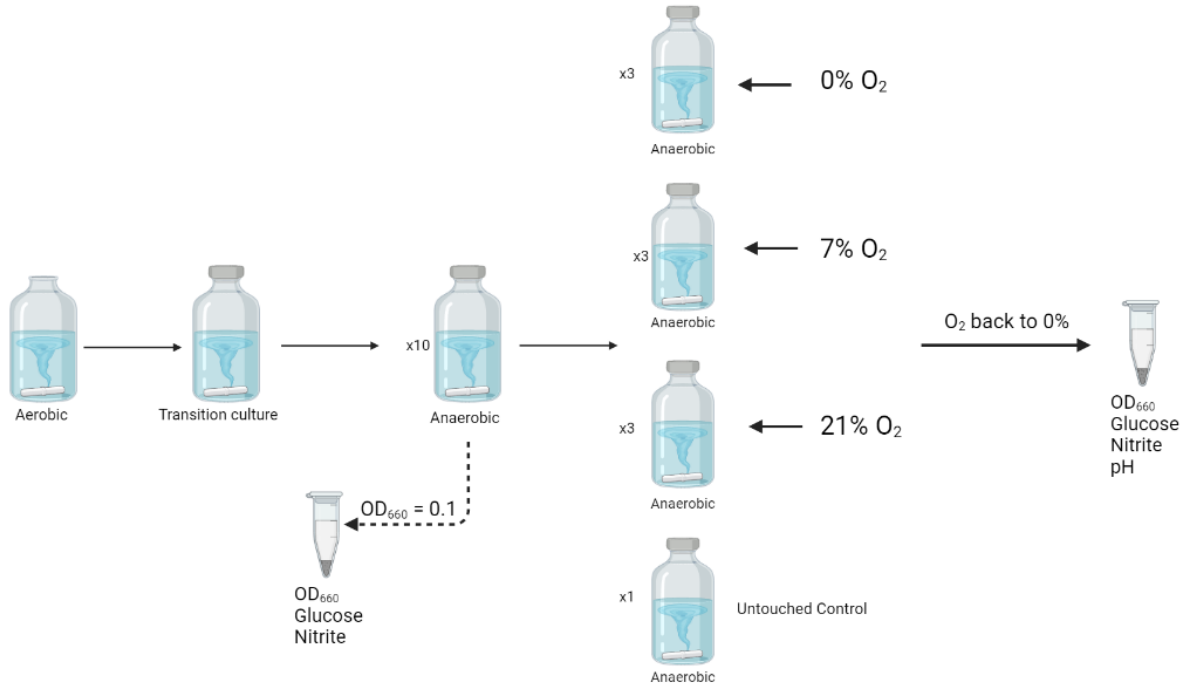

Figure 2.5 Experimental Setup for Part 1 of Aerobic Denitrification. *When the OD_{660} reached 0.10 in the anaerobic cultures, 1 mL was taken from each vial and centrifuged to measure glucose and NO_2^- concentrations. Further, O_2 was injected in triplicates, and one vial was left untouched as a control. The vials were monitored in the robot incubation system, and when oxygen was depleted, OD_{660}, pH, glucose, and NO_2^- concentrations were measured.*

Part 2 – Transcription Analysis and Sanger Sequencing

The aerobic denitrification was repeated to collect samples for DNA and RNA extraction (from now on, referred to as "DNA samples" and "RNA samples", respectively) to investigate the expression of the denitrification genes through transcription analysis and investigate potential contamination and verifying the correct organisms were used through Sanger sequencing. Biological triplicates of aerobic cultures were made for Pd1222 and GB17, using cells from aerobic pre-cultures of the respective strains. After a day of incubation, samples were taken from the aerobic vials. When sampling, 1 mL of each triplicate was taken, resulting in three samples from each sampling point. The NO_2^- concentration was checked for each sampling using the NOA system (section 2.3.3), and the remaining cells were supplied with more KNO_2 if needed to ensure the denitrification process would not stop due to NO_2^- deficiency.

Both “RNA” and “DNA” samples were taken from the aerobic vials before preparing a transition culture. Nine vials of each bacterium were inoculated anaerobically with cells from the transition cultures until an OD_{660} of ~ 0.015 was reached, allowing three sets of triplicates as entire flasks were harvested for proteomics as well (not proceeded past sampling due to time limitations). The robot monitored the denitrification process and gas accumulation. Prior to oxygen injection, “RNA” samples were taken at the following events: 1) active denitrification with OD_{660} ~ 0.03), and 2) active denitrification when the OD_{660} had increased to ~ 0.10. When the OD_{660} had reached ~ 0.30, 7% O_2 was injected into the anaerobic vials. Another three “RNA” samples were taken at the following events: 1) 0.5 hours after the oxygen injection 2) 5 hours after the oxygen injection 3) increased NO concentrations 4) re-induction/active denitrification. For the last sampling, “DNA” samples were also taken (Fig. 2.6).

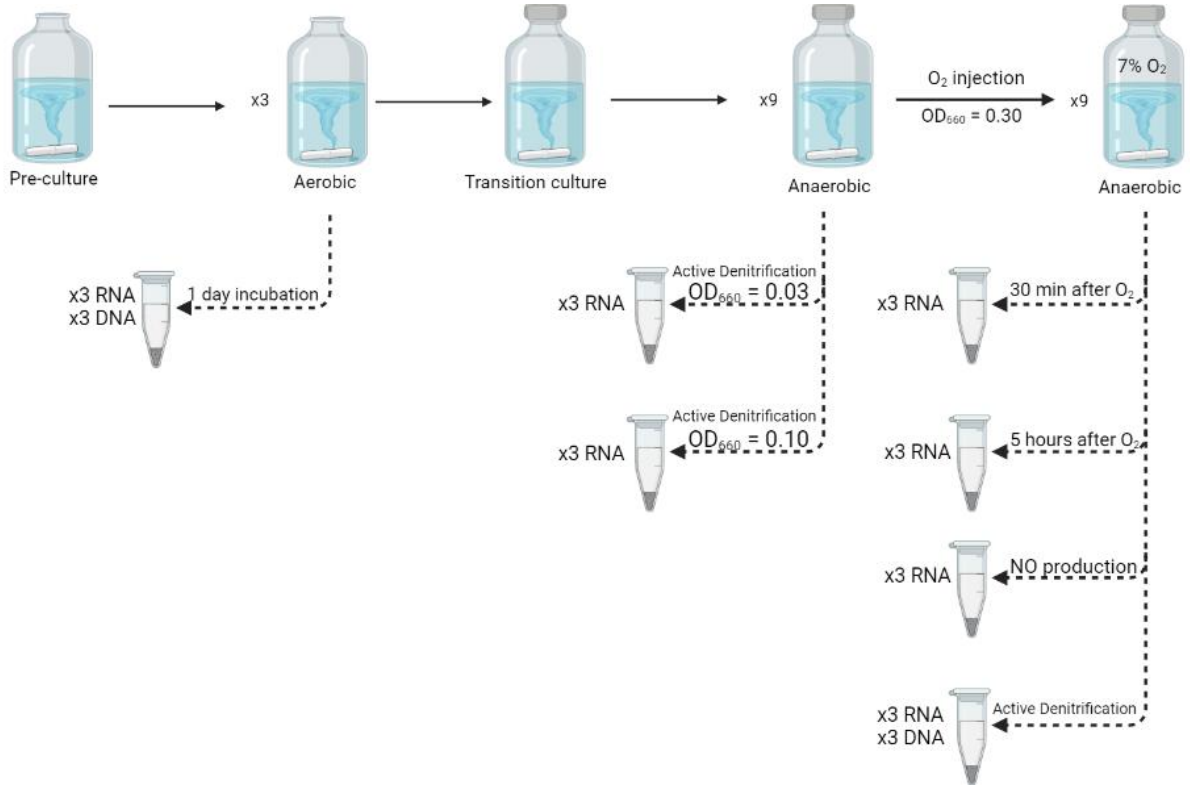

Figure 2.6 Experimental Setup for Part 2 of Aerobic Denitrification. *Samples for DNA and RNA extraction (labelled “DNA” and “RNA”, respectively) were taken from the aerobic vials prior to inoculation of transition cultures. “RNA” samples were taken from the anaerobic vials prior to oxygen injection when the cells were actively denitrifying, and the OD_{660} was 0.03 and 0.10, respectively. After the last sample was taken, 7% O_2 was injected into the vials. New “RNA” samples were taken 30 min and five hours after oxygen injection, the start of NO production. Final samples for DNA and RNA extraction were taken during active denitrification.*

The “DNA” and “RNA” samples were stored in Eppendorf tubes kept on ice. For each sample, the OD_{660} and NO_2^- concentrations were measured. Afterwards, the tubes were centrifuged at 4°C and 10 000 rcf for 5 min. The supernatant was removed, and the pellet was resuspended in 1 mL of RNAprotect® by Qiagen for the “RNA” samples and MQ water for the “DNA” samples. The samples were then centrifuged again, the supernatant was removed, and the cell pellets were stored at -80°C for the “RNA” samples and -20°C for the “DNA” samples.

The “DNA” cell pellets were lysed and purified as described (section 2.4.1), and the DNA concentration was measured using NanoDrop (Appendix E1). The clean DNA samples were used to amplify the 16S gene and to make standards for a qPCR standard curve. For the amplification of 16S, the primers listed in Table 2.9 were used for Pd1222 and GB17. The standard primers (Table 2.8) designed specifically for each gene and organism were used to make the standards for the standard curve. To assure the quality of the standards prior to making the standard curve by real-time PCR, ddPCR was performed as described (section 2.4.7).

Gel electrophoresis was performed to verify that the clean 16S and standards were correct and pure. The 16S PCR products were confirmed by inspection of the gel picture to have the expected size of 1456 bp for Pd1222 and 1467 bp for GB17 (Appendix F). The PCR products were purified (section 2.4.4) to obtain clean 16S products. The DNA concentration was measured using NanoDrop for the clean 16S products (Appendix E2) and the clean standards (Appendix E3). The clean 16S products were then prepared for Sanger sequencing by preparing two Eppendorf tubes per sample, one with 5 µL of the forward primer and one with 5 µL of the reverse primer, and 5 µL of the respective clean 16S sample in each tube.

The “RNA” cell pellets were lysed, and RNA was extracted and purified as described (section 2.4.5), and the RNA concentration was measured using NanoDrop (Appendix E4). To verify that gDNA was adequately removed, real-time qPCR was set up as described in section 2.4.7, and the cDNA was used as the template in qPCR (real-time PCR and ddPCR) performed to quantify *nirS, narG, norB* and *nosZ* transcripts, using the respective primer pairs (Table 2.7).

3 Results

3.1 Estimating Cell Count and Dry Weight

The first set of experiments aimed to estimate cell count using flow cytometry and microscopy and estimate the biomass for dry weight measurements. The motive was to couple the rapid OD_{660} measurements with dry weight and cell count, also identifying the most reliable cell counting technique. Another goal was to get specific estimates of the dry weight for both aerobic and anaerobic raised cells of Pd1222 and GB17.

3.1.1 Estimating Cell Count by Flow Cytometry

The first part of the cell counting experiment was to investigate if flow cytometry could reliably be used to estimate cells ml^{-1} OD_{660}^{-1}, and if so, which concentration of SYBR®Green and dilution (undiluted or 10x) of the sample would give the most accurate result. The SYBR®Green concentrations tested were 0.5x, 1x and 5x. Both aerobically and anaerobically raised cells were used, where some of the cells were unstained and used directly in the flow cytometer after fixation. The rest were stained with SYBR®Green after fixation. The OD_{660} was measured before the cells were fixated. The aerobic cells had an OD_{660} of 1.10 - 1.20, and the anaerobic cells had an OD_{660} of 0.60 - 0.80.

As expected, the unstained cells did not give any events mL^{-1} with the channel used for the detection of SYBR®Green fluorescence (488 – 528/46 – C3), as this channel only detects stained cells. Therefore, the estimate for unstained cells was based on the general events mL^{-1} for “bac & all”. For the aerobic, unstained cells, the cell count was approximately $2.24 \cdot 10^7$ cells ml^{-1} OD_{660}^{-1} for both organisms, whereas for the anaerobic, unstained cultures, the cell count ranged from $1.92 \cdot 10^7$ to $3.88 \cdot 10^7$ cells ml^{-1} OD_{660}^{-1} (Appendix G1).

The estimated cells ml^{-1} OD_{660}^{-1} of different SYBR®Green concentrations were compared for the 10x diluted cells of aerobically and anaerobically raised Pd1222 and GB17 (Fig. 3.1). For the stained samples, an average of 86.7% of the bacterial cells were gated as SYBR®Green positive. The undiluted samples gave heavily underestimated cell counts, with a standard deviation greater than the estimate itself, and these estimates were not included in the results (Appendix G2).

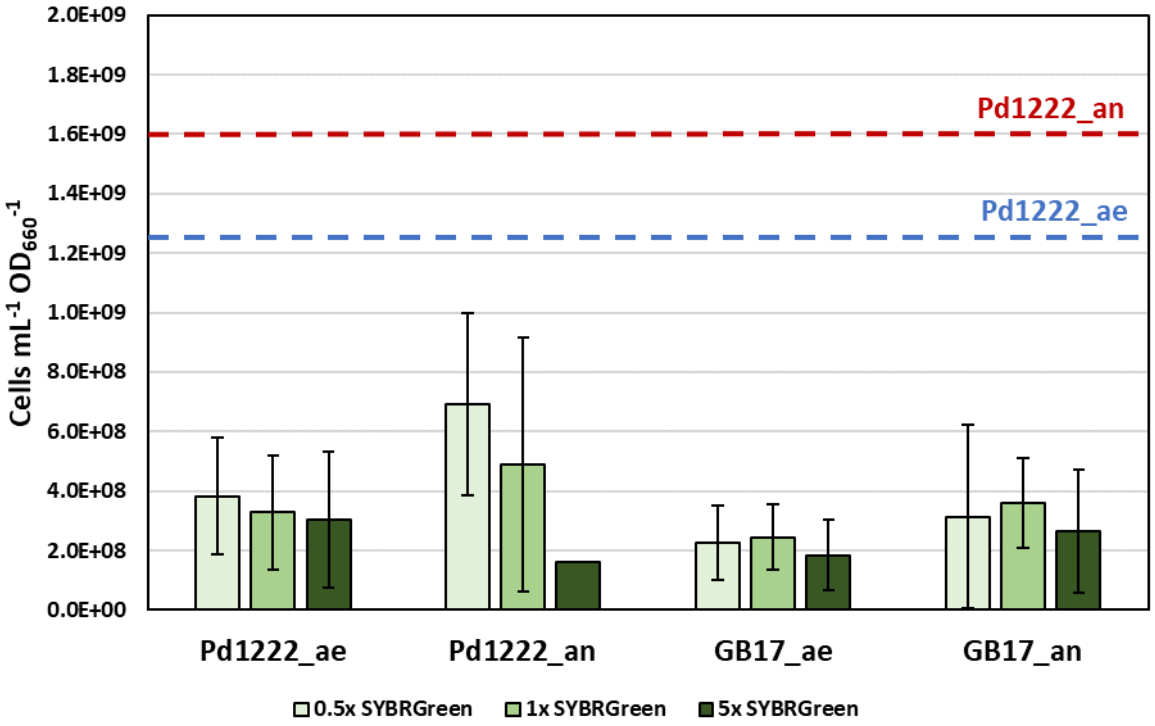

Figure 3.1 Estimated Cells mL^{-1} OD$_{660}^{-1}$ by Flow Cytometry. *Based on estimates from the 10x diluted cells stained with either 0.5x, 1x or 5x SYBR®Green for aerobic (ae) and anaerobic (an) cultures of Pd122 and GB17. The dashed lines indicate the expected cell count for aerobic (blue) and anaerobic (red) Pd1222 cultures based on previous experiments (not part of this thesis).*

Compared to unstained cells, most stained cells had an estimated cells ml^{-1} OD$_{660}^{-1}$ one order of magnitude higher. Regarding the SYBR®Green concentration, the 0.5x concentration of SYBR®Green gave the highest estimate for Pd1222, while the 1x concentration gave the highest estimate for GB17. From previous experiments (not part of this thesis), the estimated cell count for Pd1222 was $1.25 \cdot 10^9$ cells ml^{-1} OD$_{660}^{-1}$ for aerobic cells and $1.60 \cdot 10^9$ cells ml^{-1} OD$_{660}^{-1}$ for anaerobic cells. Compared to these numbers, the estimates made by flow cytometry are approximately one order of magnitude lower than expected. In addition, the standard deviation is high for all samples, indicating that the data are spread out.

3.1.2 Estimating Cell Count by Microscopy and Bürker Counting Chamber

As flow cytometry grossly underestimated the number of cells, another way to estimate the cell count was manually counting the cells by microscopy and a Bürker counting chamber (haemocytometry). The cell count was done for both aerobically and anaerobically raised cells of Pd1222 (Table 3.1) and GB17 (Table 3.2). The cells were counted from samples with known optical density, where the OD_{660} was 0.05, 0.10, 0.25, 0.50, 0.75 and 1.00. All triplicates were counted for the samples with OD_{660} = 0.05, 0.50 and 1.00. Only one sample from each was counted for the remaining samples (OD_{660} = 0.10, 0.25 and 0.75).

Table 3.1 Cell Count for Pd1222. *All data are shown as cells mL^{-1}. The number in the parentheses indicates the number of replicates.*

OD_{660}	**Aerobic**			**Anaerobic**		
0.05	$1.77 \cdot 10^7$	$\pm 7.29 \cdot 10^6$	(3)	$1.30 \cdot 10^7$	$\pm 2.15 \cdot 10^6$	(3)
0.10	$1.94 \cdot 10^7$		(1)	$3.24 \cdot 10^7$		(1)
0.25	$8.33 \cdot 10^7$		(1)	$1.94 \cdot 10^8$		(1)
0.50	$4.17 \cdot 10^8$	$\pm 2.30 \cdot 10^8$	(3)	$5.43 \cdot 10^8$	$\pm 9.21 \cdot 10^7$	(3)
0.75	$8.13 \cdot 10^8$		(1)	$7.42 \cdot 10^8$		(1)
1.00	$1.17 \cdot 10^9$	$\pm 1.86 \cdot 10^8$	(3)	$1.02 \cdot 10^9$	$\pm 2.22 \cdot 10^7$	(3)

Table 3.2 Cell Count for GB17. *All data are shown as cells mL^{-1}. The number in the parentheses indicates the number of replicates.*

OD_{660}	**Aerobic**			**Anaerobic**		
0.05	$6.76 \cdot 10^6$	$\pm 2.18 \cdot 10^6$	(3)	$5.33 \cdot 10^6$	$\pm 5.33 \cdot 10^5$	(3)
0.10	$6.93 \cdot 10^6$		(1)	$2.28 \cdot 10^7$		(1)
0.25	$1.94 \cdot 10^8$		(1)	$2.60 \cdot 10^8$		(1)
0.50	$5.45 \cdot 10^8$	$\pm 3.78 \cdot 10^7$	(3)	$6.44 \cdot 10^8$	$\pm 3.87 \cdot 10^7$	(3)
0.75	$7.69 \cdot 10^8$		(1)	$1.09 \cdot 10^9$		(1)
1.00	$1.05 \cdot 10^9$	$\pm 1.22 \cdot 10^8$	(3)	$1.31 \cdot 10^9$	$\pm 5.83 \cdot 10^7$	(3)

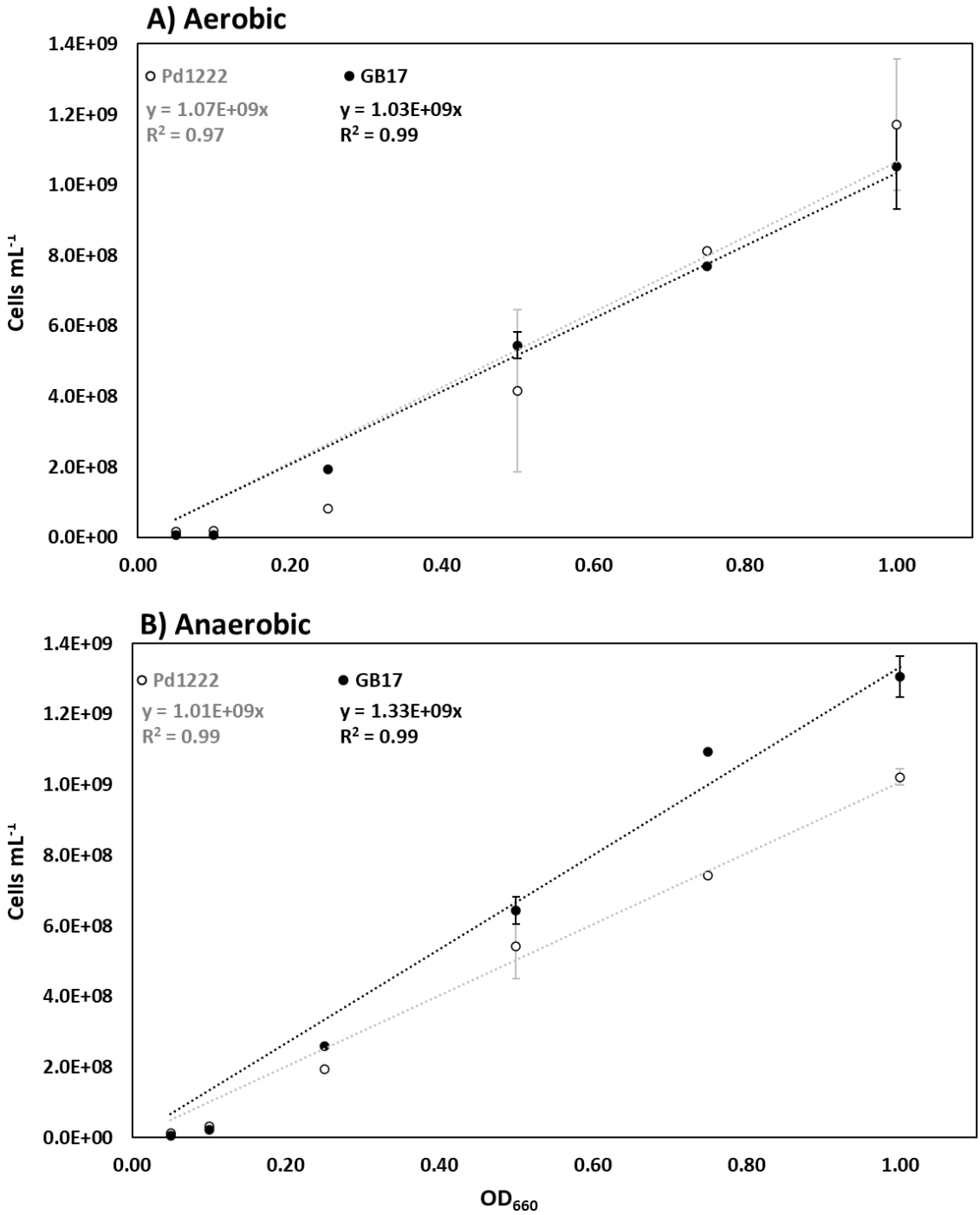

Figure 3.2 Linear relationship between cells mL^{-1} and OD_{660}. *A) Aerobically grown cells and B) Anaerobically grown cells. All are based on samples taken at the following optical densities: 0.05, 0.10, 0.25, 0.50, 0.75 and 1.00. Triplicates were counted for OD_{660} = 0.05, 0.50 and 1.00.*

The cell count was then plotted in a graph (Fig. 3.2) to visualise the linear relationship between OD_{660} and cell count. As all of the graphs have an R^2-value of 0.97 or greater, the data seem to be well fitted to the regression line, and a linear relationship between cells/mL and OD_{660} seems likely, with a small deviation for samples with low OD_{660} (<0.50).

The slope of the respective graph was used to make the following estimates for cell count based on microscopy, which are the cells mL^{-1} OD_{660}^{-1} used in all following experiments:

Pd1222 (aerobic): $1.07 \cdot 10^9$ cells mL^{-1} OD_{660}^{-1}
Pd1222 (anaerobic): $1.01 \cdot 10^9$ cells mL^{-1} OD_{660}^{-1}
GB17 (aerobic): $1.03 \cdot 10^9$ cells mL^{-1} OD_{660}^{-1}
GB17 (anaerobic): $1.33 \cdot 10^9$ cells mL^{-1} OD_{660}^{-1}

3.1.3 Estimating Dry Weight

In the last part of the cell counting experiment, the dry weight of both aerobically and anaerobically raised cells of Pd1222 and GB17 were measured. By doing so, the relationship between dry weight and OD_{660} and microscopical counts can be established. The difference between aerobic and anaerobic cells was minimal, with anaerobically raised cells having a slightly lower dry weight OD_{660}^{-1} than the aerobic. Both aerobically and anaerobically raised Pd1222 have a higher dry weight OD_{660}^{-1} than GB17 (Table 3.3).

Table 3.3 Dry weight for Aerobic and Anaerobic Cultures of Pd1222 and GB17. *The dry weight is presented as g L^{-1} OD_{660}^{-1} and pg $cell^{-1}$. The number in the parentheses indicates the number of replicates.*

Organism		**Dry Weight (g L^{-1} OD_{660}^{-1})**			**Dry Weight (pg $cell^{-1}$)**		
Pd1222	Aerobic	0.254	± 0.038	(3)	0.237	± 0.036	(3)
	Anaerobic	0.244	± 0.044	(3)	0.200	± 0.029	(3)
GB17	Aerobic	0.206	± 0.030	(3)	0.242	± 0.044	(3)
	Anaerobic	0.171	± 0.032	(3)	0.128	± 0.024	(3)

The estimated dry weight has been corrected regarding the Eppendorf tubes' weight and the natural weight loss after incubation at 100°C. Three empty Eppendorf tubes were weighed before and after the incubation. From this, the average weight loss of the tube itself was estimated to be approximately 0.16% of the original weight after incubation. Some tubes were left for several days to see if they would lose more weight after a more extended incubation period, which was proved not to be the case as the final weight remained the same after three days as for one day of incubation.

3.2 The Solubility of Carbon Species in PBS Under Different Partial Pressures

A current problem with anaerobic HCDC is that the accumulation of CO_2 leads to acidification, counteracting the pH increase driven by denitrification, thus interfering with the pH-stat (Fig. 1.4). Unless measures are taken to remove CO_2 more efficiently or somehow correct for its effect on pH, the provision of acid will become insufficient to maintain high growth rates in dense cultures, with the continuous risk of running into complete depletion of NO_3^-, and arrested growth. The aim of this experiment was thus to establish the relationship between pH and P_{CO2} and use that information to optimize the script controlling the HCDC process so that the pH setpoint is automatically adjusted depending on CO_2 in the off-gas, maintaining [HNO_3] in the low mM range.

The relationship between pH and P_{CO2} depends on the medium's buffer capacity; therefore, the experiment was done with both 20 mM and 100 mM PBS. CO_2 was injected to a P_{CO2} of 0, 0.008, 0.018, 0.030 and 0.042 atm were reached. Acidification to a pH of ~ 5.00 caused all injected CO_2 to release into headspace. The measured pH prior to acidification was then plotted against the P_{CO2} (Fig. 3.3).

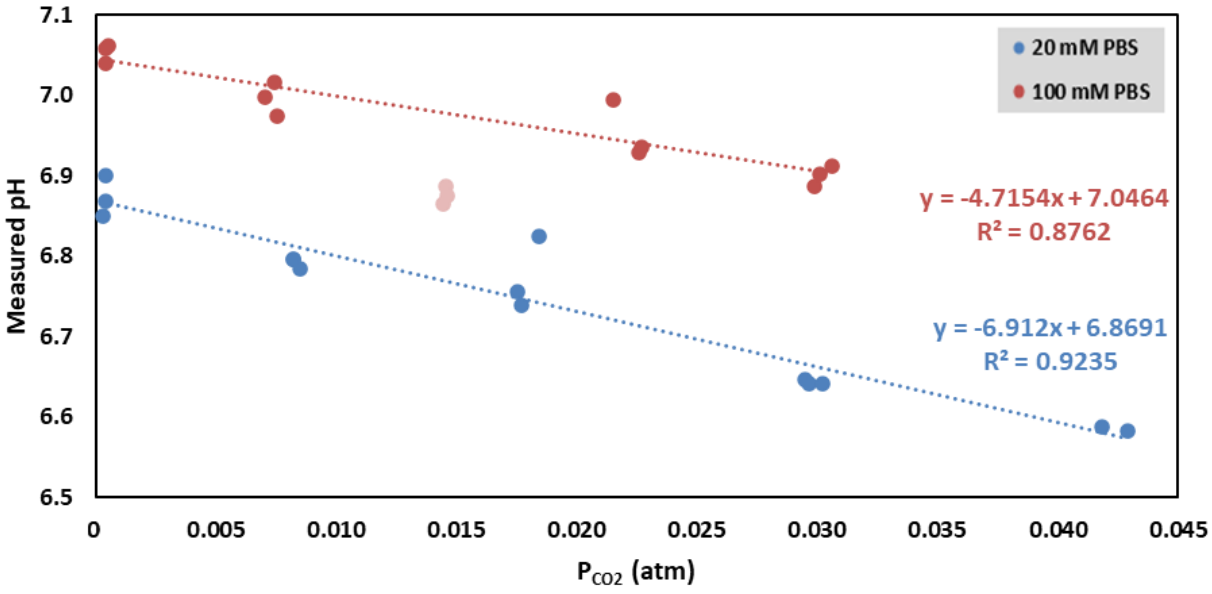

Figure 3.3 pH Plotted Against P_{CO2}. *Different volumes of pure CO_2 were injected into the vial containing PBS with either 20 mM (blue) or 100 mM (red) phosphate buffer. Each CO_2 injection was done in triplicates, and each point in the graph represents one vial. Outliers for 100 mM phosphate buffer(pink) were excluded from the regression line.*

As illustrated above, the pH declines nearly linearly when P_{CO2} increases. A general regression function can be made for both molarities within the pH range tested:

20 mM PBS: $$pH = pH_0 - P_{CO2} \cdot 6.9120 \quad (eq.1)$$

100 mM PBS: $$pH = pH_0 - P_{CO2} \cdot 4.7154 \quad (eq.2)$$

In a previous titration experiment determining pH as a function of [HNO_3] in 100 mM phosphate buffer, the relationship pH = 7.2246 – 0.0235 · [HNO_3] (R^2 = 0.9994) was found (not part of this thesis). Since this is a linear function, it can be generalized to all initial pH levels within the relevant range:

$$pH = pH_0 - 0.0235 \cdot [HNO_3] - P_{CO2} \cdot 4.7154 \quad (eq.3)$$

Thus, [HNO_3] is a simple function of measured pH and P_{CO2}.

$$[HNO_3] = \frac{pH_0 - pH - P_{CO2} \cdot 4.7154}{0.0235} \quad (eq.4)$$

Equation 4 was implemented in the HCDC process to regulate the provision of HNO_3 based on CO_2 concentration in the off-gas (Fig. 3.4). It will also improve the KinCalc spreadsheet regarding CO_2 calculations (not shown).

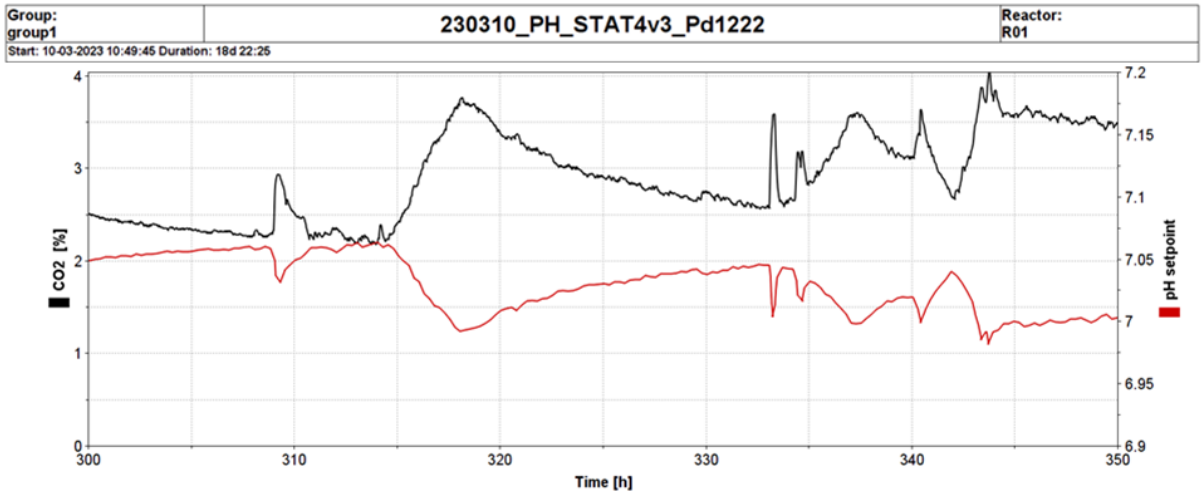

Figure 3.4 pH setpoint adjusted by CO_2. *Excerpt from a fed-batch process implementing (eq.*4*). The pH setpoint (red) continuously changes in response to changes in the concentration of CO_2 in the off-gas (black). Courtesy of Marte Mølsæter Maråk.*

3.3 Aerobic Denitrification

The main purpose of this set of experiments was to investigate the effect exposure to oxygen has on denitrifying cultures of an organism described as an aerobic denitrifier (GB17) and an organism known not to perform aerobic denitrification (Pd1222). This has implications for HCDC in terms of the vulnerability of the process to oxygen leakage and the choice of an organism (is one less vulnerable to oxidative stress than the other?).

3.3.1 Part 1 – Investigation of Gas Accumulation and Electron Flow

Anaerobically raised cells of Pd1222 and GB17 were monitored using the robot incubation system, both the gas accumulation (µmol/nmol vial^{-1}) and the electron flow, V_{e-} (µmol e$^-$ vial^{-1} h^{-1}). Triplicates of each culture were left untouched except for additions of KNO_2 (Fig. 3.5a and 3.6a), while the rest of the cultures had oxygen injected to either 7% (Fig. 3.5b and 3.6b) or 21% (Fig. 3.5c and 3.6c) in the headspace, also in triplicates. The accumulation of NO, N_2O and N_2 gas was monitored both before and after the injection of oxygen (as well as the untouched cultures for comparison) to see the effect of oxygen fluctuations and if denitrification would occur. Before the injection of oxygen, the NO_2^- concentration was measured, and KNO_2 was supplied to make sure all cultures had 4 mM NO_2^- available while oxygen was present to investigate whether O_2 and NO_2^- are reduced simultaneously or not.

In the untouched vials (0% O_2) both Pd1222 and GB17 could perform denitrification uninterruptedly, with near-negligible N_2O accumulation (N_2O_{max}: 0.03 - 0.04 µmol vial^{-1}). Inspection of V_e confirmed that the electron flow was entirely directed towards N-oxides. In the vials injected with 7% O_2, denitrification immediately stopped after the oxygen injection. A low activity, where Nos seemed more inhibited than the other reductases, resulted in some N_2O accumulation, which increased approximately 100-fold with maxima 2.71 - 4.45 µmol vial^{-1} during oxygen exposure. The further reduction to N_2 started approximately when [O_2] in the liquid was 25 µM, and the final N_2 concentration was similar to what was observed in the untouched vials. The start of denitrification was also confirmed by inspection of V_{e-}, where the graphs for oxygen reduction and N-oxide reduction cross simultaneously as the accumulation of N_2O was observed.

The last oxygen treatment was 21%, similar to the atmospheric composition. The same immediate stop of denitrification was observed when oxygen was injected into the vials. However, contrary to the 7% O_2 cultures, a much more significant accumulation of N_2O was observed before the final reduction to N_2 occurred. For Pd1222, the N_2O accumulation started when [O_2] in the liquid phase was approximately 90 µM, which goes on until the peak of 109.94 µmol vial^{-1} N_2O is reached. For GB17, the N_2O accumulation started when [O_2] in the liquid phase was approximately 75 µM, and the N_2O concentration reached a maximum level of 135.05 µmol vial^{-1}. The [O_2] in the liquid phase was approximately 30 µM when the reduction of N_2O to N_2 resumed. The final reduction to N_2 resumes for both organisms but at a lower rate than for the cells exposed to no or 7% O_2. In the time frame of the experiment, the electron flow of the 21% O_2 cultures never goes back to mainly N-oxide reduction for either of the organisms.

Summarised in Table 3.4 below is the maximum N_2O concentration (µmol vial^{-1}) measured throughout the aerobic denitrification experiment. In the samples with 7% O_2, the concentration of N_2O is almost 150x greater for Pd1222 and almost 70x greater for GB17 than the 0% O_2 samples. For the 21% O_2 samples, the N_2O concentration increases another 25x for Pd1222 and 45x for GB17 compared to the 7% O_2 samples. For both Pd1222 and GB17, the N_2O accumulation in untouched (0% O_2) cells was almost negligible.

Table 3.4. Maximum N_2O Concentration Measured. *The peak for N_2O concentration (µmol vial^{-1}) was observed in the different vials for both Pd1222 and GB17, all oxygen treatments included. The number in the parentheses indicates the number of replicates.*

Organism	Oxygen Injected	Max N_2O concentration (µmol vial^{-1})		
Pd1222	0%	0.03	±0.00	(3)
	7%	4.45	±0.21	(3)
	21%	110	±7.96	(3)
GB17	0%	0.04	±0.00	(3)
	7%	2.71	±0.41	(3)
	21%	135	±8.35	(3)

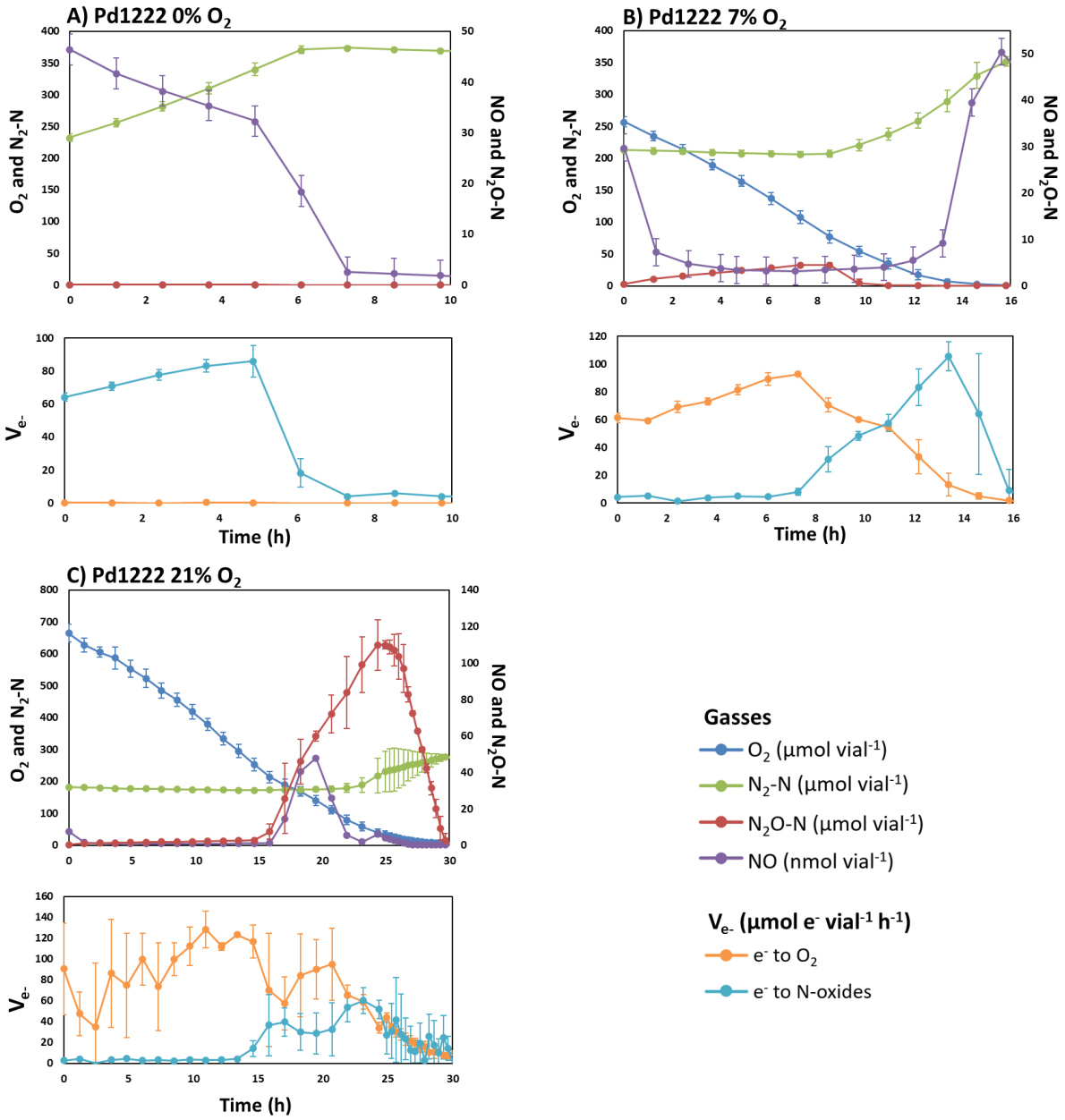

Figure 3.5. Gas Accumulation and Electron Flow for Different Oxygen Treatments of Pd1222. *Anaerobically raised Pd1222 cells were monitored in the robot incubation system regarding NO, N_2O and N_2 production before and after oxygen injection. Triplicates were made for each oxygen volume injected (0%, 7% or 21%). The panels show the gas graphs and electron flow for the following: A) 0% O_2 B) 7% O_2 C) 21% O_2. The x-axis indicates the time elapsed since the injection of oxygen.*

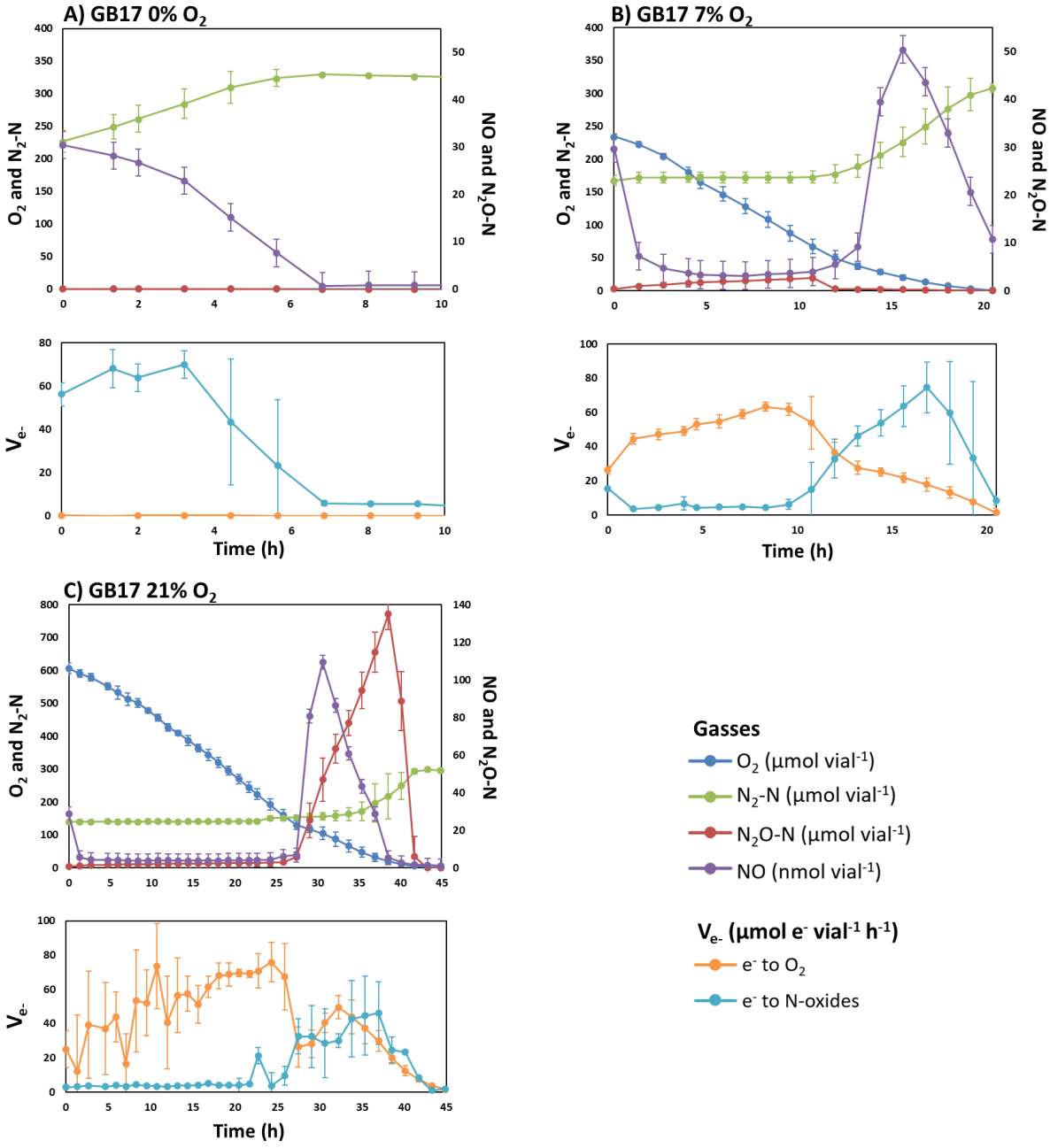

Figure 3.6 Gas Accumulation and Electron Flow for Different Oxygen Treatments of GB17. *Anaerobically raised GB17 cells were monitored in the robot incubation system regarding NO, N_2O and N_2 production before and after oxygen injection. Triplicates were made for each oxygen volume injected (0%, 7% or 21%). The panels show the gas graphs and electron flow for the following: A) 0% O_2 B) 7% O_2 C) 21% O_2. The x-axis indicates the time elapsed since the injection of oxygen.*

A closer scrutiny of the gas kinetics before, during and after oxygen exposure showed that the respective N-oxide reductases were differently affected. In vials injected with 7% O_2, there was a continuous, low activity and a slightly more potent inhibition of Nos than Nir + Nor, leading to N_2O accumulation (Fig. 3.7a and 3.7b). When oxygen approached depletion (at approx. 35 µM O_2 in liquid), denitrification resumed, with a temporarily higher N_2O activity relative to Nir + Nor (> 50%), before subsequent balanced anaerobic respiration.

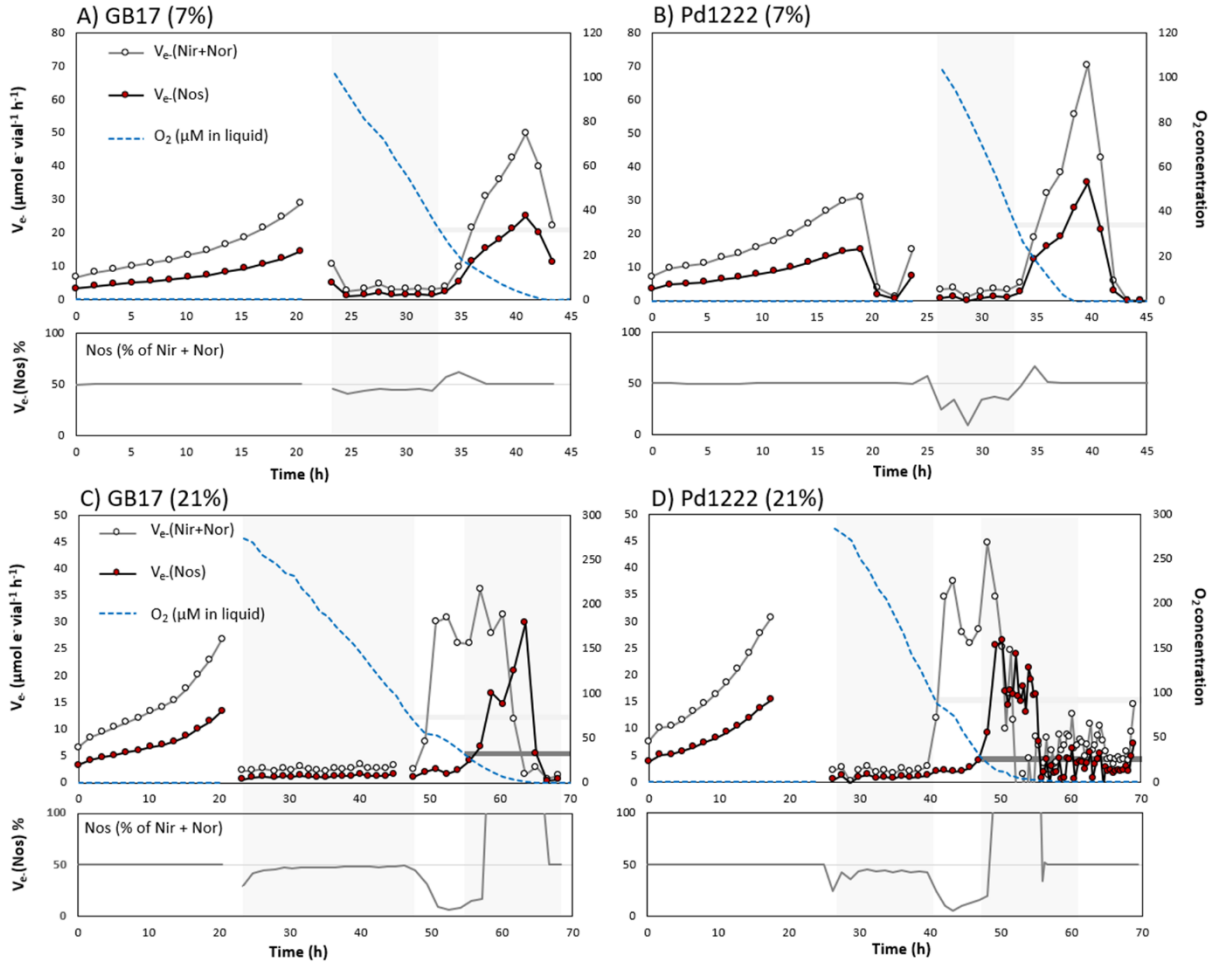

Figure 3.7 Activity of Nos and Nir + Nor Before, During and After Oxygen Exposure in Denitrifying Cultures of GB17 and Pd1222. *Large panels: electron flow (V_{e^-}, µmol e vial^{-1} h^{-1}) to Nir + Nor and Nos (left y-axis), and O_2 (µM in liquid; right Y-axis); narrow panels: % Nos activity relative to Nir + Nor throughout the experiment, in GB17 (A & C) and Pd1222 (B and D) exposed to 7 % O_2 (A & B) or 21% O_2 (C & D)—averages of triplicate vials for each time increment.*

In the cultures exposed to 21% O_2, the activity of Nos relative to Nir + Nor appeared slightly more affected in Pd1222 compared to GB17 during the oxic phase (Fig. 3.7c and 3.7d). However, the difference was minuscule and possibly coincidental. As the cultures switched to denitrification (at $O_2 \approx 90$ µM and 75 µM for Pd1222 and GB17, respectively), there was a dramatic depression in Nos activity relative to Nir + Nor, and nearly all of the available NO_2^- was transiently released as N_2O. At O_2 ~25-30 µM, Nos activity resumed in both GB17 and Pd1222. In GB17, $V_{e\text{-}(Nos)}$ increased until N_2O depletion resulting in a rapid reduction of N_2O, whereas Pd1222 showed a slightly different phenotype, where $V_{e\text{-}(Nos)}$ reached a maximum, after which it gradually dropped, while N_2O was still available. Subsequent N_2O reduction was slow (relative to GB17) and linear.

The relative activities of Nir + Nor and Nos before oxygen injection and after re-induction of denitrification in single vials showed negligible differences in apparent damage to Nos vs Nir + Nor in the cultures with 7% O_2 injected. However, they again illustrated a dramatic initial inhibition of Nos as cultures switched to denitrification after exposure to 21 % O_2 (Fig. 3.8). Moreover, in GB17, the activity of N-oxide reductases before vs after oxygen exposure appeared lower than in Pd1222, particularly pronounced in the 7% cultures (ratio $V_{e\text{-}}$ (Nir + Nor) and Nos < 0.8 and > 1 for GB17 and Pd1222, respectively).

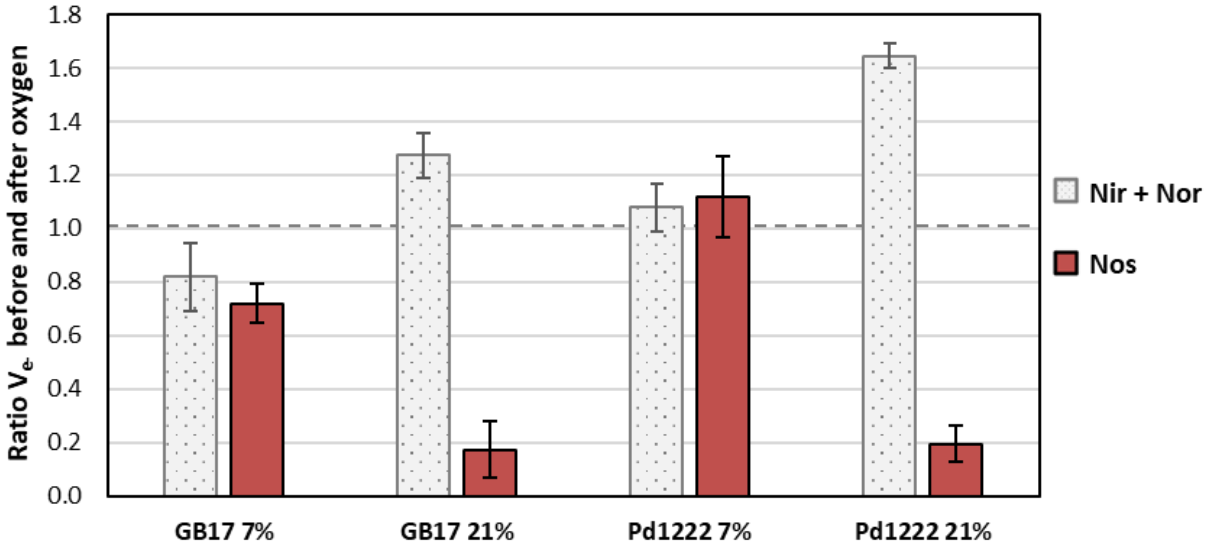

Figure 3.8 Ratio of $V_{e\text{-}(Nir + Nor)}$ and $V_{e\text{-}(Nos)}$ Before and After Oxygen Exposure. *The ratio of apparent enzyme activities in single vials (n=3 for each treatment) before injection of* oxygen *and after initial re-initiation of denitrification (the inflexion point after an initial rapid increase in $V_{e\text{-}}$ to NO-oxides and before apparent balanced anaerobic growth). A ratio of 1 indicates no change.*

The dry weight yield (g mol^{-1} e^-) in aerobic and anaerobic cultures of Pd1222 and GB17 were compared (Fig. 3.9a). The estimates for cell count (Fig. 3.2) and dry weight (Table 3.4) were used to estimate the yield per e^- based on cumulative e^--flow to terminal acceptors and measured OD_{660} in the cultures. Based on the results, GB17 seemed to have a slightly greater yield than Pd1222 for aerobic and anaerobic cultures. However, the difference was marginal (approximately 0.20 g mol^{-1} e^-), and the standard deviation for GB17 was generally higher (±0.40 g mol^{-1} e^- and ±0.20 g mol^{-1} e^- for aerobic and anaerobic cultures, respectively) than for Pd1222 (±0.33 g mol^{-1} e^- and ±0.10 g mol^{-1} e^- for aerobic and anaerobic cultures, respectively).

As well as comparing the dry weight yield of aerobic and anaerobic cultures of both organisms, the observed yield in cultures with 7% O_2 injected was compared to the expected yield in the respective cultures (Fig. 3.9 B). The observed dry weight yield was corrected for the assumed difference in dry weight yield, where anaerobic cultures are assumed to yield approximately 60% of the yield of aerobic cultures (Thauer et al., 1977). For Pd1222, the observed yield (4.31 ± 0.14 mg $vial^{-1}$) was slightly lower than the expected yield (4.80 ± 0.15 mg $vial^{-1}$). However, GB17 seemed to have a higher yield than Pd1222 and a greater observed yield (4.93 ± 0.07 mg $vial^{-1}$) than expected (4.69 ± 0.03 mg $vial^{-1}$).

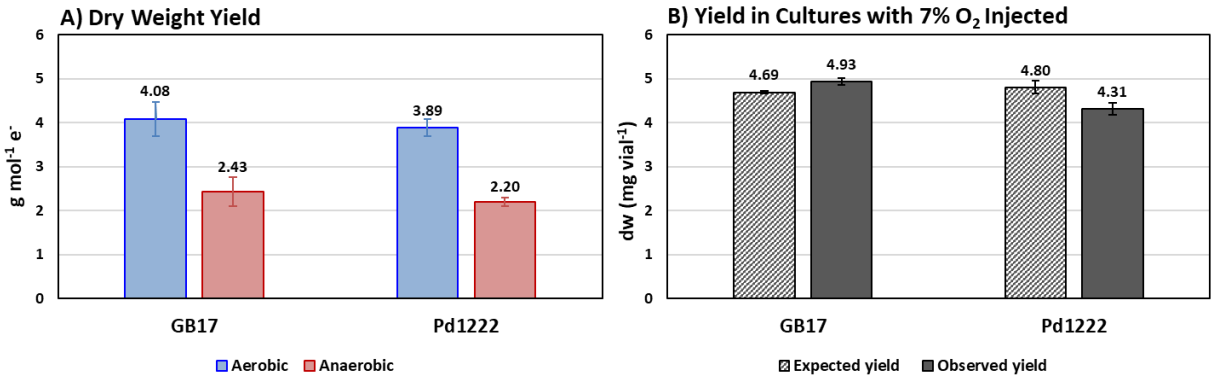

Figure 3.9 Dry Mass Yield in Aerobic, Anaerobic and Oxygen Spiked Anaerobic Cultures of Pd1222 and GB17. *Panel A: Dry mass yield (g mol^{-1} e^-) in aerobic and anaerobic cultures of GB17 and Pd1222. Panel B: expected and observed yields in cultures with 7% O_2 injected, based on cumulative e^--flow to terminal electron acceptors and observed OD_{660}.*

3.3.2 Glucose Assay

A glucose assay was performed on samples taken both prior to and after exposure to oxygen to estimate how much carbon was assimilated and how much was released as CO_2 under different conditions for both organisms. The readings from the standards were used to make a standard curve, and the slope will be used to estimate the concentration of the samples. The slope of the standard curve (Appendix B2) was:

$$y = 0.1256x \ (R^2 = 0.9974)$$

Based on the results from the plate reader, more than half of the samples showed an increased concentration of glucose, whereas the remaining showed a decrease (Appendix H). The results were surprising as no glucose was added during the oxygen exposure. The results were not trustworthy and not usable for estimations of cell yield for glucose as intended.

3.3.3 Part 2 – Collecting Samples for DNA and RNA Extraction

The aerobic denitrification experiment was repeated with only exposure to 7% O_2. The purpose was to collect samples for DNA and RNA extraction throughout the experiment for the following reasons: 1) to confirm by Sanger sequencing that there were two different organisms represented (Pd1222 and GB17), as the profiles from the previous experiment were very similar, 2) investigate by transcription analysis if there is transient inhibition of all or some of the functional genes when exposed to oxygen, and 3) investigate if there is an early transcription of *nosZ* compared to the other genes and if there was a peak in transcription at the start of complete denitrification.

The experiment was done for Pd1222 (Fig. 3.10a) and GB17 (Fig. 3.10b). Samples for both DNA and RNA extraction were collected from the aerobically raised cells prior to the inoculation of transition cultures. The anaerobically raised cells were monitored in the robot incubation system. Samples for RNA extraction were sampled at six different times during the experiment: 1) active denitrification with OD_{660} = 0.01, 2) active denitrification with OD_{660} = 0.30, 3) 30 min after oxygen injection, 4) 5 hours after oxygen injection, 5) NO-production, and 6) active denitrification. At the last sampling, samples for DNA extraction were also collected.

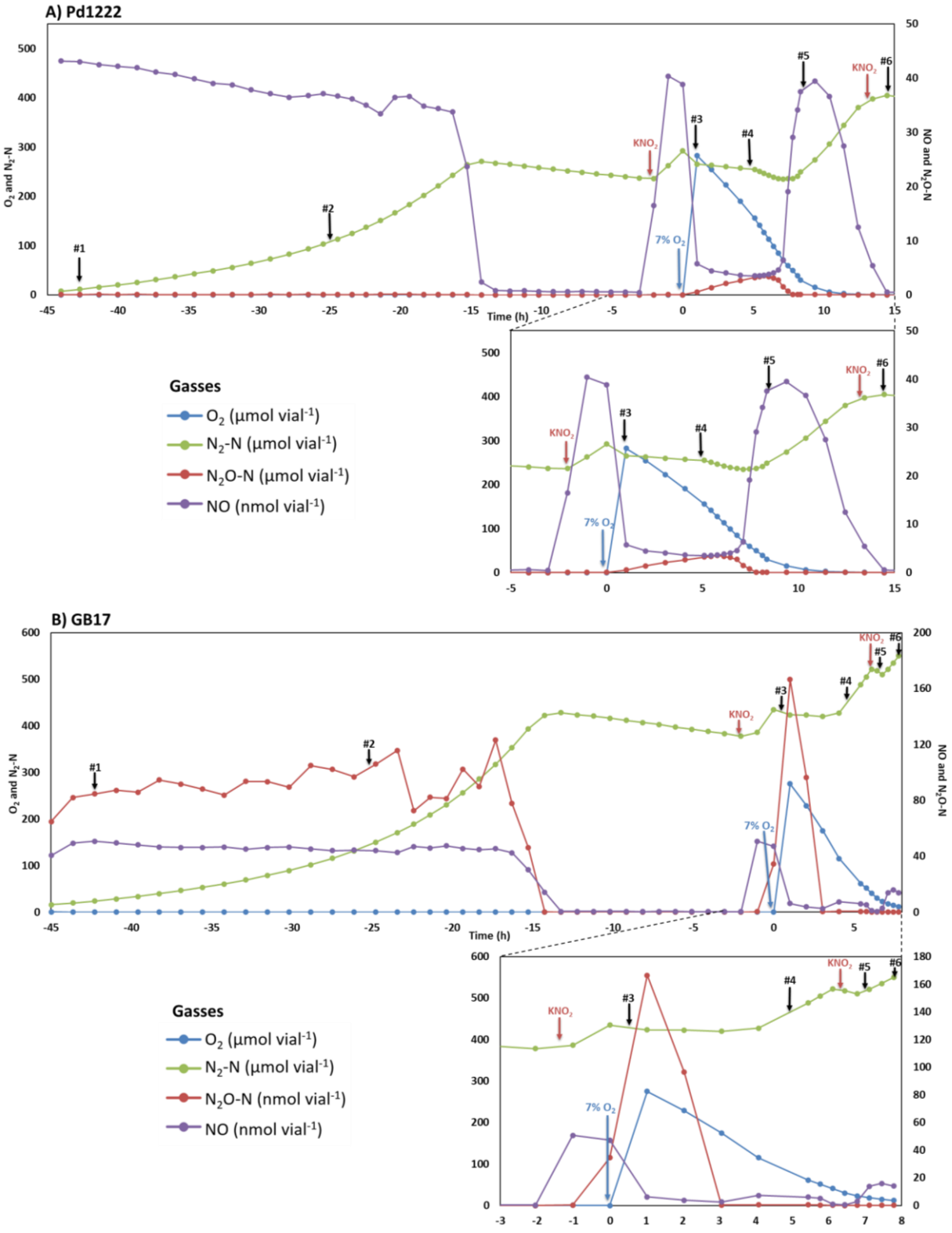

Figure 3.10 Gas Graphs from Part 2 of Aerobic Denitrification Experiment. *The x-axis shows the relative time since the* oxygen *injection. The black arrows indicate samplings. Red arrows indicate the supply of* KNO_2*, and blue arrows indicate the 7%* O_2 *injection. A) Pd1222 B) GB17*

3.3.4 Sanger Sequencing and BLAST of 16S

To verify that Pd1222 and GB17 were the actual two organisms studied in the experiment, DNA samples from the start of the experiment (aerobic) and DNA samples from the end of the experiment (anaerobic) were prepared for Sanger sequencing. The Sanger sequencing results were received as FASTA files, and two consensus sequences for both organisms (Appendix I) were made using Benchling, one based on the start samples (aerobic) and one based on the end samples (anaerobic).

NCBI's Basic Local Alignment Search Tool (BLAST®) was used to analyse the consensus sequences. For the Pd1222 samples, all of the top hits were sequences from *P. denitrificans*, and the very first hit was even strain-specific, stating Pd1222 (Accession CP000490.1). For the GB17 samples, the same was observed, with *P. pantotrophus* being all of the top hits, with hit number two being specific for DSM2944, corresponding to GB17 (Accession CP044426.1). For all the consensus sequences analysed by BLAST®, the E-value was <0.01. The E-value (expect value) is a parameter to describe the random background when searching the database, where a lower E-value is considered better. Generally, the E-value should be no higher than 0.01 to consider the match "significant" and not by random chance.

The identity percentage shows how many per cent of the base pairs in the query sequence are identical to the reference sequence. Generally, this should be greater than 98% to confirm that the query and the reference are the same species. For the consensus sequences analysed by BLAST®, the identity percentage was 99.9% for Pd1222 and 100% for GB17 (Table 3.5).

Table 3.5 Identity Percentage of Consensus Sequences Based on BLAST® Search. *Identity percentage after performing a BLAST search on the consensus sequences based on FASTA files retrieved from Sanger sequencing. The E-value for all sequences was 0.0.*

Organism	Sample Origin	Identity (%)
Pd1222	Start (Aerobic)	99.9
	End (Anaerobic)	99.9
GB17	Start (Aerobic)	100
	End (Anaerobic)	100

Alignments with Accession CP000490.1 and the consensus sequences for Pd1222 (Appendix J1) and Accession CP044426.1 and the consensus sequences for GB17 (Appendix J2) were also made. The ends of each consensus sequence were trimmed slightly to exclude a few mismatches, as mismatches at the ends are expected. The remaining few mismatches were not really mismatches, but rather a lack of signal causing undetermined bases in a few places. However, this occurred only twice for aerobically raised and once for anaerobically raised Pd1222 (Appendix J1).

3.3.5 Preparation of Standard Curve for qPCR

Before running the qPCR to amplify the denitrification genes, a standard curve was needed to calculate the number of mRNA transcripts of the different genes in the samples. The standards were made of clean DNA as the template and the standard primers (Table 2.8). Prior to making the standard curve, the primers and their Tm needed to be verified by gel electrophoresis, and a gel picture was taken for further inspection (Fig. 3.11). The first annealing temperature tested was 50°C, which resulted in one strong and clear band for *narG*, *nirS* and *norB* for Pd1222 and *narG*, *nirS* and *nosZ* for GB17. Pd1222 *nosZ* and GB17 *norB* gave no visible bands.

A new PCR was performed for these two genes, one at 50°C to eliminate the chance of something other than the Tm being wrong on the first try and one at 55°C to see if a higher annealing temperature would solve the problem. The result of this was multiple bands for Pd1222 *nosZ* at 50°C, a slightly weaker band for Pd1222 *nosZ* at 55°C, while GB17 *norB* gave a strong and clear band at both 50°C and 55°C. As the *nosZ* for Pd1222 at 50°C showed indications of another band, the annealing temperature for the subsequent runs was 55°C. For simplicity, that was the temperature used for the other genes, too, as they seemed to give similar results for 50°C and 55°C.

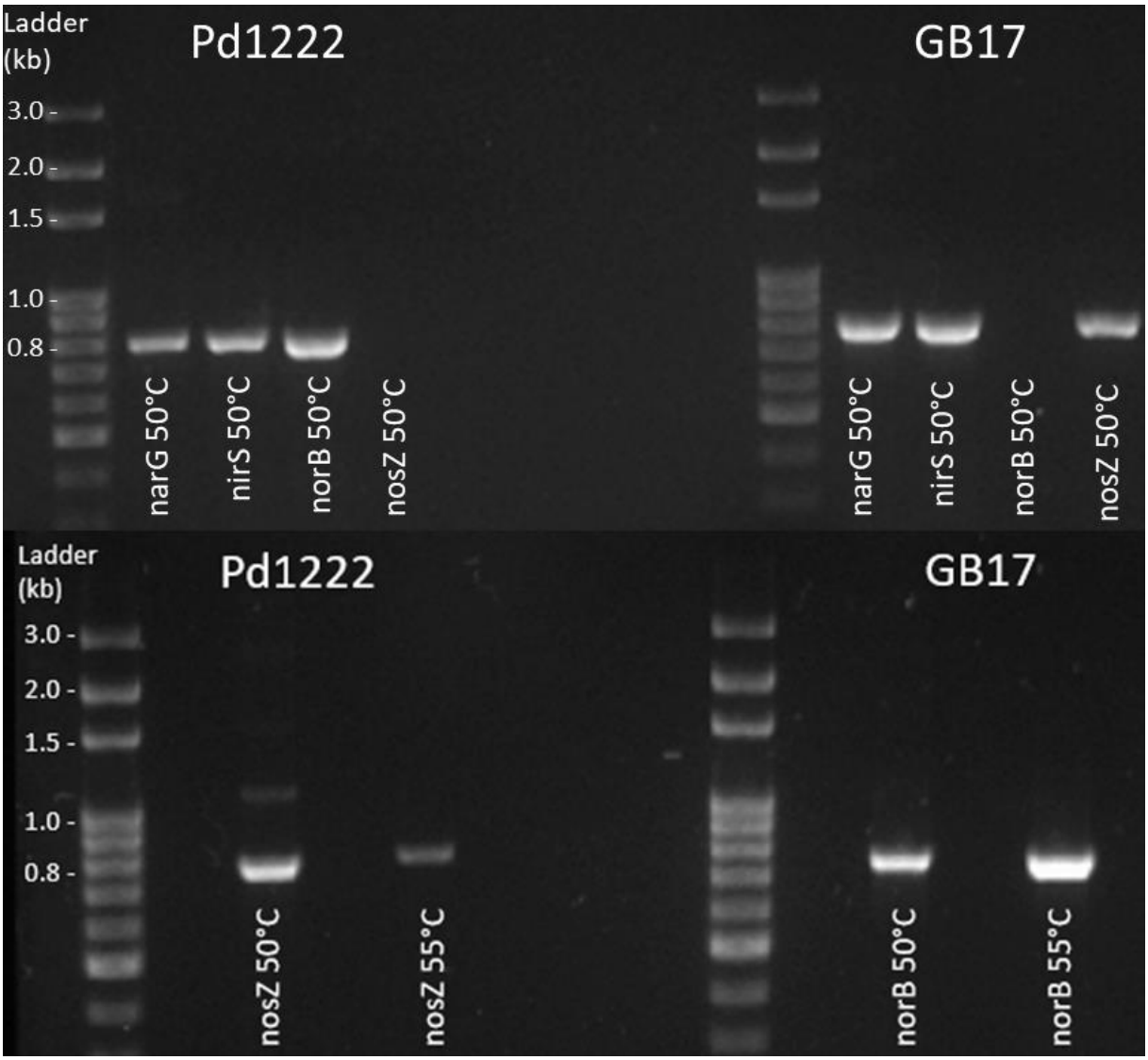

Figure 3.11 Gel Picture of Standards. *All standards for the target genes (narG, nirS, norB and nosZ) for Pd1222 and GB17 were run at 50°C. As Pd1222 nosZ and GB17 gave no bands on the first gel, they were tested again at 50°C as well as 55°C.*

The purified standards were then used as the template for ddPCR. Prior to ddPCR, estimates on the copy number μL^{-1} were needed to ensure the samples were not too saturated. The following equation was used to estimate the copy number μL^{-1}:

$$\frac{Concentration\ (ng\ \mu L^{-1}) \cdot\ 6.022\ \cdot 10^{23}}{Length\ (bp) \cdot 1\ \cdot 10^{9} \cdot 650} \qquad (eq.5)$$

The concentration in ng μL^{-1} was measured with NanoDrop, $6.022 \cdot 10^{23}$ is the Avogadro constant (number of atoms in one mole), the length of the product (estimated by using software

Benchling), $1 \cdot 10^9$ is a conversion factor, and 650 is the average mass of 1 bp dsDNA. The estimated copy number μL^{-1} for each sample is included in Appendix E3, along with the measured concentration by NanoDrop of the purified standards.

A dilution series based on the calculated copy number μL^{-1} was made, and the dilutions included were $1 \cdot 10^5$, $1 \cdot 10^4$, and $1 \cdot 10^3$ copies μL^{-1}. The ddPCR results (results not shown) were not analysed further, as multiple samples showed "no call", and there was no correlation between the estimated copy number μL^{-1} and dilutions for the rest of the samples. Even though an absolute quantification of the standards was unobtainable, the standards were used as the template for real-time PCR to make the standard curve based on Ct-values. The same dilutions based on the calculated copy number μL^{-1} were used for ddPCR, including a $1 \cdot 10^2$ copies μL^{-1} dilution. For some of the genes, graphs reminding of a standard curve were visible, but there was no correlation between the Ct-values and dilutions for most of the genes (results not shown). Based on the messy ddPCR and real-time PCR results, the plan of making a standard curve was discarded due to time limitations.

3.3.6 Purification of RNA

The initial on-column DNase treatment efficiency was tested by using the purified RNA samples as the template in real-time PCR to investigate the presence of residual gDNA in the samples. The real-time PCR was done before progressing to reverse transcription of RNA to cDNA, as gDNA would give false positives and a higher expression of genes than the actual amount. By running real-time PCR, the presence of residual gDNA was determined by the Ct-value of each sample.

The Ct-values for Pd1222 ranged from 4.89 – 37.00, with most of the samples being above 28.00, while the Ct-values for GB17 had a range of 16.96 – 39.86 with most of the samples being above 32.00 (Appendix K). Negative control for each organism was included. However, both got assigned "undetermined" regarding Ct-value; if not, the "acceptable" Ct-value for the other samples would have been 3 - 4 cycles lower than the negative control. As the negative controls had an undetermined Ct-value, the acceptable threshold was set to >35.00. Despite most samples having a Ct-value lower than desired, it was decided to proceed with reverse transcriptase as an extended treatment with TURBO™ DNase had already been done on all samples.

3.3.7 Quantification of Denitrification Genes

Before quantifying the targeted denitrification genes (*narG, nirS, norB* and *nosZ*), the purified RNA was converted to cDNA by reverse transcription as described in section 2.4.6. The concentration of cDNA (Appendix E4) was assumed to be the same as the purified RNA template (i.e., 100% conversion to cDNA).

An alternative way of quantifying the denitrification genes was explored, as no standard curve was obtained after trying both ddPCR and real-time PCR. The alternative way involved performing ddPCR on undiluted, 10^1 and 10^2 dilutions of cDNA from both Pd1222 and GB17 with primers for *narG, nirS, norB* and *nosZ*. The cDNA originated from the samplings taken during active denitrification prior to exposure to oxygen, as these samples were expected to have the highest transcription rate. This test run was done to indicate whether there was a signal and which dilution would give the best result. *nirS* and *norB* for Pd1222 gave "no call" on all concentrations. The remaining samples gave results for at least one of the dilutions, but there was no correlation between the concentration and the estimated copy number (results not shown).

A final test was done to investigate whether mRNA had degraded in the samples. ddPCR was performed with 10^2, 10^3, 10^4 and 10^5 dilutions of cDNA taken from the active denitrification prior to exposure to oxygen for both Pd1222 and GB17. Positive controls for each gene with DNA in 10^1 and 10^4 dilutions and the respective primers were also included, as well as negative controls with cDNA and DNA for both organisms, but without the primers. The results from the ddPCR (results not shown) did not give any valuable data regarding transcription analysis but confirmed that cDNA was present, which suggests mRNA degradation was most likely not the reason for the lack of results. Due to limited time, the transcription analysis attempts stopped here.

4 Discussion

Through this thesis, a series of experiments have been conducted. The first preliminary experiments included cell count estimations based on flow cytometry, microscopy and haemocytometry, followed by dry weight determinations. Next up was the experiment related to the CO_2 problem of anaerobic HCDC, where the aim was to establish the relationship between CO_2 and pH. The last set of experiments was the investigation of aerobic denitrification, whether it can occur or not, followed by Sanger sequencing and an attempt at transcription analysis.

4.1 Cell Count and Dry Weight

The preliminary experiments included cell count and dry weight measurements, intending to couple this to OD_{660} and establish which methods are the most reliable regarding cell count determination. Prior to the experiments, the given cell count estimates were $1.25 \cdot 10^9$ cells mL^{-1} OD_{660}^{-1} for aerobic cells and $1.60 \cdot 10^9$ cells mL^{-1} OD_{660}^{-1} for anaerobic cells. These were based on Pd1222 cultures grown with succinate as a carbon source, while the cultures used in this thesis were grown with glucose as a carbon source. Estimates for Pd1222 and GB17 grown under the relevant conditions used in this thesis were needed.

4.1.1 Flow Cytometry

Flow cytometry was the first method used to determine cell count. This method is way more convenient than microscopy and more direct than OD_{660} measurements, as the latter is not necessarily accurate regarding cell count under all conditions. As previously stated, both undiluted and 10x diluted cells of aerobically and anaerobically raised Pd1222 and GB17 cells were used for flow cytometry. For the results presented in section 3.1.1, only the 10x diluted cells were included. The undiluted cells gave estimates two and three orders of magnitude lower than the already low estimates based on the 10x diluted cells, assuming that the original cells mL^{-1} OD_{660}^{-1} estimates are accurate (Appendix G2). Different SYBR®Green concentrations were also tested, specifically 0.5x, 1x and 5x. The results were scattered and appeared to depend on the SYBR®Green concentration, too, as 0.5x generally gave higher estimates for Pd1222 and 1x gave higher estimates for GB17. For the cells stained with 5x SYBR®Green, only the 10x diluted cells gave an estimate. It was quickly concluded that this concentration was too high and excluded from the evaluation of which concentration would give the best result.

As well as diluting the cells prior to fixation and staining, the cells were sometimes diluted after the cells were applied to the flow cytometer when the events s^{-1} was too high. When performing flow cytometry, the desired events s^{-1} is about 300 - 400. If the events s^{-1} is higher, the samples need to be diluted. The rule of thumb is that samples with an OD_{660} between 0.1 and 1.0 need to be diluted x10 and samples with an OD_{660} above 1.0 need to be diluted 100x. In general, this happened mainly to the undiluted samples. Diluting the cells at this point also results in the dilution of the SYBR®Green used to stain them, and the final concentration might not be as intended for the experiment. Therefore, to gain the most accurate results, the dilution of samples should take place prior to fixation and staining.

The overall conclusion was that the cell count made by flow cytometry was underestimated. After a deeper analysis of the data in the CellStream™ Analysis software, a few factors seem to play a role in the low cell count. Firstly, the dot plot showing all the particles defined as bacteria shows a long "tail" on the right side of the defined gating, with increased side scatter and forward scatter (Appendix L). This "tail" suggests that the cells in the sample have aggregated, and the flow cytometer misinterprets these for bigger cells that go outside the defined gating. A possible solution is to disperse the cells by pipetting up and down a few times before applying the samples to the flow cytometer or disperse the cells using a syringe with a needle.

The protocol for preparing the samples and using the flow cytometer has been updated since the flow cytometry experiment related to this thesis was conducted. Vortexing or mixing of the samples while adding fixatives is recommended to penetrate the cells more efficiently and reduce aggregation. It is also known that samples fixated with formalin should be washed before performing flow cytometry, which was not done to the samples used in this work.

Secondly, it has now been a routine to wash the flow cytometer with 0.1% hypochlorite and then autoclaved, sterile-filtered (pore size 0.1 µm) MQ water between samples to avoid contamination of dye from the previous sample. Neglecting to do so can result in a higher cell count than the previous sample due to SYBR®Green being still present in the flow cytometer tubes, leading to a stronger signal for each run and giving false positives. However, the unstained samples and the samples stained with the lowest concentration of SYBR®Green were run first, ending with the samples with the highest concentration of SYBR®Green, meaning very strong contamination of SYBR®Green residues and false positives most likely were avoided.

In an attempt to make a conclusion based on the results from this experiment, diluting the cells 10x before staining gives the most accurate results, as undiluted cells gave a significantly underestimated cell count. Regarding the SYBR®Green concentration used to stain the cells, determining the "best" concentration is more challenging. Given that all the estimates are lower than expected, the most accurate estimate would be the highest. In other words, that will be 0.5x for Pd1222 and 1x for GB17. However, the difference between 0.5x and 1x was smaller for GB17 than for Pd1222, so if one concentration has to be regarded as the absolute best, it has to be 0.5x concentration. Based on the results, flow cytometry performed as the method was at the time of the experiment was unreliable for estimations of cell numbers in this experiment and, therefore, not used further.

4.1.2 Microscopy

As the estimate by flow cytometry seemed unreliable, another set of cell count estimates was made by microscopy and counting the cells using a Bürker counting chamber. These estimates were more similar to the original estimates based on Pd1222 grown with succinate but generally lower for both organisms and growth conditions. Even though the cells were counted manually, with the risk of making mistakes such as skipping cells or counting the same cell twice, the high R^2-value of all the regression lines (Fig. 3.2) suggests a strong linear relationship between the cells mL^{-1} and OD_{660}. As mentioned, the samples were fixated at six different OD_{660} values. Ten different squares were counted for all samples, and the mean was calculated. For three of the samples, all three of the triplicates were counted. Given the high number of squares counted and the relatively low standard deviation of those, the counting seems reliable, and not many human mistakes were made while counting. On the other hand, the linear relationship between OD_{660} and cells mL^{-1} was not as strong for samples with an OD_{660} below 0.50, as the count was generally lower than the regression line would suggest. The lower correlation could be because the samples with an OD_{660} of 0.10 and 0.25 were only based on one sample and not triplicates; in other words, only ten squares. By counting triplicates, the count will be based on 30 squares, resulting in a higher degree of statistical significance.

Automatic cell counters exist and could give an even more accurate estimate of the cell count and be more efficient and less drudgery for the user. Unfortunately, such a machine was unavailable for this experiment, and the cell count had to be done manually by haemocytometry. Counting cells by haemocytometry is a method with a high risk of errors and ranges from 20 - 30%. The high error rate can be due to chamber volume, sample volume and pipetting errors.

Regardless, counting cells using a haemocytometer is still widely used worldwide (EMS). Based on the results, the estimates based on microscopy and haemocytometry were more reliable than those based on flow cytometry. Therefore, those estimates were the ones used in further experiments.

4.1.3 Dry Weight

After the cell count estimations followed estimations of dry weight (g L^{-1} OD_{660}^{-1}). The dry weight was higher for aerobically raised cells than for anaerobically raised cells. The higher dry weight might be due to aerobically raised cells having more optimal conditions for cell growth, as oxygen is the most effective electron acceptor, resulting in maximal yield per electron acceptor (Chen & Strous, 2013).

Another reason for anaerobically raised cells' lower weight is most likely due to their smaller size and, thus, less cell mass than aerobically raised cells. The Pd1222 cells generally had a higher dry weight than GB17 cells, both for aerobically and anaerobically raised cells, where the difference was 0.05 and 0.07 g L^{-1} $OD_{660}^{-1,}$ respectively. The lower dry weight of GB17 is most likely due to the loss of cells during washing. After centrifuging to harvest the cells, the pellet was resuspended twice in 1 mL of MQ water. When removing the supernatant by pipetting, there is a risk of losing cells, and this proved to be particularly challenging with GB17 as the cell pellet was very loose compared to the firm pellets of Pd1222.

Finding other studies focused on the dry weight of Pd1222 and GB17 per OD_{660} proved difficult, except for one study by Bordel et al. (2021). They estimated a dry weight of 0.365 g L^{-1} OD_{660}^{-1} for Pd1222, which is about 0.1 g L^{-1} OD_{660}^{-1} higher than the results from this experiment. However, the carbon source available to the cells differed, as Bordel et al. used succinate. In contrast, the cells in this experiment were given glucose, suggesting the carbon source also affects the dry weight.

Another reason for the difference in dry weight might be the loss of cells during the washing steps. The washing of the cells was done similarly to what was described in Bordel et al. with the same number of replicates and washing steps, as well as using MQ water for the washing. The only difference was in the volume, as Bordel et al. used 2 mL instead of 1 mL as done in this experiment.

An alternative method to determine the bacterial cells' dry weight could be using a moisture analyser with an infrared heating source and analytical balance. This method is just as precise as the old-fashioned heating cabinet method (R^2 = 0.99), but instead of days of incubation, the dry weight is determined in less than an hour (Li & Mira de Orduña, 2010). Even though less time-consuming, the cost of such equipment might not be worth it if the only advantage is its efficiency.

4.2 The "CO_2 Problem" – Is It Solved?

As previously mentioned, one of the main challenges when performing anaerobic HCDC (Fig. 1.4) is the net change in pH being too small to trigger the acid pump due to denitrification increasing the pH but CO_2 lowering it. The aim was to investigate exactly how much CO_2 affects the pH of the medium and, based on the results, optimize the programmed pH setpoint equation to ensure HNO_3 is supplied to the cells when needed and avoid an unnecessary pause in cell growth.

4.2.1 The Reliability of the Data

The results from this experiment seem reliable as all of the triplicates from each set of treatments were highly similar, and there were no outliers within the triplicates. For the samples before acidification, the standard deviation was never greater than 0.05 for pH and pressure, but most had a standard deviation <0.01. After the acidification, the standard deviation increased slightly as the amount of H_2SO_4 varied slightly. For the samples in 20 mM PBS, the standard deviation for pH was generally around 0.4. For the samples in 100 mM PBS, however, the standard deviation for pH was <0.1 due to the medium's improved buffer capacity compared to the 20 mM. For the pressure, the standard deviation was highly similar, regardless of the molarity of the medium, acidification and presence of cells. The amount of injected CO_2 was also somewhat similar in all triplicates, which is seen as the dots being placed close to each other in the plot showing the pH as a function of P_{CO2} with few outliers within a triplicate (Figure 3.3). An entire triplicate ($P_{CO2} \approx 0.015$ atm for 100 mM PBS) was excluded when making the regression line to increase the R2-value as this triplicate seemed to be an outlier.

4.2.2 Implementation of the Results

By injecting known amounts of CO_2 into the buffer and waiting for equilibrium to be reached, the relationship between CO_2 concentration in the headspace and pH was established based on pH and pressure measurements. Knowing the start concentration of the medium and the concentration of CO_2 in the setpoint makes it possible to calculate the pH. However, this experiment was done without HNO_3, and H_2SO_4 was added at the end of the experiment to lower the pH and force all CO_2 to the headspace.

Another experiment (not a part of this thesis) was conducted without CO_2 but included HNO_3 to establish the effect HNO_3 has on the pH. Combining the results of both experiments, an equation that considers both CO2 and HNO3 was made (eq.4). All except P_{CO2} are fixed values, so the only factor affecting the pH_{SP} is the P_{CO2} which is measured in the reactor constantly. By programming the pH setpoint to follow this equation, the pH setpoint continuously changes as a response to the changes in [CO_2]. The pH of the reactor will fluctuate around the pH setpoint, resulting in the addition of HNO_3 when the pH increases, an important step towards an optimised process.

The results from the CO_2 experiment can also be implemented into KinCalc, making the calculations about C-uptake in biomass (yield) based on gas kinetics more robust. In addition to usage for purely physiological studies, it also allows more accessible and faster screening of denitrifying bacteria in search of "high yield" organisms, which in turn can be further explored as potential producers of proteins and biomass in HCDC.

4.3 Aerobic Denitrification – Does It Occur?

The other main aim of this thesis was to investigate if *P. pantotrophus* (strain GB17), previously described as an aerobic denitrifier, displays aerobic denitrification under stringently controlled conditions (mineral medium, low cell density, rigorous stirring). GB17 was also compared to the model organism *P. denitrificans* (strain Pd1222), which is not known for aerobic denitrification. Comparing their yield and electron flow to electron acceptors during and after oxygen exposure can establish if GB17 is more tolerant to oxygen, making it a more robust choice as a potential candidate for anaerobic HCDC.

4.3.1 Analysing the Gas Data from Part 1

Both organisms behaved similarly and showed a near-complete arrest of denitrification when exposed to oxygen. For both cultures with 21% O_2 injected (Fig. 3.5c and 3.6c), denitrification resumes in two pulses; First, a period with a considerable accumulation of N_2O, followed by a temporary depression and then a reduction of N_2O. One possibility is that the N_2O reduction rate is tightly coupled to O_2 concentration and is prone to a more potent inhibition than the other reductases. Another possibility is that this results from the destruction of existing Nos proteins, followed by the construction of new Nos proteins. It might also be a combination of those two. Nos was marginally more inhibited than Nir + Nor in Pd1222 under the oxygen pulse, resulting in a slightly higher concentration of N_2O in the presence of oxygen (Table 3.4). For cultures with 7% O_2 injected, the maximal N_2O concentration was observed during the oxygen pulse. However, this is unknown for cultures with 21% O_2 injected, as Table 3.4 only reports the maximal N_2O concentration for the experiment. However, the relative activity of Nir + Nor compared to Nos in cultures with 7% O_2 (Fig. 3.7a and 3.7b) and 21% O_2 (Fig. 3.7c and 3.6d) can be used as a reference for what to expect. When looking at the Nos activity after denitrification is triggered in the 21% O_2 vials, the same tendency is observed in Pd1222 compared to GB17.

As seen in the gas accumulation for GB17 exposed to 21% (Fig. 3.6c), N_2O reached a peak, but towards the end of incubation and NO_3^-/NO_2^- and NO are depleted, N_2O is reduced rapidly to N_2. This pattern is also seen in Fig. 3.7c, as V_e-(Nos) increased rapidly and peaked before the activity stopped because all N-oxides were reduced to N_2. For Pd1222, it is also observed a peak in N_2O at the same time as NO_3^-/NO_2^- and NO are depleted, but the reduction of N_2O to N_2 was slower and linear (Fig. 3.5c). This difference in reduction rate can be due to differences between the organisms but also a result of random variations. Additional experiments would have been necessary to determine this, including careful monitoring of carbon and other elements to ensure no limitations would affect the results. During balanced denitrification, the activity of Nos is 50% of the sum of Nir + Nor together, also evident in the lack of N_2O accumulation. In the presence of O_2, Nos is relatively a bit lower, and N_2O accumulation is observed. When denitrification is triggered again in the cultures exposed to 7% O_2 ($[O_2] \approx 35$ µM in the liquid phase), it appears that N_2O is activated first. The explanation for this may be that *nosZ* is transcribed at higher O_2 than *nir* and *nor,* as shown in Qu et al. (2016), resulting in a temporarily bigger pool of Nos.

Another explanation could be that the Nos pool is always relatively bigger than Nir + Nor, and the observed changes are due to the reactivation of old enzymes. When excess N_2O is reduced, the subsequent Nos activity is restricted by the activity of Nir + Nor, which provides N_2O. For the cultures with 21% O_2, it is observed that when denitrification is triggered ($[O_2] \approx 90$ μM and 75 μM for Pd1222 and GB17, respectively), the Nos activity relative to Nir + Nor is significantly reduced. The reduced activity is most likely due to the destruction of the old Nos pool and probably that the *de novo* synthesis of Nos is not activated at high O_2 concentrations. The activity of Nir + Nor starts and seems to compete with the oxidases about electrons (transient lower O_2 respiration). The activity of Nos increases dramatically when $[O_2] \sim 25$ μM. Both organisms are quite similar, but generally, Pd1222 has a slightly higher respiration rate, most likely due to the higher density.

Another matter of interest was comparing the yield of Pd1222 and GB17, both aerobically and anaerobically raised cells. When comparing aerobically and anaerobically raised cells, it is expected that the yield of anaerobically raised cells is 60% of the yield of aerobically raised cells (Thauer et al., 1977). This ratio was observed for the dry weight determinations (Fig. 3.9a), as the yield for anaerobically raised cells was 57% and 60% of the yield of aerobically raised cells for Pd1222 and GB17, respectively. When comparing the yield in cultures with 7% O_2 injected of Pd1222 and GB17 (Fig. 3.9b), minor differences are observed between the organisms, and it appears to be a slightly smaller yield for Pd1222 than for GB17. The expected yield was highly similar for both organisms, but the results show that the observed yield of GB17 was slightly above the expected yield, while the observed yield of Pd1222 was slightly below.

Suppose this minor difference is due to actual differences between the organisms, not random variations. In that case, the results suggest that GB17 might be a more robust candidate for HCDC than Pd1222, as the observed yield compared to the expected yield was not affected by the fluctuating conditions (switch from aerobic respiration to denitrification).

4.3.2 Glucose Assay

Ideally, the combination of improved estimation of CO_2 in experimental vials, final measurement of pH in sealed vials and accurate measurements of glucose would provide information about how much carbon was assimilated and how much was released as CO_2 under the different conditions for both organisms and use this knowledge in the evaluation of a potential candidate for anaerobic HCDC. However, the results from the glucose assay (Appendix H) did not make sense, as the concentration apparently increased throughout the experiment. The cells used glucose as their carbon source and were expected to consume it, leading to a lower concentration. Especially the samples exposed to 21% O_2 were expected to have a noticeable decrease in glucose concentration.

A possible reason for this is the presence of interfering components in the media. The standards used for the assay were dissolved in distilled water but could have been dissolved in the media used instead. Previous tests (not a part of this thesis) have been done where standards have been dissolved in distilled water and media and compared to each other. However, the result was only minor changes, concluding that dissolving in distilled water or media would give more or less the same results when performing a glucose assay, especially as the used medium was clearly defined and not complex. Theoretically, the assay should be sensitive enough to detect the changes in glucose concentration for this experiment, especially for the cultures injected with 21% O_2. The conclusion was that the most likely reason for the failed results was due to interfering components, and the results were not analysed further.

An alternative method to determine the yield from carbon in this experiment is to perform high-performance liquid chromatography (HPLC). HPLC is a common analytical technique to detect different components, like glucose (Galant et al., 2015; Ma et al., 2014; Wilson et al., 1981). HPLC consists of two phases, a mobile phase that dissolves the compound and a stationary phase that interacts with the compound. The compound is injected into the mobile phase, and due to the Van der Waals force between the compound and the stationary phase, the compound will move through the column at different speeds based on the affinity. A detector connected to the outlet of the columns will monitor the time the compound takes to move through the HPLC system (Gupta et al., 2012). The main disadvantages of this method are time and cost. HPLC is expensive to set up, and preparing the samples for HPLC can be challenging and time-consuming.

4.3.3 Sanger Sequencing

Sequencing of the 16S rRNA gene is a common way of identification and classification. In this experiment, the sole purpose of the 16S rRNA sequencing was to verify that Pd1222 and GB17 were indeed the two strains present in the respective vials and that the cultures were pure from start to end. If that were not the case, all the results from the previous aerobic denitrification experiment and the upcoming transcription analysis would be invalid.

Choice of Sequencing Method

The chosen method to do so was Sanger sequencing, a "first-generation" DNA sequencing method, and it is common practice to use when there are only a few samples from pure cultures to be sequenced. Sanger sequencing holds many advantages, especially for organisms that are difficult to culture. One of the main disadvantages is probably the time-consuming process of preparing the samples for sequencing and sending them to another laboratory for identification, as this is done primarily in reference laboratories. Newer methods exist, like next-generation sequencing (NGS), where the number of fragments sequenced simultaneously is much higher. However, Sanger sequencing is still used worldwide due to its simplicity and unrequired need for validation (Hagemann, 2015).

Analysing the Data

As stated in the results, all samples had a high identity match with the reference strains from NCBI's database (Accession CP000490.1 for Pd1222 and CP044426.1 for GB17). There is no doubt that the strains used for both Sanger sequencing and transcription analysis were *P. denitrificans* Pd1222 and *P. pantotrophus* GB17. This was also confirmed when making an alignment based on consensus sequences. After the ends of each consensus sequence were trimmed slightly, no "real" mismatches were present, if not counting the few undetermined bases (Appendix J). Therefore, the conclusion was that Pd1222 and GB17 were indeed the two strains present in the respective vials and that the cultures were pure from start to end.

4.3.4 Transcription Analysis

The transcription analysis intended to investigate changes in the genes for denitrifying cells before and after oxygen exposure. Due to limited time, the transcription analysis was not completed. However, the gas data from the second incubation experiment largely confirmed the observations made for cultures injected with 7% O_2 in the first aerobic denitrification experiment. The exception was a lower accumulation of N_2O in the GB17 cultures than in the first experiment, which supports the assumption of Nos in Pd1222 being marginally more sensitive to oxygen.

Lack of Standard Curves

One of the most time-consuming tasks was the attempt to make a standard curve for quantifying the denitrification genes *narG*, *nirS*, *norB* and *nosZ*. Designing the primers, amplifying and purifying the standards went smoothly, but when performing ddPCR, things started going wrong. The idea was to make a dilution series of each standard and then use three of the dilutions to make a standard curve based on the absolute quantification acquired by ddPCR. However, multiple samples got "no call", and for those who gave an estimated number of copies, there was no correlation between the dilutions, as the lower dilutions often had a higher copy number than the previous (results not shown). ddPCR was performed twice, and new dilution series was made for the second round of ddPCR.

The dilution series was made carefully, eliminating the risk of errors from that step. For the first dilution, the estimated copies μL^{-1} was 10^9, based on an equation (eq.5) and the concentrations measured by NanoDrop (Appendix E3). The samples were diluted thoroughly by pipetting up and down multiple times. New tips were used between each dilution, ensuring no residues of a higher concentrated dilution were carried over to the new one. There should therefore be no reason to believe the flaw was in the dilution series itself. After two attempts to make a standard curve based on absolute quantification by ddPCR, real-time qPCR was tried instead. However, the same issue followed here, with no clear correlation between dilutions and Ct-value (results not shown). Due to time limitations, no further attempts were made, and the standard curve was discarded. The conclusion to the problem was most likely either the choice of an assay, which here was SYBR®Green, or the primers and the PCR program regarding the annealing temperature.

Choice of Assay – SYBR®Green VS TaqMan

For the transcription analysis, SYBR®Green was used, which is a relatively cheap method based on DNA binding dye. A possible solution to the problem could be to design TaqMan assays specifically for the desired target genes in Pd1222 and GB17 instead. TaqMan assays are based on hybridization probes and 5' to 3' exonuclease activity of Taq polymerase and have multiple advantages over SYBR®Green, such as a higher specificity and efficiency (Samanthi, 2017). However, as TaqMan assays are costly, they are not the first choice when the goal is to investigate multiple genes in two organisms. Initially, a common TaqMan assay was attempted to be designed but failed due to the sequences of some genes differing too much. With more time and a higher budget, new TaqMan assays could have been designed specifically for each organism and selected genes, like *nirS* and *nosZ*. Ideally, monitoring of all the functional genes *narG, nirS, norB* and *nosZ* is of interest, but due to economic reasons, *nirS* and *nosZ* would be the main priority. The reason why *nirS* and *nosZ* are of particular interest is because of their respective enzymes' role in denitrification. Nir reduces NO_2^- to NO, which is the requirement for denitrification *sensu stricto*, while Nos is responsible for reducing the potent greenhouse gas N_2O to harmless N_2 gas. In addition, it is assumed that *nir* and *nor* are triggered and expressed quite similarly, as they are subject to the same regulators and Nor must follow Nir to prevent NO accumulation, which is lethal to the cells. Like *nir* and *nor*, *nosZ* is also regulated by NNR, but the transcription of *nosZ* is also triggered by FnrP (at least in Pd1222). *nosZ* expression and Nos activity do not necessarily follow *nir* and *nor*, and the consequence is the accumulation of N_2O.

Primer Design

Designing the primers turned out to be challenging for some of the genes. For the 16S gene primer pairs (Lane, 1991), the primers were general and well-known to many laboratories. The primers were known to work for at least Pd1222 and were confirmed to work for GB17 on the first try. The standard primer pairs (Appendix C2) were explicitly designed for Pd1222 and GB17. As mentioned earlier, most of the primers worked on the first try with an annealing temperature of 50°C, and the remaining primers worked after raising the annealing temperature to 55°C. On the other hand, the primer pairs designed for the denitrification genes (Appendix C1) turned out to be somehow problematic. Some of the primers needed to be replaced with new ones, as they would not bind to the desired area of the target genes for unknown reasons. The most likely reason is the PCR program's annealing temperature being too low.

If the experiment were to be repeated, a strategy would be to run a PCR gradient with an annealing temperature between 50°C and 65°C. By selecting the highest temperature as possible for the primer pairs in further runs, a higher level of specificity is reached for the PCR reaction. When designing the primers, many different precautions were taken. The first factor is the Tm of the primers. Primer3 and Sigma-Aldrich gave two very different Tm for all primers (Appendix C). The Tm was also calculated manually by the rule of thumb where each A and T count 2°C and each C and G count 4°C. Using this method, the Tm given by Primer3 was the most accurate. Different annealing temperatures were tried out, ranging from 50°C to 58°C. Primer dimers were avoided using the Sigma-Aldrich Oligo tool, and the primers were also controlled not to form prominent hairpin structures. The last precaution was to avoid several T and A bases at the 3'end of the primers, as G and C are considered more stable. Several co-workers were involved in the process of designing the primers to avoid obvious mistakes, and for some of the primers that would not initially work, the problem was solved. For the remaining, new primers had to be designed to replace the old ones.

Working with RNA

mRNA is easily degradable and requires careful handling. Even though the samples were quickly stabilized, some mRNA for the relevant genes are still expected to degrade. The rapid degradation is due to the half-life of mRNA, which is in the order of minutes (Chan et al., 2018). When the cells are exposed to air, the transcription of the relevant genes will presumably stop, and degradation (which takes place all the time) will dominate. Thus, the net number of mRNA for the denitrification genes is likely to be somewhat lower in cells after short exposure to oxygen (Qu et al., 2016). Another challenge was the removal of gDNA from the RNA extraction samples. The extraction and purification of RNA took place in two rounds, first for Pd1222 and then GB17. First, only the on-column DNase treatment of 15 min included in the RNA extraction kit (section 2.4.5) was used. As this was insufficient, the same on-column DNase treatment was performed with an hour of incubation instead of only 15 min. Still, the results were unsatisfactory, leading to the additional DNase treatment using TURBO™ DNase (section 2.4.5). For the Pd1222 samples, the TURBO™ DNase treatment was given after two attempts with the on-column DNase treatment. For the GB17 samples, the TURBO™ DNase treatment was given immediately after the purification. With more handling of the samples, the higher risk for degradation of mRNA and contamination of gDNA. When comparing the Ct-values of Pd1222 and GB17, the Pd1222 samples generally had lower Ct-values, indicating the presence of more gDNA, which might be due to the excessive handling compared to the GB17 samples.

5 Conclusion and Further Research

5.1 Conclusion

With an increased population in the world, food and feed production is more crucial than ever, and with a shortage of proteins, new methods of producing them are needed. Existing HCDC methods are based on aerobic respiration, with the limitations it entails. A novel HCDC method is under development, aiming at SCP production by anaerobic HCDC (Bergaust et al., 2022). Through this thesis, a series of experiments have been conducted. The first preliminary experiments included cell count estimations based on flow cytometry, microscopy and haemocytometry, followed by dry weight determinations. Next up was the experiment related to the CO_2 problem of anaerobic HCDC, where the aim was to establish the relationship between CO_2 and pH. The last set of experiments was the investigation of aerobic denitrification, whether it can occur or not, followed by Sanger sequencing and an attempt at transcription analysis.

As initially stated, there were two main aims of this thesis: The first was to investigate the effect CO_2 has on pH in the hope of helping optimise the anaerobic HCDC method and solve the so-called "CO_2 problem". Together with the results of another experiment not a part of this thesis, a new equation (eq.4) was made and used in programming the pH-stat. So far, it seems like this has been successful, and a step in the right direction has been taken in optimising the anaerobic HCDC method. Moreover, the now-established relationship between CO_2 dissolved in liquid and pH has led to the optimisation of the carbonate chemistry algorithm of KinCalc, which will be helpful in future experiments.

The second main aim was to investigate aerobic denitrification, specifically in *P. pantotrophus*, as an aerobic denitrifier would be the perfect candidate for anaerobic HCDC due to potential oxygen leakages. Contrary to previous reports of *P. pantotrophus* being an aerobic denitrifier (Robertson & Kuenen, 1983; 1984; 1985), the results in this thesis do not imply this is the case. However, these results are insufficient to prove or reject this, and more research is needed. Besides this, more knowledge of how oxygen fluctuations lead to the emission of N_2O and NO is acquired, showing how much the accumulation increases under different oxygen concentrations.

In addition to the main aims of the thesis, more data has been collected regarding the relationship between optical density, cell count and dry weight of both *P. denitrificans* and *P. pantotrophus*. Knowledge like this was not only beneficial for the experiments conducted as a part of this thesis, but can also help make better and faster estimates of cell count and dry weight in future experiments as well, by only doing the fast and easy spectrophotometrically measurement of OD_{660}. The estimates of cell count, dry weight and OD_{660} were also used to investigate and compare the yield per mol e^- in Pd1222 and GB17 under aerobic and anaerobic conditions and when challenged with exposure to oxygen during active denitrification.

In an attempt to draw a tentative conclusion based on the results of this thesis, *P. pantotrophus* type strain GB17 appears to be marginally better for SCP production by anaerobic HCDC than *P. denitrificans* strain Pd1222 regarding the observed dry weight yield per mol e^- and robustness of Nos when exposed to oxygen.

5.2 Further Research

A similar aerobic denitrification experiment can be designed if granted one more year of working on this thesis. However, instead of just one injection of oxygen, the cells can be exposed to oxygen in multiple fluxes, which simulates the natural environment more precisely than just one single wave of oxygen. Doing such an experiment would give information about how the strains cope with being exposed to oxygen fluctuations; maybe they handle multiple exposures to oxygen just as well as the first, or maybe the first flux is destroying their ability to rebuild the necessary apparatus back to the original, and their ability to cope will be reduced for each new exposure? As implied in section 4.3.4, to investigate the changes in the transcriptome of the bacteria, a new analysis should be performed with TaqMan assays instead of the SYBR®Green assay used. Such analyses would increase the understanding of how oxygen fluctuations affect the transcription of genes encoding the denitrification-related reductases.

As well as performing a better and more specialized transcriptome analysis, proteomics analysis can also be done, which was intended for this thesis. However, due to limited time, it never proceeded past the sampling of cells. Proteomics analyses would be helpful combined with detailed gas kinetics and transcriptional analysis to obtain a comprehensive picture. At the same time, the presence of a peptide does not necessarily mean one has a functional protein.

Proteomics analyses are used to separate and identify the proteins expressed by the genome (Le et al., 2019) and have already been performed on Pd1222 to explore the denitrification proteome (Olaya-Abril et al., 2018). It would be interesting to compare the proteome before and after exposure to oxygen, investigate the relative differences, and compare the widely studied model organism *P. denitrificans* to *P. pantotrophus*, which is not investigated as much. The implications of this work, especially if it is continued, may increase our understanding of which mechanisms drive N_2O emission in complex systems and have implications for the biotechnological application of denitrification, e.g., in HCDC.

References

Ambus, P., & Zechmeister-Boltenstern, S. (2007). Chapter 22 - Denitrification and N-Cycling in Forest Ecosystems. In H. Bothe, S. J. Ferguson, & W. E. Newton (Eds.), *Biology of the Nitrogen Cycle* (pp. 343-358). Elsevier. https://doi.org/https://doi.org/10.1016/B978-044452857-5.50023-0

Appelo, C. A. J., & Postma, D. (1993). *Geochemistry, Groundwater and Pollution*. A.A. Balkema.

Appelo, C. A. J., & Postma, D. (2004). *Geochemistry, Groundwater and Pollution*. CRC Press. https://doi.org/10.1201/9781439833544

Bakken, L. R., Bergaust, L., Liu, B., & Frostegård, Å. (2012). Regulation of denitrification at the cellular level: a clue to the understanding of N ₂ O emissions from soils. *Philosophical Transactions of the Royal Society B: Biological Sciences*, *367*(1593), 1226-1234. https://doi.org/10.1098/rstb.2011.0321

Barney, B. M., Lee, H.-I., Dos Santos, P. C., Hoffman, B. M., Dean, D. R., & Seefeldt, L. C. (2006). Breaking the N2 triple bond: insights into the nitrogenase mechanism [10.1039/B517633F]. *Dalton Transactions*(19), 2277-2284. https://doi.org/10.1039/B517633F

Baumann, B., Van Der Meer, J. R., Snozzi, M., & Zehnder, A. J. B. (1997). *Antonie van Leeuwenhoek*, *72*(3), 183-189. https://doi.org/10.1023/a:1000342125891

Beijerinck, M. W., & Minkman, D. C. J. (1910). Bildung und Verbrauch von Stickoxydul durch Bakterien. *Zentralblatt für Bakteriologie, Parasitenkunde und Infektionskrankheiten und Hygiene*, *25*, 30-63.

Bergaust, L., Bakken, Lars R., & Frostegård, Å. (2011). Denitrification regulatory phenotype, a new term for the characterization of denitrifying bacteria. *Biochemical Society Transactions*, *39*(1), 207-212. https://doi.org/10.1042/bst0390207

Bergaust, L., Horn, S. J., & Bakken, L. R. (2022). *Method of culture//2019_13 NIMIPROD* UK patent application No. 2200070.7).

Bergaust, L., Mao, Y., Bakken, L. R., & Frostegård, Å. (2010). Denitrification Response Patterns during the Transition to Anoxic Respiration and Posttranscriptional Effects of Suboptimal pH on Nitrogen Oxide Reductase in Paracoccus denitrificans. *Applied and environmental microbiology*, *76*(19), 6387-6396. https://doi.org/doi:10.1128/AEM.00608-10

Bergaust, L., Van Spanning, R. J. M., Frostegård, Å., & Bakken, L. R. (2012). Expression of nitrous oxide reductase in Paracoccus denitrificans is regulated by oxygen and nitric oxide through FnrP and NNR. *Microbiology*, *158*(3), 826-834. https://doi.org/10.1099/mic.0.054148-0

Berks, B. C., Ferguson, S. J., Moir, J. W., & Richardson, D. J. (1995). Enzymes and associated electron transport systems that catalyse the respiratory reduction of nitrogen oxides and oxyanions. *Biochimica et Biophysica Acta (BBA)-Bioenergetics*, *1232*(3), 97-173.

Berry, E. A., Guergova-Kuras, M., Huang, L. S., & Crofts, A. R. (2000). Structure and function of cytochrome bc complexes. *Annu Rev Biochem*, *69*, 1005-1075. https://doi.org/10.1146/annurev.biochem.69.1.1005

Bertero, M. G., Rothery, R. A., Palak, M., Hou, C., Lim, D., Blasco, F., Weiner, J. H., & Strynadka, N. C. (2003). Insights into the respiratory electron transfer pathway from the structure of nitrate reductase A. *Nature structural & molecular biology*, *10*(9), 681-687.

Bordel, S., Van Spanning, R. J. M., & Santos-Beneit, F. (2021). Imaging and modelling of poly(3-hydroxybutyrate) synthesis in Paracoccus denitrificans. *AMB Express*, *11*(1). https://doi.org/10.1186/s13568-021-01273-x

Bothe, H., Ferguson, S., & Newton, W. (2007). In Elsevier (Ed.), *Biology of the nitrogen cycle*.
Burns, L. C., Stevens, R. J., & Laughlin, R. J. (1996). Production of nitrite in soil by simultaneous nitrification and denitrification. *Soil Biology and Biochemistry*, *28*(4), 609-616. https://doi.org/https://doi.org/10.1016/0038-0717(95)00175-1
Chan, L. Y., Mugler, C. F., Heinrich, S., Vallotton, P., & Weis, K. (2018). Non-invasive measurement of mRNA decay reveals translation initiation as the major determinant of mRNA stability. *eLife*, *7*, e32536. https://doi.org/10.7554/eLife.32536
Chen, J., & Strous, M. (2013). Denitrification and aerobic respiration, hybrid electron transport chains and co-evolution. *Biochimica et Biophysica Acta (BBA) - Bioenergetics*, *1827*(2), 136-144. https://doi.org/https://doi.org/10.1016/j.bbabio.2012.10.002
Davis, D. H. S., Doudoroff, M. J., Stanier, R. Y., & Mandel, M. (1969). Proposal to reject the genus Hydrogenomonas: Taxonomic implications. *International Journal of Systematic and Evolutionary Microbiology*, *19*, 375-390.
De Vries, G. E., Harms, N., Hoogendijk, J., & Stouthamer, A. H. (1989). Isolation and characterization of Paracoccus denitrificans mutants with increased conjugation frequencies and pleiotropic loss of a (nGATCn) DNA-modifying property. *Archives of Microbiology*, *152*(1), 52-57. https://doi.org/10.1007/bf00447011
Eldor, A. (2015). Nitrogen Transformations. In Elsevier (Ed.), *Soil microbiology, ecology, and biochemistry* (4 ed.).
EMS. Neubauer Haemocytometry. In: Electron Microscopy Sciences.
Flock, U., Lachmann, P., Reimann, J., Watmough, N. J., & Ädelroth, P. (2009). Exploring the terminal region of the proton pathway in the bacterial nitric oxide reductase. *Journal of inorganic biochemistry*, *103*(5), 845-850.
Galant, A., Kaufman, R., & Wilson, J. (2015). Glucose: Detection and analysis. *Food chemistry*, *188*, 149-160.
Garcia-Ochoa, F., & Gomez, E. (2009). Bioreactor scale-up and oxygen transfer rate in microbial processes: an overview. *Biotechnol Adv*, *27*(2), 153-176. https://doi.org/10.1016/j.biotechadv.2008.10.006
Gibson, U. E., Heid, C. A., & Williams, P. M. (1996). A novel method for real time quantitative RT-PCR. *Genome research*, *6*(10), 995-1001.
Godden, J., Turley, S., Teller, D. C., Adman, E. T., Liu, M., Payne, W., & LeGall, J. (1991). The 2.3 angstrom X-ray structure of nitrite reductase from Achromobacter cycloclastes. *Science*, *253*(5018), 438-442.
Grady Jr, C. L., Daigger, G. T., Love, N. G., & Filipe, C. D. (2011). *Biological wastewater treatment*. CRC press.
Gupta, V., Jain, A. D. K. J., N.S, G., & Guptan, K. (2012). Development and validation of HPLC method - a review. *International Research Journal of Pharmaceutical and Applied Sciences*, *2*(4), 17-25. https://scienztech.org/index.php/irjpas/article/view/307
Hagemann, I. S. (2015). Chapter 1 - Overview of Technical Aspects and Chemistries of Next-Generation Sequencing. In S. Kulkarni & J. Pfeifer (Eds.), *Clinical Genomics* (pp. 3-19). Academic Press. https://doi.org/https://doi.org/10.1016/B978-0-12-404748-8.00001-0
Hahnke, S., Moosmann, P., Erb, T., & Strous, M. (2014). An improved medium for the anaerobic growth of Paracoccus denitrificans Pd1222 [Original Research]. *Frontiers in Microbiology*, *5*. https://doi.org/10.3389/fmicb.2014.00018
Hallin, S., Philippot, L., Löffler, F. E., Sanford, R. A., & Jones, C. M. (2018). Genomics and ecology of novel N2O-reducing microorganisms. *Trends in Microbiology*, *26*(1), 43-55.
Hassan, J., Bergaust, L. L., Wheat, I. D., & Bakken, L. R. (2014). Low Probability of Initiating nirS Transcription Explains Observed Gas Kinetics and Growth of Bacteria Switching

from Aerobic Respiration to Denitrification. *PLoS Computational Biology*, *10*(11), e1003933. https://doi.org/10.1371/journal.pcbi.1003933

Hayatsu, M., Tago, K., & Saito, M. (2008). Various players in the nitrogen cycle: Diversity and functions of the microorganisms involved in nitrification and denitrification. *Soil Science & Plant Nutrition*, *54*, 33-45. https://doi.org/10.1111/j.1747-0765.2007.00195.x

Hino, T., Nagano, S., Sugimoto, H., Tosha, T., & Shiro, Y. (2012). Molecular structure and function of bacterial nitric oxide reductase. *Biochimica et Biophysica Acta (BBA)-Bioenergetics*, *1817*(4), 680-687.

Hu, H.-W., & He, J.-Z. (2017). Comammox—a newly discovered nitrification process in the terrestrial nitrogen cycle. *Journal of Soils and Sediments*, *17*(12), 2709-2717. https://doi.org/10.1007/s11368-017-1851-9

Huang, Y. T., & Kinsella, J. E. (1986). Functional properties of phosphorylated yeast protein: solubility, water-holding capacity, and viscosity. *Journal of Agricultural and Food Chemistry*, *34*(4), 670-674. https://doi.org/10.1021/jf00070a020

Højberg, O., Binnerup, S. J., & Sørensen, J. (1997). Growth of silicone-immobilized bacteria on polycarbonate membrane filters, a technique to study microcolony formation under anaerobic conditions. *Applied and environmental microbiology*, *63*(7), 2920-2924. https://doi.org/doi:10.1128/aem.63.7.2920-2924.1997

Jetten, M. S., Wagner, M., Fuerst, J., van Loosdrecht, M., Kuenen, G., & Strous, M. (2001). Microbiology and application of the anaerobic ammonium oxidation ('anammox') process. *Curr Opin Biotechnol*, *12*(3), 283-288. https://doi.org/10.1016/s0958-1669(00)00211-1

Ji, B., Yang, K., Zhu, L., Jiang, Y., Wang, H., Zhou, J., & Zhang, H. (2015). Aerobic denitrification: A review of important advances of the last 30 years. *Biotechnology and Bioprocess Engineering*, *20*(4), 643-651. https://doi.org/10.1007/s12257-015-0009-0

Kleman, G. L., & Strohl, W. R. (1994). Developments in high cell density and high productivity microbial fermentation. *Curr Opin Biotechnol*, *5*(2), 180-186. https://doi.org/10.1016/s0958-1669(05)80033-3

Koutný, M., Kučera, I., Tesařík, R., Turánek, J., & Van Spanning, R. J. (1999). Pseudoazurin mediates periplasmic electron flow in a mutant strain of Paracoccus denitrificans lacking cytochrome c550. *FEBS letters*, *448*(1), 157-159.

Kraft, B., Strous, M., & Tegetmeyer, H. E. (2011). Microbial nitrate respiration--genes, enzymes and environmental distribution. *J Biotechnol*, *155*(1), 104-117. https://doi.org/10.1016/j.jbiotec.2010.12.025

Kuenen, J. G. (2008). Anammox bacteria: from discovery to application. *Nature Reviews Microbiology*, *6*(4), 320-326. https://doi.org/10.1038/nrmicro1857

Lane, D. J. (1991). 16S/23S rRNA sequencing. In E. Stackebrandt & M. Goodfellow (Eds.), *Nucleic acid techniques in bacterial systematics* (pp. 115-175). Wiley.

Le, T. T., Zhao, D., & Larsen, L. B. (2019). Chapter 5 - Analytical Methods for Measuring or Detecting Whey Proteins. In H. C. Deeth & N. Bansal (Eds.), *Whey Proteins* (pp. 155-184). Academic Press. https://doi.org/https://doi.org/10.1016/B978-0-12-812124-5.00005-9

Lee, S. Y. (1996). High cell-density culture of Escherichia coli. *Trends in Biotechnology*, *14*(3), 98-105. https://doi.org/https://doi.org/10.1016/0167-7799(96)80930-9

Li, E., & Mira de Orduña, R. (2010). A rapid method for the determination of microbial biomass by dry weight using a moisture analyser with an infrared heating source and an analytical balance. *Letters in Applied Microbiology*, *50*(3), 283-288. https://doi.org/10.1111/j.1472-765X.2009.02789.x

Lin, Y. (2016). *Introduction of Droplet Digital PCR*. National Veterinary Diagnostic Center Ministry of Agriculture, P.R. China. https://rr-asia.woah.org/wp-content/uploads/2020/06/6_introduction-of-ddpcr.pdf

Liu, B., Frostegård, Å., & Bakken, L. R. (2014). Impaired Reduction of N_2O to N_2 in Acid Soils Is Due to a Posttranscriptional Interference with the Expression of *nosZ*. *mBio*, *5*(3), e01383-01314. https://doi.org/doi:10.1128/mBio.01383-14

Liu, B., Mørkved, P. T., Frostegård, A., & Bakken, L. R. (2010). Denitrification gene pools, transcription and kinetics of NO, N2O and N2 production as affected by soil pH. *FEMS Microbiol Ecol*, *72*(3), 407-417. https://doi.org/10.1111/j.1574-6941.2010.00856.x

Liu, S., Dai, J., Wei, H., Li, S., Wang, P., Zhu, T., Zhou, J., & Qiu, D. (2021). Dissimilatory Nitrate Reduction to Ammonium (DNRA) and Denitrification Pathways Are Leveraged by Cyclic AMP Receptor Protein (CRP) Paralogues Based on Electron Donor/Acceptor Limitation in Shewanella loihica PV-4. *Applied and environmental microbiology*, *87*(2), e01964-01920. https://doi.org/doi:10.1128/AEM.01964-20

Ludwig, W., Mittenhuber, G., & Friedrich, C. G. (1993). Transfer of Thiosphaera pantotropha to Paracoccus denitrificans. *International Journal of Systematic Bacteriology*, *43*(2), 363-367. https://doi.org/10.1099/00207713-43-2-363

Lycus, P., Lovise Bøthun, K., Bergaust, L., Peele Shapleigh, J., Reier Bakken, L., & Frostegård, Å. (2017). Phenotypic and genotypic richness of denitrifiers revealed by a novel isolation strategy. *The ISME Journal*, *11*(10), 2219-2232. https://doi.org/10.1038/ismej.2017.82

Lycus, P., Soriano-Laguna, M. J., Kjos, M., Richardson, D. J., Gates, A. J., Milligan, D. A., Frostegård, Å., Bergaust, L., & Bakken, L. R. (2018). A bet-hedging strategy for denitrifying bacteria curtails their release of N ₂ O. *Proceedings of the National Academy of Sciences*, *115*(46), 11820-11825. https://doi.org/10.1073/pnas.1805000115

Ma, C., Sun, Z., Chen, C., Zhang, L., & Zhu, S. (2014). Simultaneous separation and determination of fructose, sorbitol, glucose and sucrose in fruits by HPLC–ELSD. *Food chemistry*, *145*, 784-788.

Martinez-Espinosa, R. M., Dridge, E. J., Bonete, M. J., Butt, J. N., Butler, C. S., Sargent, F., & Richardson, D. J. (2007). Look on the positive side! The orientation, identification and bioenergetics of 'Archaeal'membrane-bound nitrate reductases. *FEMS microbiology letters*, *276*(2), 129-139.

Mathekga, B. S. P., Nxumalo, Z., & Thimiri Govinda Raj, D. B. (2022). Chapter Four - Micro and nanofluidics for high throughput drug screening. In A. Pandya & V. Singh (Eds.), *Progress in Molecular Biology and Translational Science* (Vol. 187, pp. 93-120). Academic Press. https://doi.org/https://doi.org/10.1016/bs.pmbts.2021.07.020

Matsumoto, Y., Tosha, T., Pisliakov, A. V., Hino, T., Sugimoto, H., Nagano, S., Sugita, Y., & Shiro, Y. (2012). Crystal structure of quinol-dependent nitric oxide reductase from Geobacillus stearothermophilus. *Nature structural & molecular biology*, *19*(2), 238-245.

McKinnon, K. M. (2018). Flow Cytometry: An Overview. *Current Protocols in Immunology*, *120*(1). https://doi.org/10.1002/cpim.40

Moir, J. W., Baratta, D., Richardson, D. J., & Ferguson, S. J. (1993). The purification of a cd1-type nitrite reductase from, and the absence of a copper-type nitrite reductase from, the aerobic denitrifier Thiosphaera pantotropha; the role of pseudoazurin as an electron donor. *European journal of biochemistry*, *212*(2), 377-385.

Molstad, L., Dörsch, P., & Bakken, L. R. (2007). Robotized incubation system for monitoring gases (O2, NO, N2O N2) in denitrifying cultures. *J Microbiol Methods*, *71*(3), 202-211. https://doi.org/10.1016/j.mimet.2007.08.011

Mørkved, P. T., Dörsch, P., & Bakken, L. R. (2007). The N2O product ratio of nitrification and its dependence on long-term changes in soil pH. *Soil Biology and Biochemistry*, *39*(8), 2048-2057. https://doi.org/https://doi.org/10.1016/j.soilbio.2007.03.006

Nasseri, A., Rasoul-Amini, S., Morowvat, M., & Ghasemi, Y. (2011). Single cell protein: production and process. *American Journal of food technology*, *6*(2), 103-116.

Nokhal, T. H., & Schlegel, H. G. (1983). Taxonomic Study of Paracoccus denitrificans. *International Journal of Systematic Bacteriology*, *33*(1), 26-37. https://doi.org/10.1099/00207713-33-1-26

Olaya-Abril, A., Hidalgo-Carrillo, J., Luque-Almagro, V. M., Fuentes-Almagro, C., Urbano, F. J., Moreno-Vivián, C., Richardson, D. J., & Roldán, M. D. (2018). Exploring the Denitrification Proteome of Paracoccus denitrificans PD1222 [Original Research]. *Frontiers in Microbiology*, *9*. https://doi.org/10.3389/fmicb.2018.01137

Pepper, I. L., Gerba, C. P., & Gentry, T. J. (2015a). Municipal Wastewater Treatment. In *Environmental Microbiology* (3 ed., pp. 590-591). Academic Press.

Pepper, I. L., Gerba, C. P., & Gentry, T. J. (2015b). Nitrogen Cycle. In *Environmental Microbiology* (3 ed., pp. 352-353). Academic Press.

Postgate, J. R. (1982). Biology Nitrogen Fixation: Fundamentals. *Philosophical Transactions of the Royal Society of London. Series B, Biological Sciences*, *296*(1082), 375-385. http://www.jstor.org/stable/2395691

Qu, Z., Bakken, L. R., Molstad, L., Frostegård, Å., & Bergaust, L. L. (2016). Transcriptional and metabolic regulation of denitrification in Paracoccus denitrificans allows low but significant activity of nitrous oxide reductase under oxic conditions. *Environ Microbiol*, *18*(9), 2951-2963. https://doi.org/10.1111/1462-2920.13128

Rainey, F. A., Kelly, D. P., Stackebrandt, E., Burghardt, J., Hiraishi, A., Katayama, Y., & Wood, A. P. (1999). A re-evaluation of the taxonomy of Paracoccus denitrificans and a proposal for the combination Paracoccus pantotrophus comb. nov. *Int J Syst Bacteriol*, *49 Pt 2*, 645-651. https://doi.org/10.1099/00207713-49-2-645

Ravishankara, A. R., Daniel, J. S., & Portmann, R. W. (2009). Nitrous Oxide (N₂O): The Dominant Ozone-Depleting Substance Emitted in the 21st Century. *Science*, *326*(5949), 123-125. https://doi.org/doi:10.1126/science.1176985

Richardson, D., Berks, B., Russell, D., Spiro, S., & Taylor, C. (2001). Multi-author Review-New perspectives on prokaryotic and eukaryotic nitrate reduction-Functional, biochemical and genetic diversity of prokaryotic nitrate reductases. *CMLS-Cellular and Molecular Life Sciences*, *58*(2), 165-178.

Richardson, D. J. (2000). Bacterial respiration: a flexible process for a changing environment. *Microbiology*, *146*(3), 551-571.

Riesenberg, D. (1991). High-cell-density cultivation of Escherichia coli. *Curr Opin Biotechnol*, *2*(3), 380-384. https://doi.org/10.1016/s0958-1669(05)80142-9

Riesenberg, D., & Guthke, R. (1999). High-cell-density cultivation of microorganisms. *Applied Microbiology and Biotechnology*, *51*(4), 422-430. https://doi.org/10.1007/s002530051412

Robertson, L. A., & Kuenen, J. G. (1983). Thiosphaera pantotropha gen. nov. sp. nov., a facultatively anaerobic, facultatively autotrophic sulfur bacterium. *J. Gen. Microbiol.*(129), 2847–2855.

Robertson, L. A., & Kuenen, J. G. (1984). Aerobic denitrification: a controversy revived. *Archives of Microbiology*, *139*(4), 351-354. https://doi.org/10.1007/bf00408378

Robertson, L. A., & Kuenen, J. G. (1985). Further evidence for aerobic denitrification by Thiosphaera pantotropha. *Anton. Leeuw. Int. J. G.*(51), 561.

Russow, R., Stange, C. F., & Neue, H. U. (2009). Role of nitrite and nitric oxide in the processes of nitrification and denitrification in soil: Results from 15N tracer experiments. *Soil*

Biology and Biochemistry, *41*(4), 785-795. https://doi.org/https://doi.org/10.1016/j.soilbio.2009.01.017

Rümer, S., Krischke, M., Fekete, A., Lesch, M., Mueller, M., & Kaiser, W. (2016). Methods to Detect Nitric Oxide in Plants: Are DAFs Really Measuring NO? In (Vol. 1424, pp. 57-68). https://doi.org/10.1007/978-1-4939-3600-7_6

Samanthi. (2017). *Difference Between SYBR Green and Taqman*. https://www.differencebetween.com/difference-between-sybr-green-and-vs-taqman/

Sanford, R. A., Wagner, D. D., Wu, Q., Chee-Sanford, J. C., Thomas, S. H., Cruz-García, C., Rodríguez, G., Massol-Deyá, A., Krishnani, K. K., & Ritalahti, K. M. (2012). Unexpected nondenitrifier nitrous oxide reductase gene diversity and abundance in soils. *Proceedings of the National Academy of Sciences*, *109*(48), 19709-19714.

Sazanov, L. A., & Hinchliffe, P. (2006). Structure of the hydrophilic domain of respiratory complex I from Thermus thermophilus. *Science*, *311*(5766), 1430-1436. https://doi.org/10.1126/science.1123809

Schneider, L. K., Wüst, A., Pomowski, A., Zhang, L., & Einsle, O. (2014). No Laughing Matter: The Unmaking of the Greenhouse Gas Dinitrogen Monoxide by Nitrous Oxide Reductase. In (pp. 177-210). Springer Netherlands. https://doi.org/10.1007/978-94-017-9269-1_8

Seefeldt, L. C., Hoffman, B. M., & Dean, D. R. (2009). Mechanism of Mo-Dependent Nitrogenase. *Annual Review of Biochemistry*, *78*(1), 701-722. https://doi.org/10.1146/annurev.biochem.78.070907.103812

Shapleigh, J. P. (2006). The denitrifying prokaryotes. *The prokaryotes*, *2*, 769-792.

Shi, M., Zhao, Y., Zhu, L., Song, X., Tang, Y., Qi, H., Cao, H., & Wei, Z. (2020). Denitrification during composting: Biochemistry, implication and perspective. *International Biodeterioration & Biodegradation*, *153*, 105043. https://doi.org/10.1016/j.ibiod.2020.105043

Simon, J., van Spanning, R. J., & Richardson, D. J. (2008). The organisation of proton motive and non-proton motive redox loops in prokaryotic respiratory systems. *Biochimica et Biophysica Acta (BBA)-Bioenergetics*, *1777*(12), 1480-1490.

Sistrom, W. R. (1960). A Requirement for Sodium in the Growth of Rhodopseudomonas spheroides. *Journal of General Microbiology*, *22*(3), 778-785. https://doi.org/10.1099/00221287-22-3-778

Skaar, I., & Aasen, E.-M. (2021). BIO336 Mycology Laboratory Exercises.

Stehfest, E., & Bouwman, L. (2006). N2O and NO emission from agricultural fields and soils under natural vegetation: summarizing available measurement data and modeling of global annual emissions. *Nutrient Cycling in Agroecosystems*, *74*(3), 207-228. https://doi.org/10.1007/s10705-006-9000-7

Strock, J. S. (2008). Ammonification. In S. E. Jørgensen & B. D. Fath (Eds.), *Encyclopedia of Ecology* (pp. 162-165). Academic Press. https://doi.org/https://doi.org/10.1016/B978-008045405-4.00256-1

Strohm, T. O., Griffin, B., Zumft, W. G., & Schink, B. (2007). Growth Yields in Bacterial Denitrification and Nitrate Ammonification. *Applied and environmental microbiology*, *73*(5), 1420-1424. https://doi.org/10.1128/aem.02508-06

Subramaniam, R., Thirumal, V., Chistoserdov, A., Bajpai, R., Bader, J., & Popovic, M. (2018). *Chem Biochem Eng Q*, *32*(4), 451-464.

Suharti, Heering, H. A., & De Vries, S. (2004). NO Reductase from Bacillus azotoformans Is a Bifunctional Enzyme Accepting Electrons from Menaquinol and a Specific Endogenous Membrane-Bound Cytochrome c₅₅₁. *Biochemistry*, *43*(42), 13487-13495. https://doi.org/10.1021/bi0488101

Suzuki, T., Yamane, T., & Shimizu, S. (1987). Mass production of thiostrepton by fed-batch culture of Streptomyces laurentii with pH-stat modal feeding of multi-substrate. *Applied Microbiology and Biotechnology*, *25*(6). https://doi.org/10.1007/bf00252011

Thauer, R. K., Jungermann, K., & Decker, K. (1977). Energy conservation in chemotrophic anaerobic bacteria. *Bacteriol Rev*, *41*(1), 100-180. https://doi.org/10.1128/br.41.1.100-180.1977

Thompson, R. L., Lassaletta, L., Patra, P. K., Wilson, C., Wells, K. C., Gressent, A., Koffi, E. N., Chipperfield, M. P., Winiwarter, W., Davidson, E. A., Tian, H., & Canadell, J. G. (2019). Acceleration of global N2O emissions seen from two decades of atmospheric inversion. *Nature Climate Change*, *9*(12), 993-998. https://doi.org/10.1038/s41558-019-0613-7

Tian, H., Lu, C., Ciais, P., Michalak, A. M., Canadell, J. G., Saikawa, E., Huntzinger, D. N., Gurney, K. R., Sitch, S., Zhang, B., Yang, J., Bousquet, P., Bruhwiler, L., Chen, G., Dlugokencky, E., Friedlingstein, P., Melillo, J., Pan, S., Poulter, B., . . . Wofsy, S. C. (2016). The terrestrial biosphere as a net source of greenhouse gases to the atmosphere. *Nature*, *531*(7593), 225-228. https://doi.org/10.1038/nature16946

Van Spanning, R. J. M., De Boer, A. P. N., Reijnders, W. N. M., Westerhoff, H. V., Stouthamer, A. H., & Van Der Oost, J. (1997). FnrP and NNR of Paracoccus denitrificans are both members of the FNR family of transcriptional activators but have distinct roles in respiratory adaptation in response to oxygen limitation. *Molecular Microbiology*, *23*(5), 893-907. https://doi.org/10.1046/j.1365-2958.1997.2801638.x

van Spanning, R. J. M., Richardson, D. J., & Ferguson, S. J. (2007). Chapter 1 - Introduction to the Biochemistry and Molecular Biology of Denitrification. In H. Bothe, S. J. Ferguson, & W. E. Newton (Eds.), *Biology of the Nitrogen Cycle* (pp. 3-20). Elsevier. https://doi.org/https://doi.org/10.1016/B978-044452857-5.50002-3

Veening, J.-W., Smits, W. K., & Kuipers, O. P. (2008). Bistability, Epigenetics, and Bet-Hedging in Bacteria. *Annual Review of Microbiology*, *62*(1), 193-210. https://doi.org/10.1146/annurev.micro.62.081307.163002

Vikromvarasiri, N., Boonyawanich, S., & Pisutpaisal, N. (2015). Comparative Performance of Halothiobacillus Neapolitanus and Paracoccus Pantotrophus in Sulphur Oxidation. *Energy Procedia*, *79*, 885-889. https://doi.org/10.1016/j.egypro.2015.11.582

Wang, Z., Vishwanathan, N., Kowaliczko, S., & Ishii, S. (2023). Clarifying Microbial Nitrous Oxide Reduction under Aerobic Conditions: Tolerant, Intolerant, and Sensitive. *Microbiology Spectrum*, *11*(2), e04709-04722. https://doi.org/doi:10.1128/spectrum.04709-22

Ward, B. B. (2008). Nitrification. In S. E. Jørgensen & B. D. Fath (Eds.), *Encyclopedia of Ecology* (pp. 2511-2518). Academic Press. https://doi.org/https://doi.org/10.1016/B978-008045405-4.00280-9

Wilhelm, E., Battino, R., & Wilcock, R. J. (1977). Low-pressure solubility of gases in liquid water. *Chemical Reviews*, *77*(2), 219-262. https://doi.org/10.1021/cr60306a003

Wilson, A., Work, T., Bushway, A., & Bushway, R. (1981). HPLC determination of fructose, glucose, and sucrose in potatoes. *Journal of Food Science*, *46*(1), 300-301.

Wood, N. J., Alizadeh, T., Bennett, S., Pearce, J., Ferguson, S. J., Richardson, D. J., & Moir, J. W. B. (2001). Maximal Expression of Membrane-Bound Nitrate Reductase in Paracoccus Is Induced by Nitrate via a Third FNR-Like Regulator Named NarR. *Journal of bacteriology*, *183*(12), 3606-3613. https://doi.org/10.1128/jb.183.12.3606-3613.2001

Xi, H., Zhou, X., Arslan, M., Luo, Z., Wei, J., Wu, Z., & Gamal El-Din, M. (2022). Heterotrophic nitrification and aerobic denitrification process: Promising but a long way

to go in the wastewater treatment. *Science of The Total Environment*, *805*, 150212. https://doi.org/https://doi.org/10.1016/j.scitotenv.2021.150212

Yoon, S., Nissen, S., Park, D., Sanford, R. A., & Löffler, F. E. (2016). Nitrous oxide reduction kinetics distinguish bacteria harboring clade I NosZ from those harboring clade II NosZ. *Applied and environmental microbiology*, *82*(13), 3793-3800.

Zumft, W. G. (1997). Cell biology and molecular basis of denitrification. *Microbiology and Molecular Biology Reviews*, *61*(4), 533–616.

Appendices

Appendix A – Media and Buffers

Table A1. *Preparation of 10x Sistrom's medium (Sistrom, 1960)*

Component	Amount [g]	Concentration [mM]
K_2HPO_4	34.8	200
NH_4Cl	1.95	36.4
Succinate	40.0	340
L-glutamic acid	1.0	6.7
L-aspartic acid	0.4	2.5
NaCl	5.0	85
Nitrilotriacetic acid	2.0	
$MgSO_4 \cdot 7H_2O$	3.0	12
$CaCl_2 \cdot 2H_2O$	0.15	1.0
$FeSO_4 \cdot 7H_2O$	0.02	0.07
$(NH_4)_6Mo_7O_{24}$ (1% solution)	0.2 mL	
Trace elements solution	1 mL	
Vitamins solution	1 mL	

Table A2. *Preparation of 10x Sistrom's medium without any carbon source*

Component	Amount [g]	Concentration [mM]
K_2HPO_4	34.8	200
NH_4Cl	1.95	36.4
NaCl	5.0	85
Nitrilotriacetic acid	2.0	
$MgSO_4 \cdot 7H_2O$	3.0	12
$CaCl_2 \cdot 2H_2O$	0.15	1.0
$FeSO_4 \cdot 7H_2O$	0.02	0.07
$(NH_4)_6Mo_7O_{24}$ (1% solution)	0.2 mL	
Trace elements solution	1 mL	
Vitamins solution	1 mL	

Table A3. *Trace elements solution for Sistrom's medium A*

Component	Amount [g/100 mL]
EDTA	1.765
$ZnSO_4 \cdot 7H_2O$	10.95
$FeSO_4 \cdot 7H_2O$	5.00
$MnSO_4 \cdot H_2O$	1.54
$CuSO_4 \cdot 5H_2O$	0.392
$Co(NO_3)_2 \cdot 6H_2O$	0.248
H_3BO_3	0.114

Table A4. *Vitamin Solution for Sistrom's medium A*

Component	Amount [g/100 mL]
Nicotinic Acid	1.0
Thiamine HCl	0.5
Biotin	0.01

Table A5. *Phosphate Buffered Saline (PBS) pH 7.0 per L.*

Component	20 mM	100 mM
$Na_2HPO_4 \cdot 2H_2O$	1.377 g	6.886 g
$NaH_2PO_4 \cdot H_2O$	1.692 g	8.4605 g

Appendix B – Standard Curves

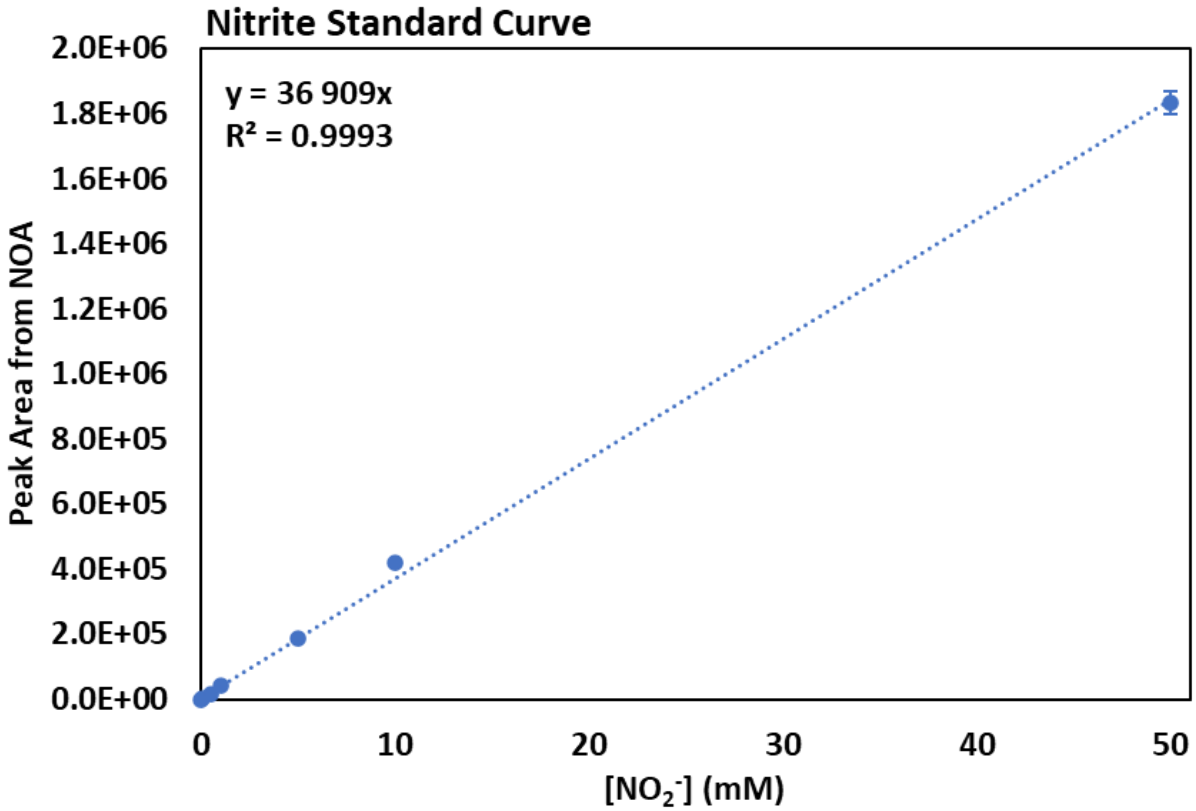

Figure B1. *Standard Curve for Nitrite Concentrations.*

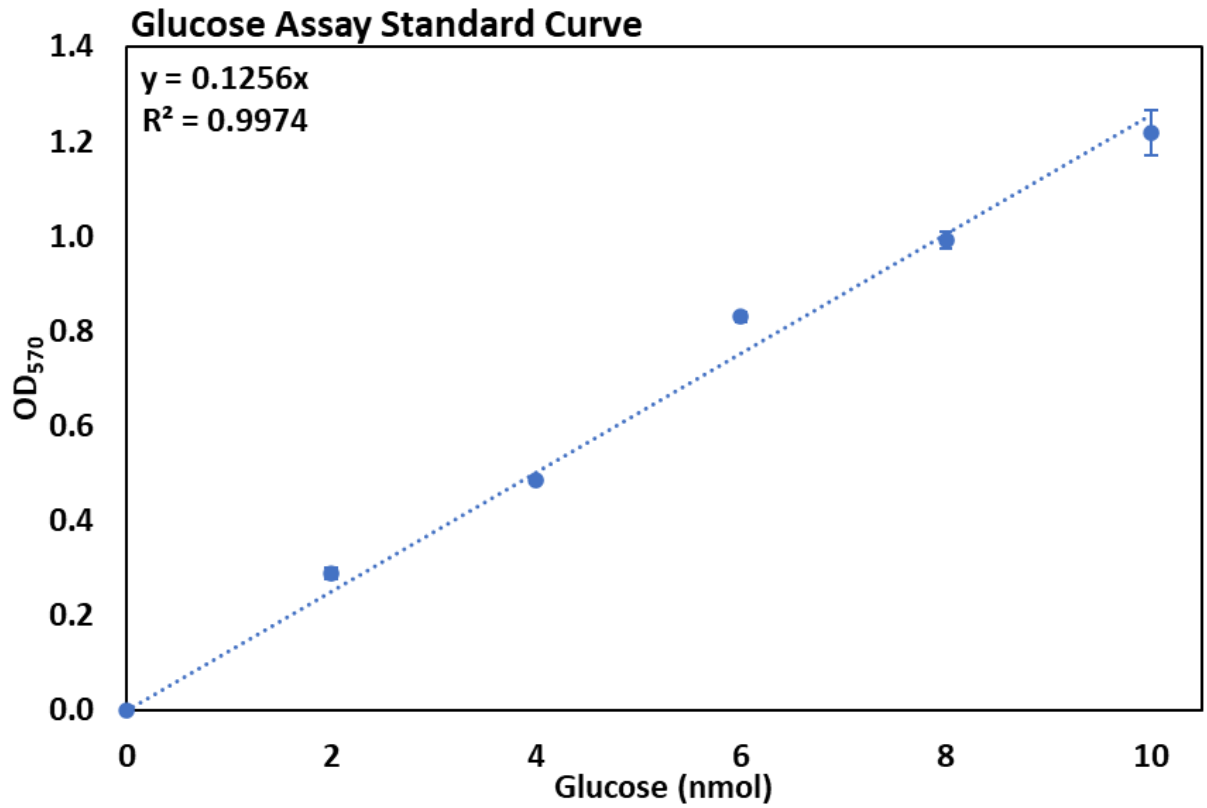

Figure B2. *Standard Curve for Glucose Assay.*

Appendix C - Primers

Table C1. Primers for Denitrification Genes. *Primer pairs designed to amplify the denitrification genes narG, nirS, norB and nosZ. The primer names indicate which organism and gene it is designed for. Both the Tm estimated by Sigma-Aldrich and Primer3 are listed, as well as the primer length and the product length, both in bp.*

Primer	Sequence	Tm (°C) Sigma	Tm (°C) Primer3	Length (bp)	Product (bp)
GB17_*narG*_FWD	GAACACCTCGGACATGCATC	65.6	59.0	20	641
GB17_*narG*_REV	TGGGCGAGGAGATGATCTTC	66.6	59.0	20	
GB17_*nirS*_FWD	GATCAAGATCGGCTCGGAGG	68.2	60.0	20	645
GB17_*nirS*_REV	TTCGGGTGCGTCTTGATGAA	68.9	60.0	20	
GB17_*norB*_FWD	TCGCCTTCCTGATGCTCAAG	67.8	60.1	20	605
GB17_*norB*_REV	GTCCTGCACGTCCATGAAGA	66.4	60.0	20	
GB17_*nosZ*_FWD	TCTCGACCTCCTACAACTCG	62.0	58.3	20	603
GB17_*nosZ*_REV	CCTTCGAGAACTTGCACAGC	65.1	59.5	20	
Pd1222_*narG*_FWD	GAAGTTCGGCGACATCTGG	66.1	58.6	19	596
Pd1222_*narG*_REV	CCCGGTCCAGGCTGTAATTG	66.0	60.8	20	
Pd1222_*nirS*_FWD	GACGCCCAATACAACGAAGC	66.6	59.9	20	625
Pd1222_*nirS*_REV	TGGCGTATTTGTCCTCCCAG	67.1	59.8	20	
Pd1222_*norB*_FWD	CCTTGCCTTCCTGATGCTCA	67.7	60.0	20	607
Pd1222_*norB*_REV	GTCCTGCACGTCCATGAAGA	66.4	60.0	20	
Pd1222_*nosZ*_FWD	TGGAGGACGTGGCGAATTAC	67.1	60.1	20	635
Pd1222_*nosZ*_REV	CAGCTTGTCCTTGATCGGGT	66.4	60.0	20	

Table C2. Primers for Standards. *Primer pairs designed to amplify the denitrification genes narG, nirS, norB and nosZ and cover the previous primers. The primer names indicate which organism and gene it is designed for. Both the Tm estimated by Sigma-Aldrich and Primer3 are listed, as well as the primer length and the product length, both in bp.*

Primer	Sequence	Tm (°C) Sigma	Tm (°C) Primer3	Length (bp)	Product (bp)
GB17_STD_*narG*_FWD	TGCTGGTGACGATCGACTT	64.7	59.0	19	794
GB17_STD_*narG*_REV	CTCATGCACGTTGGTCCAG	65.6	58.8	19	
GB17_STD_*nirS*_FWD	CTGTGGATGAAGGAGCCCA	66.4	59.0	19	795
GB17_STD_*nirS*_REV	GGTCTTGAACTCGGGGTCC	65.9	59.7	19	
GB17_STD_*norB*_FWD	ATACTGGTGGTGGGTCATCC	63.5	58.8	20	751
GB17_STD_*norB*_REV	CACCGCATAGATGAACAGCA	64.9	58.3	20	
GB17_STD_*nosZ*_FWD	GAACGTCTTCACCGCTGTC	63.6	58.9	19	781
GB17_STD_*nosZ*_REV	CATCTGGTCGCCCGAAATG	68.8	59.0	19	
Pd1222_STD_*narG*_FWD	CGCGCATTTCTATACCGAGG	66.4	58.9	20	775
Pd1222_STD_*narG*_REV	CTGGATGATCTTGTCGCGAC	65.9	58.8	20	
Pd1222_STD_*nirS*_FWD	AGGATCACAAGACCAAGACG	61.8	57.3	20	780
Pd1222_STD_*nirS*_REV	TCTCGCCGTCCATGATGAC	67.6	59.6	19	
Pd1222_STD_*norB*_FWD	ATACTGGTGGTGGGTCATCC	63.5	58.8	20	751
Pd1222_STD_*norB*_REV	CACGGCATAGATGAACAGCA	64.9	58.3	20	
Pd1222_STD_*nosZ*_FWD	GTCAACGACGGCACCAAC	65.5	59.4	18	755
Pd1222_STD_*nosZ*_REV	CGGTCCTTCGAGAACTTGGA	66.5	59.4	20	

Appendix D - Ladders

Figure D1. 100 bp DNA Ladder. *The ladder used on the agarose gel for gel electrophoresis is the 100 bp DNA Ladder Ready to Load from Solis Biodyne.* *https://solisbiodyne.com/EN/product/name=100-bp-DNA-Ladder-Ready-to-Load&catno=07-11-0000S*

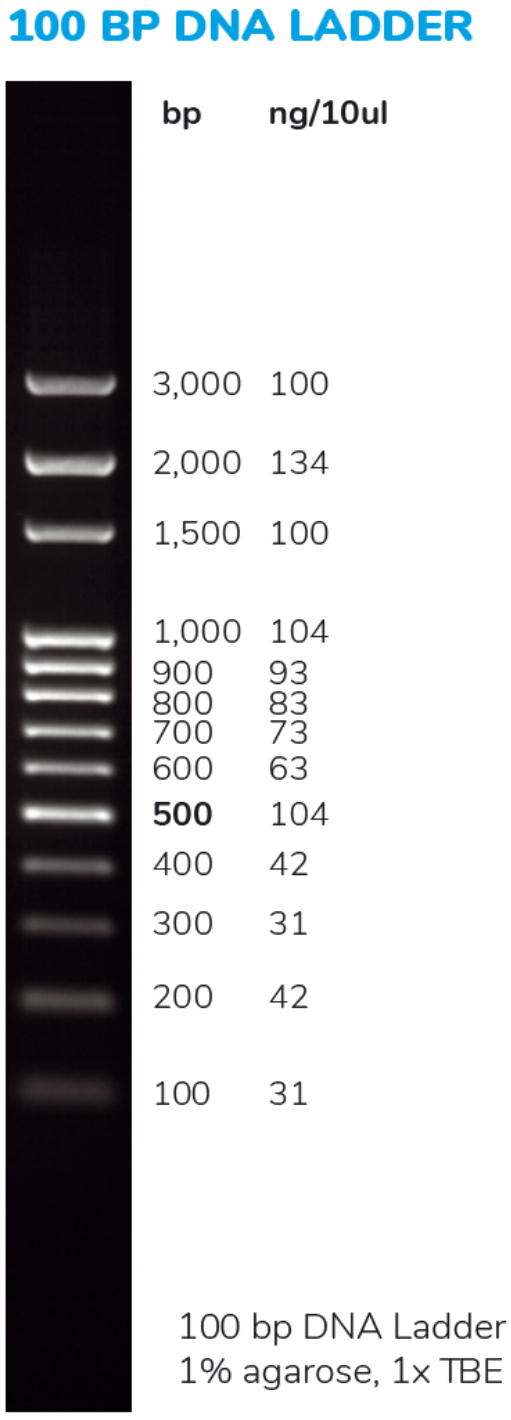

Appendix E – NanoDrop

Table E1. NanoDrop of Clean DNA.

Organism	Culture	Sample	Abs	260/280	ng/µL
Pd1222	Aerobic	1	0.088	2.55	1.7
		2	0.066	1.30	2.9
		3	0.033	5.16	1.8
	Anaerobic	7	0.186	2.23	9.0
		8	0.021	2.50	4.0
		9	0.089	1.99	4.5
GB17	Aerobic	1	0.043	1.43	1.5
		2	0.068	6.35	0.7
		3	0.018	1.23	0.4
	Anaerobic	7	0.199	1.80	7.3
		8	0.197	2.01	9.8
		9	0.161	1.68	7.0

Table E2. NanoDrop of Clean 16S PCR Product.

Organism	Culture	Sample	Abs	260/280	ng/µL
Pd1222	Aerobic	1	2.215	1.96	28.2
		2	0.256	2.29	16.2
		3	0.866	1.99	30.2
	Anaerobic	7	2.660	2.07	31.6
		8	0.448	2.06	30.8
		9	0.348	2.02	26.3
GB17	Aerobic	1	0.352	1.96	23.2
		2	0.306	2.13	21.5
		3	0.633	2.33	37.9
	Anaerobic	7	0.202	2.19	10.8
		8	0.290	1.98	19.2
		9	0.465	2.19	28.7

Table E3. NanoDrop of Clean Standards and Copies µL^{-1}.

Organism	Gene	Abs	260/280	ng/µL	Copies µL^{-1}
Pd1222	*narG*	0.212	1.89	18.0	2.12E+10
	nirS	0.293	2.17	15.7	1.84E+10
	norB	0.28	1.93	20.0	2.43E+10
	nosZ	0.212	1.77	10.9	1.32E+10
GB17	*narG*	0.173	2.05	15.3	1.76E+10
	nirS	0.203	2.23	14.2	1.63E+10
	norB	0.160	1.84	14.6	1.77E+10
	nosZ	0.231	2.38	13.1	1.53E+10

Table E4. NanoDrop of Clean RNA.

Organism	Culture	Sample	Abs	260/280	ng/µL
Pd1222	Aerobic	1.1	2.846	1.25	63.6
		1.2	1.034	1.67	8.9
		1.3	0.672	0.76	1.7
	Anaerobic	2.1	0.841	1.11	5.3
		2.2	0.793	0.74	1.1
		2.3	1.87	1.41	24.7
		3.1	0.829	1.86	5.7
		3.2	1.228	1.13	3.3
		3.3	0.600	0.80	1.4
		4.1	0.579	1.54	3.9
		4.2	0.961	1.31	4.9
		4.3	4.169	1.46	87.1
		5.1	1.017	1.20	5.9
		5.2	0.702	2.30	6.4
		5.3	0.695	1.58	4.3
		6.1	1.235	1.32	6.3
		6.2	1.326	1.52	13.3
		6.3	0.636	1.44	5.3
		7.1	2.289	1.66	11.5
		7.2	0.968	1.82	14.1
		7.3	0.880	1.51	11.6
GB17	Aerobic	1.1	2.387	1.56	5.8
		1.2	1.319	1.70	4.7
		1.3	1.489	2.02	5.0
	Anaerobic	2.1	1.426	1.53	5.7
		2.2	1.265	1.35	4.0
		2.3	1.723	1.54	4.0
		3.1	1.578	2.10	4.8
		3.2	1.801	1.63	5.7
		3.3	1.808	1.39	4.0
		4.1	1.547	1.46	5.0
		4.2	1.888	2.12	6.1
		4.3	1.753	2.16	6.8
		5.1	2.236	1.46	5.4
		5.2	1.273	2.07	7.7
		5.3	2.482	1.59	7.9
		6.1	2.224	1.44	9.1
		6.2	1.482	1.80	7.4
		6.3	2.150	1.69	8.7
		7.1	2.070	1.57	11.3
		7.2	2.700	1.71	8.8
		7.3	1.951	1.59	11.0

Appendix F – Gel Pictures

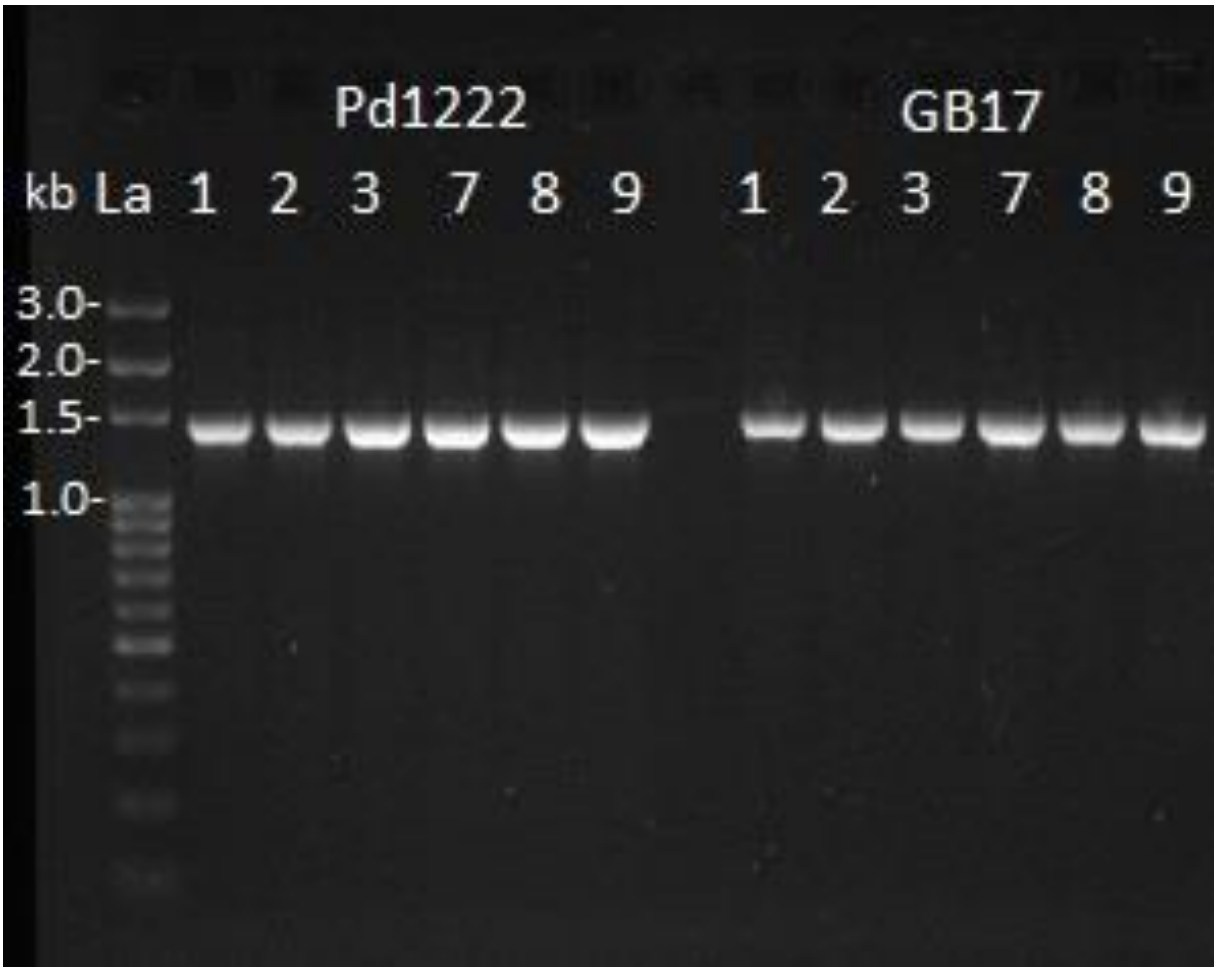

Figure F1. Gel Picture of 16S Samples. *The numbers represent the sample number applied to the well, where 1 - 3 are the aerobic DNA samples and 7 - 9 are the anaerobic DNA samples. The expected size of the 16S rRNA gene for both Pd1222 and GB17 was ~ 1.4 kb.*

Appendix G – Cell Count by Flow Cytometry

Table G1. Estimated Cells mL^{-1} OD$_{660}^{-1}$ by Flow Cytometry (Unstained cells). *The number in the parentheses indicates the number of replicates.*

Organism	Cells mL^{-1} OD$_{660}^{-1}$	
Pd1222 Aerobic	$2.23 \cdot 10^7 \pm 1.58 \cdot 10^7$	(3)
Pd1222 Anaerobic	$3.88 \cdot 10^7 \pm 2.85 \cdot 10^7$	(5)
GB17 Aerobic	$2.25 \cdot 10^7 \pm 1.89 \cdot 10^7$	(3)
GB17 Anaerobic	$1.92 \cdot 10^7 \pm 1.38 \cdot 10^7$	(3)

Table G2. Estimated Cells mL^{-1} OD$_{660}^{-1}$ by Flow Cytometry (Stained cells). *The number in the parentheses indicates the number of replicates.*

	SYBR®Green					
Organism	**0.5x**		**1x**		**5x**	
UD Pd1222 Aerobic	$2.67 \cdot 10^8 \pm 2.76 \cdot 10^8$	(3)	$5.51 \cdot 10^5$	(1)	N/A	
10x Pd1222 Aerobic	$3.83 \cdot 10^8 \pm 1.95 \cdot 10^8$	(2)	$3.29 \cdot 10^8 \pm 1.93 \cdot 10^8$	(2)	$3.02 \cdot 10^8 \pm 2.29 \cdot 10^8$	(2)
UD Pd1222 Anaerobic	$4.46 \cdot 10^8 \pm 4.55 \cdot 10^8$	(3)	$4.32 \cdot 10^6$	(1)	N/A	
10x Pd1222 Anaerobic	$6.93 \cdot 10^8 \pm 3.07 \cdot 10^8$	(2)	$4.90 \cdot 10^8 \pm 4.27 \cdot 10^8$	(2)	$1.61 \cdot 10^8$	(1)
UD GB17 Aerobic	$7.98 \cdot 10^7 \pm 1.01 \cdot 10^8$	(2)	$5.61 \cdot 10^6$	(1)	N/A	
10x GB17 Aerobic	$2.28 \cdot 10^8 \pm 1.25 \cdot 10^8$	(2)	$2.45 \cdot 10^8 \pm 1.09 \cdot 10^8$	(2)	$1.84 \cdot 10^8 \pm 1.18 \cdot 10^8$	(2)
UD GB17 Anaerobic	$8.18 \cdot 10^6$	(1)	$4.62 \cdot 10^6$	(1)	N/A	
10x GB17 Anaerobic	$3.14 \cdot 10^8 \pm 3.08 \cdot 10^8$	(2)	$3.59 \cdot 10^8 \pm 1.50 \cdot 10^8$	(2)	$2.64 \cdot 10^8 \pm 2.07 \cdot 10^8$	(2)

Appendix H – Glucose Assay

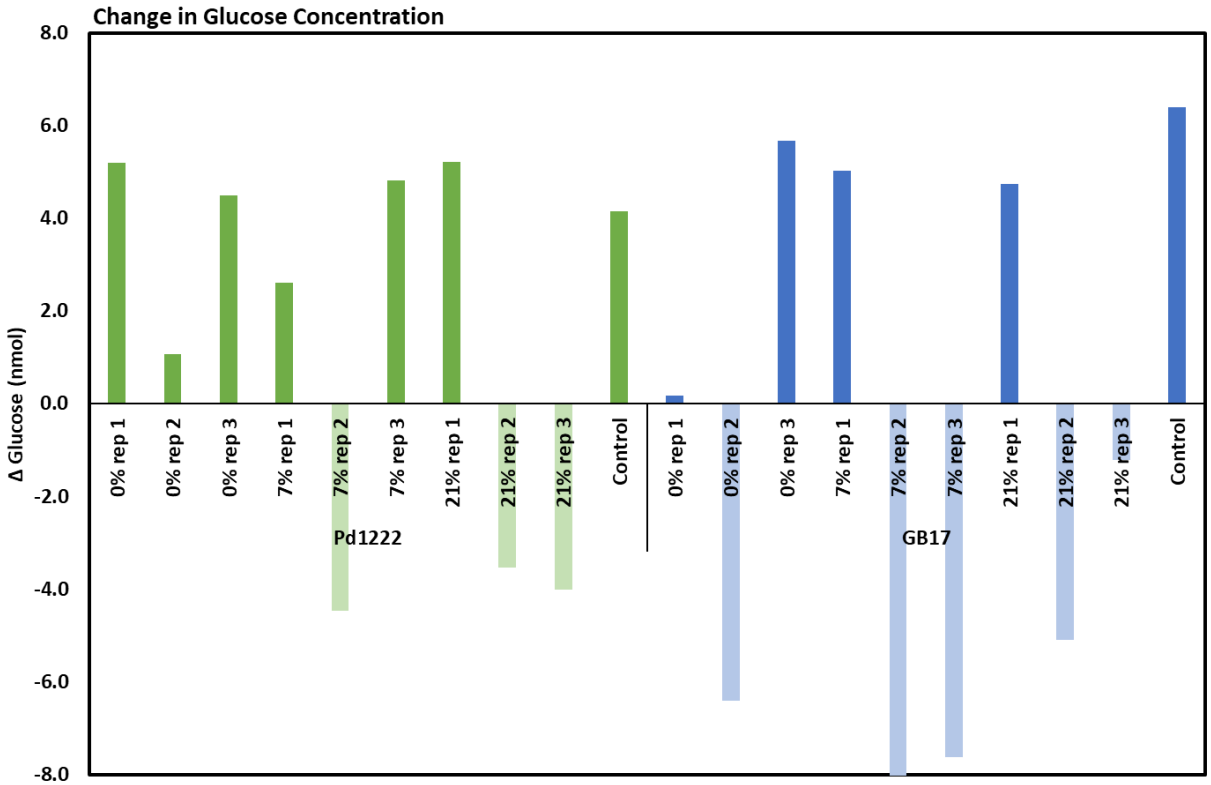

Figure H1. Change in Glucose Concentration. *Calculated change in glucose concentrations based on glucose assay performed on samples taken prior to and after aerobic denitrification. The bars show how much the glucose concentration had increased or decreased for all* O_2 *concentrations and replicates for Pd1222 and GB17.*

Appendix I – Consensus Sequences

>Pd1222_aerobic

agtcgagcgaacccttcggggttagcggcggacgggtgagtaacgcgtgggaatatgccctttgctacggaatagccccgggaaactggg
agtaataccgtatacgccctttgggggaaagatttatcggcaaaggattagcccgcgttggattaggtagttggtggggtaatggcctaccaag
ccgacgatccatagctggtttgagaggatgatcagccacactgggactgagacacggcccagactcctacgggaggcagcagtggggaat
cttagacaatgggggcaaccctgatctagccatgccgcgtgagtgatgaaggccctagggttgtaaagctctttcagctgggaagataatgac
ggtaccagcagaagaagccccggctaactccgtgccagcagccgcggtaatacggaggggctagcgttgttcggaattactgggcgtaa
agcgcacgtaggcggaccggaaagttgggggtgaaatcccggggctcaacctcggaactgccttcaaaactatcggtctggagttcgaga
gaggtgagtggaattccgagtgtagaggtgaaattcgtagatattcggaggaacaccagtggcgaaggcggctcactggctcgatactgac
gctgaggtgcgaaagcgtggggagcaaacaggattagataccctggtagtccacgccgtaaacgatgaatgccagtcgtcgggcagcatg
ctgttcggtgacacacctaacggattaagcattccgcctggggagtacggtcgcaagattaaaactcaaaggaattgacgggggcccgcac
aagcggtggagcatgtggtttaattcgaagcaacgcgcagaaccttaccaacccttgacatcgcaggaccgctccagagatggagttttctcg
taagagacctgtggacaggtgctgcatggctgtcgtcagctcgtgtcgtgagatgttcgggttaagtccgggcaacgagcgcaacccacact
cttagttgccagcatttggttgggcactctaagagaactgccgatgataagtcggaggaaggtgtggatgaagtcaagtcctcatggcccttac
gggttgggctacacacgtgctacaatggtggtgacagtgggttaatccccaaaagccatctcagttcggattggggtctgcaactcgacccca
tgaagttggaatcgctagtaatcgcggaacagcatgccgcggtgaatacgttcccgggccttgtacacaccgcccgtcacaccatggg-agt
tgggtctacccgacggccgtgcgctaaccagc

>Pd1222_anaerobic

agtcgagcgaacccttcggggttagcggcggacgggtgagtaacgcgtgggaatatgccctttgctacggaatagccccgggaaactggg
agtaataccgtatacgccctttgggggaaagatttatcggcaaaggattagcccgcgttggattaggtagttggtggggtaatggcctaccaag
ccgacgatccatagctggtttgagaggatgatcagccacactgggactgagacacggcccagactcctacgggaggcagcagtggggaat
cttagacaatgggggcaaccctgatctagccatgccgcgtgagtgatgaaggccctagggttgtaaagctctttcagctgggaagataatgac
ggtaccagcagaagaagccccggctaactccgtgccagcagccgcggtaatacggaggggctagcgttgttcggaattactgggcgtaa
agcgcacgtaggcggaccggaaagttgggggtgaaatcccggggctcaacctcggaactgccttcaaaactatcggtctggagttcgaga
gaggtgagtggaattccgagtgtagaggtgaaattcgtagatattcggaggaacaccagtggcgaaggcggctcactggctcgatactgac
gctgaggtgcgaaagcgtggggagcaaacaggattagataccctggtagtccacgccgtaaacgatgaatgccagtcgtcgggcagcatg
ctgttcggtgacacacctaacggattaagcattccgcctggggagtacggtcgcaagattaaaactcaaaggaattgacgggggcccgcac
aagcggtggagcatgtggtttaattcgaagcaacgcgcagaaccttaccaacccttgacatcgcaggaccgctccagagatggagttttctcg
taagagacctgtggacaggtgctgcatggctgtcgtcagctcgtgtcgtgagatgttc-ggttaagtcc-ggcaacgagcgcaacccacactc
ttagttgccagcatttggttgggcactctaagagaactgccgatgataagtcggaggaaggtgtggatgaagtcaagtcctcatggcccttacg
ggttgggctacacacgtgctacaatggtggtgacagtgggttaatccccaaaagccatctcagttcggattggggtctgcaactcgaccccat
gaagttggaatcgctagtaatcgcggaacagcatgccgcggtgaatacgttcccgggccttgtacacaccgcccgtcacaccatgggtagtt
gggtctacccgacggccgtgcgctaaccagc

>GB17_aerobic

acacatgcaagtcgagcgcacccttcggggtgagcggcggacgggtgagtaacgcgtgggaatatgccctttggtacggaatagtcctgg
gaaactgggggtaataccgtatgcgcccttcgggggaaagatttatcgccaaaggattagcccgcgttggattaggtagttggtggggtaatg
gcctaccaagccgacgatccatagctggtttgagaggatgatcagccacactgggactgagacacggcccagactcctacgggaggcagc
agtggggaatcttagacaatgggggcaaccctgatctagccatgccgcgtgagtgatgaaggccctagggttgtaaagctctttcagctggg
aagataatgacggtaccagcagaagaagccccggctaactccgtgccagcagccgcggtaatacggaggggctagcgttgttcggaatt
actgggcgtaaagcgcacgtaggcggaccggaaagttgggggtgaaatcccggggctcaaccccggaactgccttcaaaactatcggtct
ggagttcgagaggtgagtggaattccgagtgtagaggtgaaattcgtagatattcggaggaacaccagtggcgaaggcggctcactggc
tcgatactgacgctgaggtgcgaaagcgtggggagcaaacaggattagataccctggtagtccacgccgtaaacgatgaatgccagtcgtc
gggcagcatgctgttcggtgacacacctaacggattaagcattccgcctggggagtacggtcgcaagattaaaactcaaaggaattgacggg
ggcccgcacaagcggtggagcatgtggtttaattcgaagcaacgcgcagaaccttaccaacccttgacatcccaggaccggcccggagac
gggtctttcacttcggtgacctggagacaggtgctgcatggctgtcgtcagctcgtgtcgtgagatgttcggttaagtccggcaacgagcgca
acccacactcttagttgccagcatttggttgggcactctaagagaactgccgatgataagtcggaggaaggtgtggatgacgtcaagtcctcat
ggcccttacgggttgggctacacacgtgctacaatggtggtgacagtgggttaatccccaaaagccatctcagttcggattggggtctgcaac
tcgaccccatgaagttggaatcgctagtaatcgcggaacagcatgccgcggtgaatacgttcccgggccttgtacacaccgcccgtcacacc
atgggagttgggtctacccgacggccgtgcgctaaccagcaatgggg

>GB17_anaerobic

acacatgcaagtcgagcgcacccttcggggtgagcggcggacgggtgagtaacgcgtgggaatatgccctttggtacggaatagtcctgg
gaaactgggggtaataccgtatgcgcccttcgggggaaagatttatcgccaaaggattagcccgcgttggattaggtagttggtggggtaatg
gcctaccaagccgacgatccatagctggtttgagaggatgatcagccacactgggactgagacacggcccagactcctacgggaggcagc
agtggggaatcttagacaatgggggcaaccctgatctagccatgccgcgtgagtgatgaaggccctagggttgtaaagctctttcagctggg
aagataatgacggtaccagcagaagaagccccggctaactccgtgccagcagccgcggtaatacggaggggctagcgttgttcggaatt
actgggcgtaaagcgcacgtaggcggaccggaaagttgggggtgaaatcccggggctcaaccccggaactgccttcaaaactatcggtct
ggagttcgagaggtgagtggaattccgagtgtagaggtgaaattcgtagatattcggaggaacaccagtggcgaaggcggctcactggc
tcgatactgacgctgaggtgcgaaagcgtggggagcaaacaggattagataccctggtagtccacgccgtaaacgatgaatgccagtcgtc
gggcagcatgctgttcggtgacacacctaacggattaagcattccgcctggggagtacggtcgcaagattaaaactcaaaggaattgacggg
ggcccgcacaagcggtggagcatgtggtttaattcgaagcaacgcgcagaaccttaccaacccttgacatcccaggaccggcccggagac
gggtctttcacttcggtgacctggagacaggtgctgcatggctgtcgtcagctcgtgtcgtgagatgttcggttaagtccggcaacgagcgca
acccacactcttagttgccagcatttggttgggcactctaagagaactgccgatgataagtcggaggaaggtgtggatgacgtcaagtcctcat
ggcccttacgggttgggctacacacgtgctacaatggtggtgacagtgggttaatccccaaaagccatctcagttcggattggggtctgcaac
tcgaccccatgaagttggaatcgctagtaatcgcggaacagcatgccgcggtgaatacgttcccgggccttgtacacaccgcccgtcacacc
atgggagttgggtctacccgacggccgtgcgctaaccagcaatgggg

Appendix J - Alignments

Appendix J1 - Alignment for Pd1222.

```
Page 1 Pd1222 Alignment

                1                                                                                                  78
Pd1222 16S rRNA  agucgagcgaacccuucgggguuagcggcggacgggugaguaacgcgugggaauaugcccuuugcuacggaauagccc
Pd1222 Aerobic   agtcgagcgaacccttcggggttagcggcggacgggtgagtaacgcgtgggaatatgccctttgctacggaatagccc
Pd1222 Anaerobic agtcgagcgaacccttcggggttagcggcggacgggtgagtaacgcgtgggaatatgccctttgctacggaatagccc

.....

                79                                                                                                 156
Pd1222 16S rRNA  cgggaaacugggaguaauaccguauacgcccuuuggggggaaagauuuaucggcaaaggauuagcccgcguuggauuag
Pd1222 Aerobic   cgggaaactgggagtaataccgtatacgccctttgggggaaagatttatcggcaaaggattagcccgcgttggattag
Pd1222 Anaerobic cgggaaactgggagtaataccgtatacgccctttgggggaaagatttatcggcaaaggattagcccgcgttggattag

.....

                157                                                                                                234
Pd1222 16S rRNA  guaguuggugggguaauggccuaccaagccgacgauccauagcugguuugagaggaugaucagccacacugggacuga
Pd1222 Aerobic   gtagttggtggggtaatggcctaccaagccgacgatccatagctggtttgagaggatgatcagccacactgggactga
Pd1222 Anaerobic gtagttggtggggtaatggcctaccaagccgacgatccatagctggtttgagaggatgatcagccacactgggactga

.....

                235                                                                                                312
Pd1222 16S rRNA  gacacggcccagacuccuacgggaggcagcaguggggaaucuuagacaaugggggcaacccugaucuagccaugccgc
Pd1222 Aerobic   gacacggcccagactcctacgggaggcagcagtggggaatcttagacaatgggggcaaccctgatctagccatgccgc
Pd1222 Anaerobic gacacggcccagactcctacgggaggcagcagtggggaatcttagacaatgggggcaaccctgatctagccatgccgc

.....

                313                                                                                                390
Pd1222 16S rRNA  gugagugaugaaggcccuaggguuguaaagcucuuucagcugggaagauaaugacgguaccagcagaagaagccccgg
Pd1222 Aerobic   gtgagtgatgaaggccctagggttgtaaagctctttcagctgggaagataatgacggtaccagcagaagaagccccgg
Pd1222 Anaerobic gtgagtgatgaaggccctagggttgtaaagctctttcagctgggaagataatgacggtaccagcagaagaagccccgg

.....

                391                                                                                                468
Pd1222 16S rRNA  cuaacuccgugccagcagccgcgguaauacggaggggcuagcguuguucggaauuacugggcguaaagcgcacguag
Pd1222 Aerobic   ctaactccgtgccagcagccgcggtaatacggaggggctagcgttgttcggaattactgggcgtaaagcgcacgtag
Pd1222 Anaerobic ctaactccgtgccagcagccgcggtaatacggaggggctagcgttgttcggaattactgggcgtaaagcgcacgtag

.....

                469                                                                                                546
Pd1222 16S rRNA  gcggaccggaaaguugggggugaaaucccggggcucaaccucggaacugccuucaaaacuaucggucuggaguucgag
Pd1222 Aerobic   gcggaccggaaagttgggggtgaaatcccggggctcaacctcggaactgccttcaaaactatcggtctggagttcgag
Pd1222 Anaerobic gcggaccggaaagttgggggtgaaatcccggggctcaacctcggaactgccttcaaaactatcggtctggagttcgag

.....

                547                                                                                                624
Pd1222 16S rRNA  agaggugaguggaauuccgaguguagaggugaaaauucguagauauucggaggaacaccaguggcgaaggcggcucacu
Pd1222 Aerobic   agaggtgagtggaattccgagtgtagaggtgaaattcgtagatattcggaggaacaccagtggcgaaggcggctcact
Pd1222 Anaerobic agaggtgagtggaattccgagtgtagaggtgaaattcgtagatattcggaggaacaccagtggcgaaggcggctcact

.....

                625                                                                                                702
Pd1222 16S rRNA  ggcucgauacugacgcugaggugcgaaagcgugggagcaaacaggauuagauacccugguaguccacgccguaaacg
Pd1222 Aerobic   ggctcgatactgacgctgaggtgcgaaagcgtggggagcaaacaggattagataccctggtagtccacgccgtaaacg
Pd1222 Anaerobic ggctcgatactgacgctgaggtgcgaaagcgtggggagcaaacaggattagataccctggtagtccacgccgtaaacg

.....
```

```
                703                                                                 780
Pd1222 16S rRNA  augaaugccagucgucgggcagcaugcuguucggugacacaccuaacggauuaagcauuccgccuggggaguacgguc
Pd1222 Aerobic   atgaatgccagtcgtcgggcagcatgctgttcggtgacacacctaacggattaagcattccgcctggggagtacggtc
Pd1222 Anaerobic atgaatgccagtcgtcgggcagcatgctgttcggtgacacacctaacggattaagcattccgcctggggagtacggtc

.....

                781                                                                 858
Pd1222 16S rRNA  gcaagauuaaaacucaaaggaauugacgggggcccgcacaagcgguggagcaugugguuuaauucgaagcaacgcgca
Pd1222 Aerobic   gcaagattaaaactcaaaggaattgacgggggcccgcacaagcggtggagcatgtggtttaattcgaagcaacgcgca
Pd1222 Anaerobic gcaagattaaaactcaaaggaattgacgggggcccgcacaagcggtggagcatgtggtttaattcgaagcaacgcgca

.....

                859                                                                 936
Pd1222 16S rRNA  gaaccuuaccaacccuugacaucgcaggaccgcuccagagauggaguuuucucguaagagaccuguggacaggugcug
Pd1222 Aerobic   gaaccttaccaacccttgacatcgcaggaccgctccagagatggagttttctcgtaagagacctgtggacaggtgctg
Pd1222 Anaerobic gaaccttaccaacccttgacatcgcaggaccgctccagagatggagttttctcgtaagagacctgtggacaggtgctg

.....

                937                                                                1014
Pd1222 16S rRNA  cauggcugucgucagcucgugucgugagauguuc-gguuaagucc-ggcaacgagcgcaacccacacucuuaguugcc
Pd1222 Aerobic   catggctgtcgtcagctcgtgtcgtgagatgttcgggttaagtccgggcaacgagcgcaacccacactcttagttgcc
Pd1222 Anaerobic catggctgtcgtcagctcgtgtcgtgagatgttc-ggttaagtcc-ggcaacgagcgcaacccacactcttagttgcc

.....

                1015                                                               1092
Pd1222 16S rRNA  agcauuugguugggcacucuaagagaacugccgaugauaagucggaggaaggugguggaugaagucaaguccucauggc
Pd1222 Aerobic   agcatttggttgggcactctaagagaactgccgatgataagtcggaggaaggtgtggatgaagtcaagtcctcatggc
Pd1222 Anaerobic agcatttggttgggcactctaagagaactgccgatgataagtcggaggaaggtgtggatgaagtcaagtcctcatggc

.....

                1093                                                               1170
Pd1222 16S rRNA  ccuuacgggguugggcuacacacgugcuacaauggugguugacaguggguuaaucccccaaaagccaucucaguucggauu
Pd1222 Aerobic   ccttacgggttgggctacacacgtgctacaatggtggtgacagtgggttaatccccaaaagccatctcagttcggatt
Pd1222 Anaerobic ccttacgggttgggctacacacgtgctacaatggtggtgacagtgggttaatccccaaaagccatctcagttcggatt

.....

                1171                                                               1248
Pd1222 16S rRNA  ggggucugcaacucgaccccaugaaguuggaaucgcuaguaaucgcggaacagcaugccgcggugaauacguucccgg
Pd1222 Aerobic   ggggtctgcaactcgaccccatgaagttggaatcgctagtaatcgcggaacagcatgccgcggtgaatacgttcccgg
Pd1222 Anaerobic ggggtctgcaactcgaccccatgaagttggaatcgctagtaatcgcggaacagcatgccgcggtgaatacgttcccgg

.....

                1249                                                        1315
Pd1222 16S rRNA  gccuuguacacaccgcccgucacaccaugggaguugggucuacccgacggccgugcgcuaaccagc
Pd1222 Aerobic   gccttgtacacaccgcccgtcacaccatgggagttgggtctacccgacggccgtgcgctaaccagc
Pd1222 Anaerobic gccttgtacacaccgcccgtcacaccatgggtagttgggtctacccgacggccgtgcgctaaccagc

.....
```

Appendix J2 - Alignment for GB17

Page 1 GB17 Alignment

```
                1                                                                                                  78
GB17 16S rRNA   acacaugcaagucgagcgcacccuucggggugagcggcggacgggugaguaacgcgugggaauaugcccuuugguacg
GB17 Aerobic    acacatgcaagtcgagcgcacccttcggggtgagcggcggacgggtgagtaacgcgtgggaatatgccctttggtacg
GB17 Anaerobic  acacatgcaagtcgagcgcacccttcggggtgagcggcggacgggtgagtaacgcgtgggaatatgccctttggtacg

                ....................................................................................................

                79                                                                                                156
GB17 16S rRNA   gaauaguccugggaaacuggggguaauaccguaugcgcccuucgggggaaagauuuaucgccaaaggauuagcccgcg
GB17 Aerobic    gaatagtcctgggaaactgggggtaataccgtatgcgcccttcgggggaaagatttatcgccaaaggattagcccgcg
GB17 Anaerobic  gaatagtcctgggaaactgggggtaataccgtatgcgcccttcgggggaaagatttatcgccaaaggattagcccgcg

                ....................................................................................................

                157                                                                                               234
GB17 16S rRNA   uuggauuagguaguuggugggguaauggccuaccaagccgacgauccauagcugguuugagaggaugaucagccacac
GB17 Aerobic    ttggattaggtagttggtggggtaatggcctaccaagccgacgatccatagctggtttgagaggatgatcagccacac
GB17 Anaerobic  ttggattaggtagttggtggggtaatggcctaccaagccgacgatccatagctggtttgagaggatgatcagccacac

                ....................................................................................................

                235                                                                                               312
GB17 16S rRNA   ugggacugagacacggcccagacuccuacgggaggcagcaguggggaaucuuagacaaugggggcaacccugaucuag
GB17 Aerobic    tgggactgagacacggcccagactcctacgggaggcagcagtggggaatcttagacaatgggggcaaccctgatctag
GB17 Anaerobic  tgggactgagacacggcccagactcctacgggaggcagcagtggggaatcttagacaatgggggcaaccctgatctag

                ....................................................................................................

                313                                                                                               390
GB17 16S rRNA   ccaugccgcgugagugaugaaggcccuaggguuguaaagcucuuucagcugggaagauaaugacgguaccagcagaag
GB17 Aerobic    ccatgccgcgtgagtgatgaaggccctagggttgtaaagctctttcagctgggaagataatgacggtaccagcagaag
GB17 Anaerobic  ccatgccgcgtgagtgatgaaggccctagggttgtaaagctctttcagctgggaagataatgacggtaccagcagaag

                ....................................................................................................

                391                                                                                               468
GB17 16S rRNA   aagccccggcuaacuccgugccagcagccgcgguaauacggaggggcuagcguuguucggaauuacugggcguaaag
GB17 Aerobic    aagccccggctaactccgtgccagcagccgcggtaatacggagggggctagcgttgttcggaattactgggcgtaaag
GB17 Anaerobic  aagccccggctaactccgtgccagcagccgcggtaatacggagggggctagcgttgttcggaattactgggcgtaaag

                ....................................................................................................

                469                                                                                               546
GB17 16S rRNA   cgcacguaggcggaccggaaaguuggggguaaaucccggggcucaaccccggaacugccuucaaaacuaucggucug
GB17 Aerobic    cgcacgtaggcggaccggaaagttgggggtgaaatcccggggctcaaccccggaactgccttcaaaactatcggtctg
GB17 Anaerobic  cgcacgtaggcggaccggaaagttgggggtgaaatcccggggctcaaccccggaactgccttcaaaactatcggtctg

                ....................................................................................................

                547                                                                                               624
GB17 16S rRNA   gaguucgagagaggugaguggaauuccgaguguagaggugaaauucguagauauucggaggaacaccaguggcgaagg
GB17 Aerobic    gagttcgagagaggtgagtggaattccgagtgtagaggtgaaattcgtagatattcggaggaacaccagtggcgaagg
GB17 Anaerobic  gagttcgagagaggtgagtggaattccgagtgtagaggtgaaattcgtagatattcggaggaacaccagtggcgaagg

                ....................................................................................................

                625                                                                                               702
GB17 16S rRNA   cggcucacuggcucgauacugacgcugaggugcgaaagcgugggggagcaaacaggauuagauacccugguaguccacg
GB17 Aerobic    cggctcactggctcgatactgacgctgaggtgcgaaagcgtggggagcaaacaggattagataccctggtagtccacg
GB17 Anaerobic  cggctcactggctcgatactgacgctgaggtgcgaaagcgtggggagcaaacaggattagataccctggtagtccacg

                ....................................................................................................
```

```
               703                                                                 780
GB17 16S rRNA  ccguaaacgaugaaugccagucgucgggcagcaugcuguucggugacacaccuaacggauuaagcauuccgccuggggg
GB17 Aerobic   ccgtaaacgatgaatgccagtcgtcgggcagcatgctgttcggtgacacacctaacggattaagcattccgcctgggg
GB17 Anaerobic ccgtaaacgatgaatgccagtcgtcgggcagcatgctgttcggtgacacacctaacggattaagcattccgcctgggg

...............................................................................................

               781                                                                 858
GB17 16S rRNA  aguacggucgcaagauuaaaacucaaaggaauugacgggggcccgcacaagcgguggagcaugugguuuaauucgaag
GB17 Aerobic   agtacggtcgcaagattaaaactcaaaggaattgacgggggcccgcacaagcggtggagcatgtggtttaattcgaag
GB17 Anaerobic agtacggtcgcaagattaaaactcaaaggaattgacgggggcccgcacaagcggtggagcatgtggtttaattcgaag

...............................................................................................

               859                                                                 936
GB17 16S rRNA  caacgcgcagaaccuuaccaacccuugacaucccaggaccggcccggagacgggucuuucacuucggugaccuggaga
GB17 Aerobic   caacgcgcagaaccttaccaacccttgacatcccaggaccggcccggagacgggtctttcacttcggtgacctggaga
GB17 Anaerobic caacgcgcagaaccttaccaacccttgacatcccaggaccggcccggagacgggtctttcacttcggtgacctggaga

...............................................................................................

               937                                                                1014
GB17 16S rRNA  caggugcugcauggcugucgucagcucgugucgugagauguucgguuaaguccggcaacgagcgcaacccacacucuu
GB17 Aerobic   caggtgctgcatggctgtcgtcagctcgtgtcgtgagatgttcggttaagtccggcaacgagcgcaacccacactctt
GB17 Anaerobic caggtgctgcatggctgtcgtcagctcgtgtcgtgagatgttcggttaagtccggcaacgagcgcaacccacactctt

...............................................................................................

               1015                                                               1092
GB17 16S rRNA  aguugccagcauuugguugggcacucuaagagaacugccgaugauaagucggaggaaggugguggaugacgucaagucc
GB17 Aerobic   agttgccagcatttggttgggcactctaagagaactgccgatgataagtcggaggaaggtgtggatgacgtcaagtcc
GB17 Anaerobic agttgccagcatttggttgggcactctaagagaactgccgatgataagtcggaggaaggtgtggatgacgtcaagtcc

...............................................................................................

               1093                                                               1170
GB17 16S rRNA  ucauggcccuuacgggguugggcuacacacgugcuacaauggugguugacaguggguuaaucccccaaaagccaucucagu
GB17 Aerobic   tcatggcccttacgggttgggctacacacgtgctacaatggtggtgacagtgggttaatccccaaaagccatctcagt
GB17 Anaerobic tcatggcccttacgggttgggctacacacgtgctacaatggtggtgacagtgggttaatccccaaaagccatctcagt

...............................................................................................

               1171                                                               1248
GB17 16S rRNA  ucggauuggggucugcaacucgaccccaugaaguuggaaucgcuaguaaucgcggaacagcaugccgcggugaauacg
GB17 Aerobic   tcggattggggtctgcaactcgaccccatgaagttggaatcgctagtaatcgcggaacagcatgccgcggtgaatacg
GB17 Anaerobic tcggattggggtctgcaactcgaccccatgaagttggaatcgctagtaatcgcggaacagcatgccgcggtgaatacg

...............................................................................................

               1249                                                               1326
GB17 16S rRNA  uucccgggccuuguacacaccgcccgucacaccaugggaguugggucuacccgacggccgugcgcuaaccagcaaugg
GB17 Aerobic   ttcccgggccttgtacacaccgcccgtcacaccatgggagttgggtctacccgacggccgtgcgctaaccagcaatgg
GB17 Anaerobic ttcccgggccttgtacacaccgcccgtcacaccatgggagttgggtctacccgacggccgtgcgctaaccagcaatgg

...............................................................................................

               1327
GB17 16S rRNA  gg
GB17 Aerobic   gg
GB17 Anaerobic gg

...............................................................................................
```

Appendix K – qPCR

Table K1. The Efficiency of DNase Treatment. *Ct-values were obtained by qPCR of the purified RNA samples after on-column DNase treatment and TURBO™ DNase treatment.*

Organism	Culture	Sample	Ct-value
Pd1222	Aerobic	1.1	Undetermined
		1.2	34.37
		1.3	28.82
	Anaerobic	2.1	Undetermined
		2.2	20.73
		2.3	19.88
		3.1	37.00
		3.2	Undetermined
		3.3	34.24
		4.1	35.00
		4.2	30.45
		4.3	35.15
		5.1	29.03
		5.2	29.14
		5.3	31.87
		6.1	30.32
		6.2	10.98
		6.3	34.63
		7.1	4.89
		7.2	32.02
		7.3	28.75
		Negative Control	Undetermined
GB17	Aerobic	1.1	35.86
		1.2	32.91
		1.3	Undetermined
	Anaerobic	2.1	32.91
		2.2	33.11
		2.3	34.68
		3.1	35.38
		3.2	34.57
		3.3	39.86
		4.1	33.17
		4.2	35.16
		4.3	16.96
		5.1	33.08
		5.2	Undetermined
		5.3	37.13
		6.1	32.66
		6.2	32.53
		6.3	Undetermined
		7.1	29.97
		7.2	35.32
		7.3	Undetermined
		Negative Control	Undetermined

Appendix L – Flow Cytometry Gating

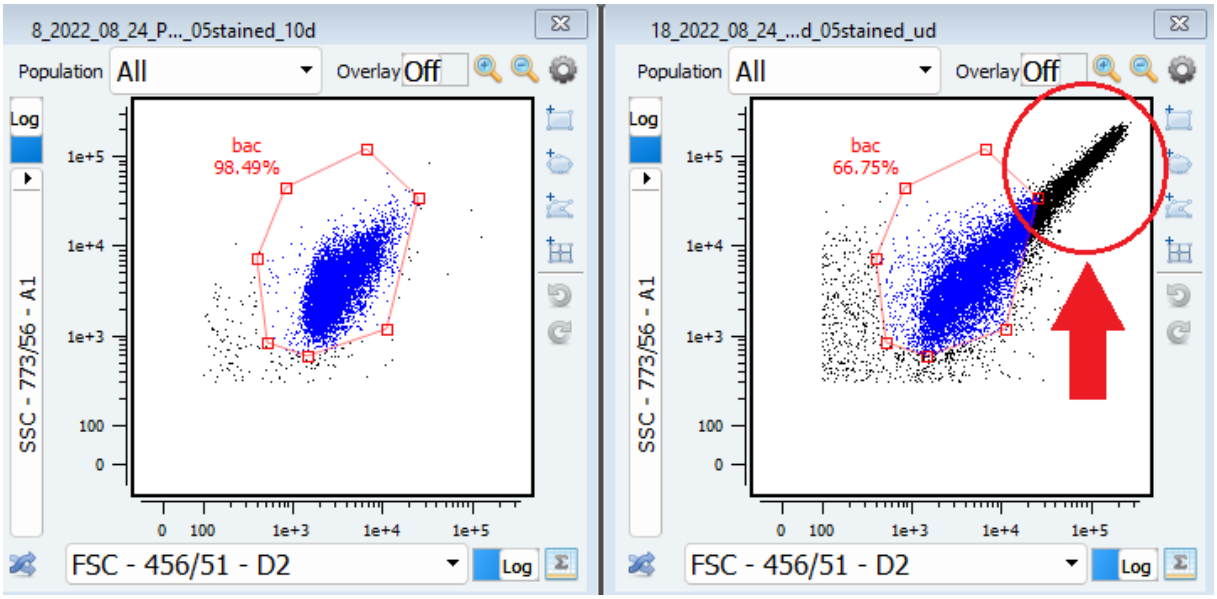

Figure L1. Observed "Tail" in Flow Cytometry Plots. *To the left is a screenshot of a typical sample where most particles are within the defined gating. To the right is a screenshot of what a sample with a tail looks like.*

This page intentionally left blank

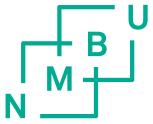

Norges miljø- og biovitenskapelige universitet
Noregs miljø- og biovitskapelege universitet
Norwegian University of Life Sciences

Postboks 5003
NO-1432 Ås
Norway